Non-Redfield carbon model for the Baltic Sea (ERGOM version 1.2) – Implementation and Budget estimates

Thomas Neumann[1], Hagen Radtke[1], Bronwyn Cahill[1], Martin Schmidt[1], and Gregor Rehder[1]

[1]Leibniz Institute for Baltic Sea Research Warnemünde, Seestr. 15, 18119 Rostock, German

Correspondence: Thomas Neumann (thomas.neumann@io-warnemuende.de)

Abstract. Redfield stoichiometry based marine biogeochemical models suffer from underestimating carbon fixation by primary production. The most pronounced indication of this is the overestimation of the dissolved inorganic carbon concentration and, consequently, the partial pressure of carbon dioxide in surface waters. The reduced production of organic carbon will impact most biogeochemical processes.

We propose a marine biogeochemical model allowing for a non-Redfieldian carbon fixation. The updated model is able to reproduce observed partial pressure of carbon dioxide and other variables of the ecosystem, like nutrients and oxygen, reasonably well. The additional carbon uptake is realized in the model by an extracellular release of dissolved organic matter from phytoplankton. Dissolved organic matter is subject to flocculation and the sinking particles remove carbon from surface waters. This approach is mechanistically different from existing non-Redfieldian models, which allow for flexible element ratios for the living cells of the phytoplankton itself. The performance of the model is demonstrated as an example for the Baltic Sea. We have chosen this approach because of a reduced computational effort, which is beneficial for large scale and long-term model simulations.

Budget estimates for carbon illustrate that the Baltic Sea acts as a carbon sink. For alkalinity, the Baltic Sea is a source due to internal alkalinity generation by denitrification. Owing to the underestimated model alkalinity, there exists still an unknown alkalinity source or underestimated land based fluxes.

1 Introduction

We introduce the non-Redfieldian carbon uptake implemented in the biogeochemical model ERGOM 1.2. In a previous publication (Neumann et al., 2021), the optical model of ERGOM 1.2 is described. In this paper, we focus on the non-Redfieldian carbon uptake in ERGOM 1.2. We decided to split the description of ERGOM 1.2 into two parts because we think both parts could be used separately in other models as well.

Models for the marine carbon cycle often fail if carbon fixation by autotrophs is restricted to the elemental Redfield ratio (Redfield et al., 1963). As an example, the surface CO_2 partial pressure ($sp\mathrm{CO}_2$) for the Baltic Sea can hardly be represented correctly (Omstedt et al., 2009, 2014). A prominent disagreement is the overestimated $sp\mathrm{CO}_2$ in Redfield ratio based models (e.g. Kuznetsov et al., 2011). In Fig. 1, we show the $sp\mathrm{CO}_2$ climatology in the central Baltic Sea from observations and from a previous, Redfield version of our model ERGOM. There is

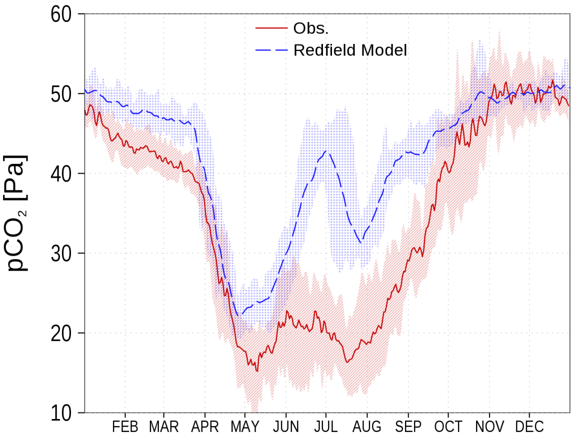

Figure 1. $sp\mathrm{CO}_2$ in the central Baltic Sea from a previous, Redfield stoichiometry version of ERGOM (blue) and observations (red) as climatology (2003–2016) at station BY15 (Fig.6). Shaded areas show the range between the 10th and 90th percentile. Observations are available from SOCAT (see *code and data availability*).

clear observational evidence that carbon fixation continues after the depletion of nitrate during the spring bloom period, which has been termed post-nitrate production (Schneider and Müller, 2018). As this production cannot be sustained in a strictly Redfield-defined parameterization, the simulated $sp\mathrm{CO}_2$ strongly deviates from the onset of nitrate-depletion, which in the central Gotland Sea usually starts by mid-April (Fig. 1, see also Schneider and Müller (2018), their Figure 5.13). The $sp\mathrm{CO}_2$ overestimation vanishes in fall when primary production subsides and deeper mixing occurs. Consequently, the model primary production fixes considerably less carbon compared to *in situ* conditions (Fig. 1). The missing organic carbon impacts all biogeochemical processes of the ecosystem. However, the relatively large freedom in calibration allows one to tune the models to match observed variables like nutrient concentrations.

Fransner et al. (2018) demonstrated the considerable improvement by introducing non-Redfieldian dynamics, which allow for an excess carbon uptake. Established methods for implementing a non-Redfieldian carbon fixation in ecosystem models are the cell quota model by Droop (1973) and/or additional carbon uptake due to dissolved organic matter (DOM) production (Fransner et al., 2018).

Several studies prove that the stoichiometry of healthy phytoplankton cells do not considerably deviate from the Redfield ratio. Ho et al. (2003) showed in an experimental setup for marine phytoplankton that the biomass composition is generally close to the Redfield ratio. In situ data of particulate organic matter (POM) by Martiny et al. (2016) display only moderate deviations from the Redfield ratio. Considering that POM constitutes not only of phytoplankton, other particles like heterotrophs or detritus may impact the observed ratios. Sharoni and Halevy (2020) showed with the aid of model experiments that variations in POM stoichiometry are best explained by taxonomic composition of phytoplankton compared to phenotypic plasticity. That is, phytoplankton with a minimum flexibility of the nutrient cell quota, but a variation between adapted groups, fits best the observed elemental ratio variations on a global scale. Engel (2002) stated that "the fundamental need for N and P for biomass synthesis does not allow large deviations from Redfield".

DOM in the ocean is one of Earth's major carbon reservoirs (Hansell et al., 2009). Many production, degradation and consumption processes control its dynamics. An excellent review of DOM dynamics is given by Carlson and Hansell (2015). We will summarize some facts from this review which we think are important to guide our model development: The main producer of DOM is phytoplankton within the euphotic zone due to extracellular release (ER). Two common models exist to explain mechanisms for ER: (i) The overflow model and (ii) the passive diffusion model. The overflow model assumes an active DOM release by healthy cells. This process is directly coupled to primary production (PP) and regulates the frequently mismatching availability of irradiation and nutrients. The active ER will be used to dissipate energy from the photosynthetic machinery and protect it from damage. In the passive diffusion model, ER is controlled by different concentrations of DOM inside and outside of the cell. The concentration gradient forces an ER across the cell membrane. This process is more strongly coupled to phytoplankton biomass instead of primary production. For both models, experimental evidence exists and it is possible that both are valid and depending on environmental conditions, one or the other process is more active.

Although ER is coupled to PP in the overflow model, there is not a constant fraction of produced DOM. In fact, fractionation depends on nutrient availability and phytoplankton composition (Carlson et al., 1998). Phytoplankton ER consists to up to 80% of carbohydrates which are important precursors for the formation of transparent exopolymer particles (TEP). TEP are sticky and aggregate into larger particles which may sink down (Engel et al., 2004) and are methodically often counted as particulate organic carbon (POC) (Carlson and Hansell, 2015). Therefore, not considering TEP production results in underestimating ER (Wetz and Wheeler, 2007).

Considering the fact that biogeochemical models for the Baltic Sea with a Redfield carbon fixation are not able to reproduce the observed carbon cycle (see also Fig 1) and a strong observational evidence for an ER of DOM (Hoikkala et al., 2015), we develop a model able to fix carbon beyond the classical Redfield ratio. In this study, we introduce a non-Redfiedian carbon uptake by maintaining Redfield composition of living biomass, but allowing ER of highly carbon-enriched DOM in the model ERGOM 1.2 and show selected budgets derived from the model simulations.

2 Methods and data

2.1 Biogeochemical model

We start with explaining the biogeochemical model ERGOM (Leibniz Institute for Baltic Sea Research, 2015), which describes cycles of the elements nitrogen, phosphorus, carbon, oxygen, and partly sulfur.

Primary production, forced by photosynthetically active radiation (PAR), is provided by three functional phytoplankton groups (large cells, small cells, and cyanobacteria). The chlorophyll concentration used in the optical model is estimated from the phytoplankton groups (Neumann et al., 2021). Dead particles accumulate in the detritus state variable. A bulk zooplankton grazes on phytoplankton and is the highest trophic level considered in the model. Phytoplankton and detritus can sink down in the water column and accumulate in a sediment layer. In the water column and in the sediment, detritus is mineralized into dissolved inorganic nitrogen and phosphorus. Mineralization is controlled by water temperature and oxygen concentration. Oxygen is produced by primary production and consumed due to all other processes, e.g., metabolism and mineralization.

The stoichiometry in all organic carbon components of the model is confined to the classical Redfield ratio (Redfield et al., 1963). The advantage of this approach is the model's simplicity. However, observations of the carbon cycle in the Baltic Sea reveal the shortcomings of this kind of model (e.g. Fransner et al., 2018). Based on the findings presented in Sec. 1, specifically the underestimation of carbon fixation, we extended our model by introducing a non-Redfieldian stoichiometry into carbon fixation. The aim of this extension is to allow for carbon fixation beyond the part limited by the availability of nutrients.

Our basic idea is that the element composition in vegetative phytoplankton cells remains at the Redfield ratio and under certain circumstances, extracellular dissolved organic matter (DOM) is produced. This extracellular DOM has a fairly flexible elemental ratio. The produced DOM is subject to flocculation (TEP formation) with a certain rate and eventually sinks down as particulate organic matter (POM). In order to realize the elemental flexibility in DOM, we introduce three different DOM state variables together with the POM counterparts. We call the DOM state variables dissolved organic carbon (DOC), dissolved organic nitrogen (DON), and dissolved organic phosphorus (DOP). The model considers DOC as polysaccharides (COH_2), and DON and DOP as DOC with additional nitrogen (N) and phosphorus (P), respectively. In DON and DOP, the elemental ratio is fixed to the Redfield ratio and they are counted in units of N and P: DON - $(COH_2)_{106/16}N$ and DOP - $(COH_2)_{106}P$. Altogether, model DOM has a flexible elemental ratio with the restriction that the carbon fraction is never below the Redfield ratio. That is, DOM is usually enriched by carbon compared to the Redfield ratio. One could also have used one DOM state variable with a completely free elemental ratio. However, we used the different DOM compartments because we may consider a different fate for DOC, DON, and DOP later.

The production of DOC, DON, and DOP by phytoplankton is controlled by light availability and nutrient concentrations. Under optimal conditions, primary production increases phytoplankton biomass. When nutrients become limiting, DOM production increases while the production of phytoplankton biomass decreases. A schematic is shown in Figure 2. In case of N limitation, DOP is produced and under P limitation, DON is produced. If both N and P becoming exhausted, the fraction of produced DOC increases. We have to note that only phytoplankton is able to produce DOM. That means, if phytoplankton biomass decreases because a net growth is not possible due to e.g. nutrient limitation, the DOM production will decrease as well. In particular, the DOM production is controlled by

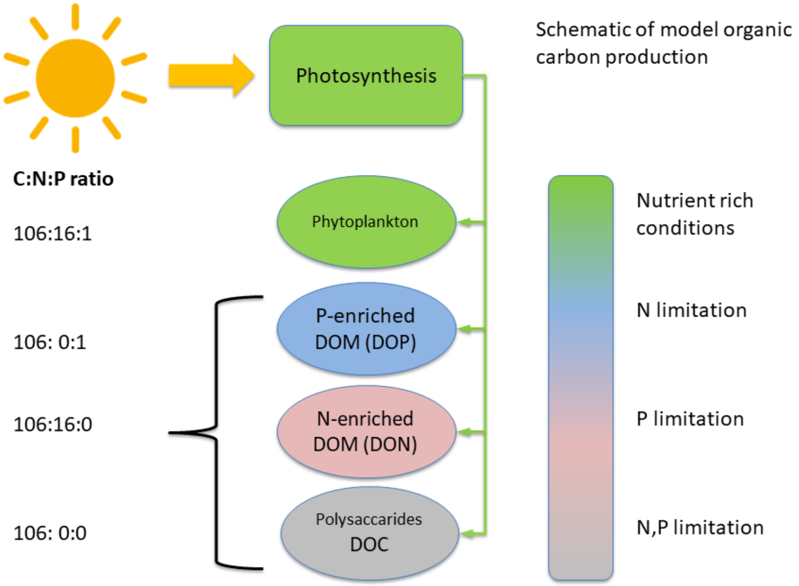

Figure 2. Schematic of DOM production. In case of sufficient nitrients nitrogen (N) and phosphorus (P), phytoplankton biomass is produced. If N becomes depleted, DOP is produced and if P is depleted, DON is produced. If both N and P are depleted, DOC is produced.

a reversal of the phytoplankton nutrient limitation. Gross phytoplankton growth in our model is:

$$\frac{\mathrm{d}PY}{\mathrm{d}t} = r_0 \cdot PY \cdot \min(l_N, l_P, l_L) \cdot l_T \tag{1}$$

PY is the phytoplankton biomass, r_0 the maximum uptake rate, and l_n are limitation functions ranging between zero and one. Subscripts N, P, and L are for nitrogen, phosphorus, and light. l_T is a (possible) temperature impact on uptake. For nutrient limitation (l_N, l_P), we use a squared Monod kinetik (Monod, 1949; Neumann et al., 2002). Light limitation (l_L) follows Steele (1974) and for temperature control (l_T), a Q10 rule is applied (Eppley, 1972) meaning doubling of growth rates with a 10 Kelvin temperature increase. For the temporal development of the DOM compartments we formulate:

$$\frac{\mathrm{d}DON}{\mathrm{d}t} = r_0 \cdot PY \cdot \min(1 - l_P, l_N, l_L)\, l_T \tag{2}$$

$$\frac{\mathrm{d}DOP}{\mathrm{d}t} = r_0 \cdot PY \cdot \min(l_P, 1 - l_N, l_L)\, l_T \tag{3}$$

$$\frac{\mathrm{d}DOC}{\mathrm{d}t} = r_0 \cdot PY \cdot \min(\max(1 - l_P, 1 - l_N), l_L)\, l_T \tag{4}$$

The dependence of nutrients uptake in relation to carbon uptake on nutrient concentrations is shown in Fig. 3. For this purpose, we divide the nutrient assimilation for nutrients N and P by the carbon assimilation. The assimilation

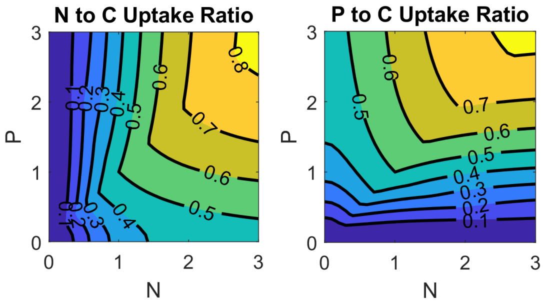

Figure 3. Nutrients (N, P) to carbon uptake ratios as a function of nutrient concentrations. Nutrient concentrations are normalized by the half saturation constant in the limitation function and the uptake is normalized by the Redfield ratio. A ratio of one means uptake in the classical Redfield ratio and values less then one describe an excess carbon uptake.

consists of phytoplankton growth (Redfield ratio) and ER defined in equation 1 and equations 2 to 4, respectively. 125 The nutrient concentrations are normalized by the half saturation constant from the Monod kinetics. A value of one in Fig. 3 denotes a carbon uptake in the Redfield ratio while smaller values indicate an excess carbon uptake. In case of low N concentrations, the N:C uptake ratio declines to zero. The P:C uptake ratio in this case depends on P concentrations and asymptotically approaches 0.5 for high P concentrations. That is, ER consists of DOC and DOP in equal shares. Figure 4 demonstrates the different carbon uptake rates with a realistic example from our 130 model simulations for station BY15 (Fig. 6) in 2017. In spring, when nutrients are available in high concentrations, phytoplankton biomass production dominates. Later in spring, N becomes exhausted and the fraction of DOP production increases. DOC production dominates in summer when both N and P are at low concentrations. DON production is always at a low level at this station because the winter concentration of P is in excess to the N concentration with respect to the Redfield ratio. Altogether, carbon fixation is solely mediated by phytoplankton. 135 Depending on the nutrient concentrations, organic carbon production ends up in phytoplankton, DOC, DON, and DOP. The fractionation is controlled by the limitation functions which ensure a smooth transition and co-existence of the different carbon fixation pathways.

Extracellular DOM eventually forms particles (POC, PON, POP) which constitute transparent exopolymer particles (TEP). Engel (2002) shows a linear relation between dissolved inorganic carbon (DIC) uptake and TEP 140 production implying a direct transfer from DOM to TEP. Therefore, we chose a simple rate equation for DOC flocculation:

$$\frac{\mathrm{d}POC}{\mathrm{d}t} = rf \cdot DOC \tag{5}$$

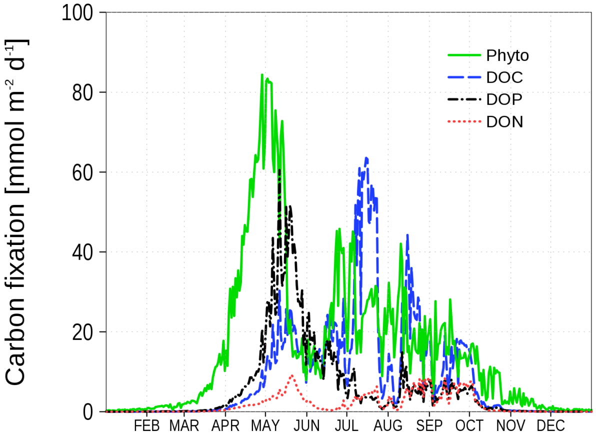

Figure 4. Vertically integrated carbon uptake rates at station BY15 (Fig. 6) in 2017. Shown are production rates for different organic matter compartments phytoplankton, DOC, DOP, and DON.

rf is a constant rate for POC formation. The same equation applies for DON and DOP forming their counterparts PON and POP.

For particle sinking, we apply a Martin curve (Martin et al., 1987) which means a linear increase of the sinking speed with depth.

$$w = a \cdot z \tag{6}$$

w is the sinking speed, a a constant, and z the depth. This approach is investigated by e.g. Kriest et al. (2012) and yields good results for the deep ocean. In the Baltic Sea application, we could improve the simulated oxygen concentrations by using the non-constant sinking speed.

A schematic of ERGOM is shown in Fig.5. Ellipses are for state variables and rectangles for processes. The complete set of equations is given in appendix B.

The relation between model state variables and observed dissolved organic carbon ($\mathrm{DOC_{obs}}$) in carbon units is:

$$DOC_{obs} = DOC + \frac{106}{16} DON + 116\, DOP \tag{7}$$

Taking into account that model state variables DON and DOP are counted in nitrogen and phosphorus units (see Tab. 1), they correspond to the observed nitrogen and phosphorus in DOM. We have to note that our model DOM (DOC, DON, DOP) constitutes only the labile part of DOM existing in the Baltic Sea. Usually, the refractory DOM fraction, not considered in the model, is much larger than the labile fraction.

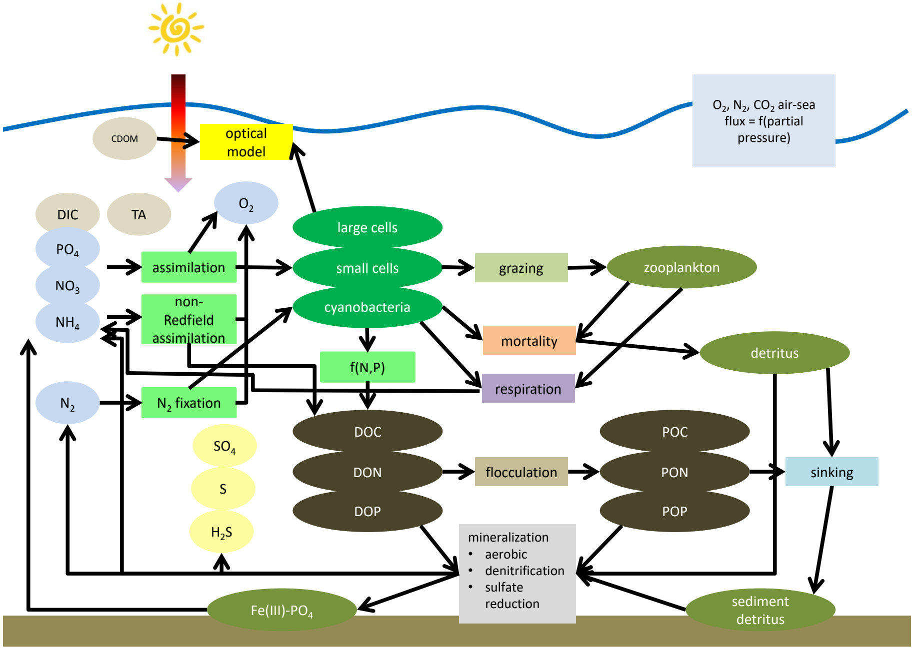

Figure 5. Simplified schematic of the ERGOM model. State variables are shown as ellipses and processes as rectangles. State variables are explained in Tab. 1. Arrows show fluxes of elements mediated by processes. Not all arrows are shown for simplicity of the schematic, e.g. oxygen demanding processes do not show arrows from the oxygen state variable.

2.2 Rationale for model design

The model design was guided by the main principle of keeping the model as simple as possible. This is especially important for model applications in a 3D environment and at long time scales like climate change as well as in ensemble approaches because we want to keep the computational effort at a feasible level. Therefore, we decided to implement ER which allows flexible nutrients to carbon uptake ratios. A cell quota approach was not implemented since it requires a number of additional state variables.

We do not doubt the flexibility in phytoplankton stoichiometry. However, from a modeler's point of view, we consider a fixed elemental ratio in phytoplankton as a reasonable simplification with the advantage of less model complexity. We proved this concept by the application for the Baltic Sea. Measurable state variables agree well with the model data (Sec. A). Especially for $sp\mathrm{CO}_2$, we achieved a considerable improvement. Improvement of the carbon cycle mass balances was the main focus of our model development since it plays a vital role in the energy cascade of the marine ecosystem.

For this reason, we decided to transfer the intracellular deviation from a fixed elemental ratio into dissolved organic matter with a flexible ratio as extracellular release. We justify this assumption by the small effect of intracellular

Table 1. State variables of the biogeochemical model ERGOM shown in Fig. 5.

Symbol	State Variable	Units <element> [mol kg^{-1}]
O_2	dissolved oxygen	dioxygen
N_2	dissolved nitrogen	dinitrogen
CDOM	colored dissolved organic matter	carbon
DIC	dissolved inorganic carbon	carbon
TA	total alkalinity	molar equivalent
NH_4	ammonium	nitrogen
NO_3	nitrate	nitrogen
PO_4	phosphate	phosphorus
SO_4	sulfate	sulfur
S	sulfur	sulfur
H_2S	hydrogen sulfide	sulfur
large cells	large cell phytoplankton	nitrogen
small cells	small cell phytoplankton	nitrogen
cyanobacteria	cyanobacteria	nitrogen
zooplankton	bulk zooplankton	nitrogen
detritus	detritus	nitrogen
DOC	dissolved organic carbon	carbon
DON	DOC with additional nitrogen	nitrogen
DOP	DOC with additional phosphorus	phosphorus
POC	particulate organic carbon	carbon
PON	POC with additional nitrogen	nitrogen
POP	POC with additional phosphorus	phosphorus
sediment detritus	detritus accumulated in the sediment layer	nitrogen [mol m^{-2}]
$Fe(III)-PO_4$	phosphate adsorbed to iron-3 minerals in the sediment	phosphorus [mol m^{-2}]

Sediment state variable units are mol m^{-2}.

flexibility on carbon uptake (see also Sec. 2.3) which is a focus of our model development. Furthermore, observations of C/N/P ratios which distinguish between living cells and POM are still missing in the Baltic Sea area. In the following, we review literature supporting our assumptions.

In Kuznetsov et al. (2011, 2008), we applied the Larsson et al. (2001) findings for diazotrophs. However, these elemental ratios do not explain observed $sp\mathrm{CO}_2$, although the C/P ratio in diazotrophs increases up to fourfold and an additional, artificial spring blooming species of diazotrophs was introduced. Larsson et al. (2001) did their study with filamentous cyanobacteria. Filaments consist not only of vegetative cells but also of akinetes, heterocysts, and vacuoles which together are not necessarily composed according the Redfield ratio. Especially, vacuoles develop in a later state of the bloom and may explain an increasing C/P ratio. These mechanisms are not explicitly formulated in our model and parameterized instead by extracellular release.

Nausch et al. (2009) showed that the elemental C/P ratio (up to 400) is elevated especially in cyanobacteria (their Fig. 7) similar to Larsson et al. (2001). However, the C/P ratio (100-200) in POM at the same station is much lower (same Fig.). Taking the high C/P ratio of cyanobacteria into account, the C/P ratio of the remaining POM is close to the Redfield ratio (~100). In their Tab. 2, C/N ratios in POM are given (7-9) which appear close to Redfield. The slight C enrichment in POM cannot explain observed $sp\mathrm{CO}_2$ (Kuznetsov et al., 2011).

Kreus et al. (2015) introduced extracellular release and cell quota into their model and run it in an 1D environment in the central Baltic Sea. Two experiments have been performed (a) variable quotas, and (b) fixed quotas. POC/PON ratios are virtually the same for both experiments while POC/POP ratios show a different seasonality. However, they conclude that fueling the summer cyanobacteria bloom controlling the carbon cycle and nitrogen dynamics is determined by DOM which is also part of our model. The shortcoming in the DIP cycle in experiment (b) of Kreus et al. (2015) has been solved with our approach. In summary, one can conclude that cell quotas do not have an impact on the nitrogen and carbon cycle (their Fig. 5).

2.3 Differences to earlier approaches

Omstedt et al. (2009) inferred that the carbon dynamics in the Baltic Sea cannot be correctly represented with a strict Redfield based model. Since this time, several carbon cycle models have been proposed for the Baltic Sea. We will review a few of them and highlight the differences to our approach.

Kuznetsov et al. (2008, 2011) used an elevated C/P ratio in cyanobacteria. However, they demonstrated that non-Redfieldian biomass, at least during summer since only cyanobacteria are considered, is by far not sufficient to reproduce observed $sp\mathrm{CO}_2$. We use this result also as an argument to focus on extracellular release.

Wan et al. (2011) changed the N/P uptake and mineralization ratios but did not introduce a flexible elemental uptake ratio. This approach may violate the mass conservation.

Fransner et al. (2018) introduced both non-Redfieldian phytoplankton biomass and extracellular release of DOC. They found that for the Gulf of Bothnia “A substantial part of the fixed carbon is directly exuded as semilabile extracellular DOC” (26%-52%). Their study is limited to the northern Baltic. Therefore, it has not been shown that the model works reasonably for the whole Baltic Sea. Unfortunately, the authors do not show any deep water properties like oxygen which may be impacted by the increased downward carbon flux.

The model used in Kreus et al. (2015) was applied at a station in the central Baltic Sea. Thus, it is not shown that the model gives reasonable results in a 3D environment. It uses a similar approach as in Fransner et al. (2018) with a flexible elemental ratio in phytoplankton and ER of DOM. From our point of view, it involves the disadvantage of enhanced computational effort but do not proof that cell quotas improve the carbon cycle dynamics (Sec. 2.2).

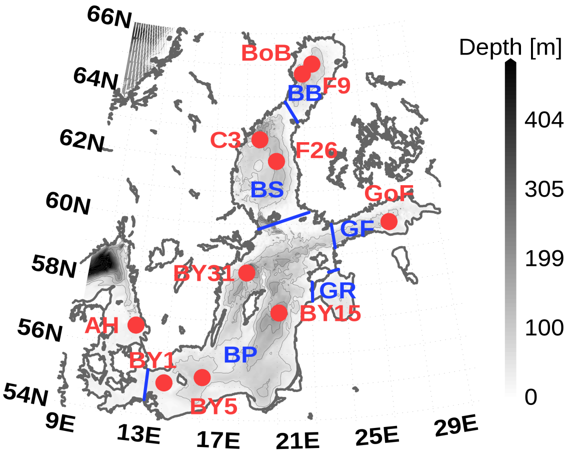

Figure 6. Model domain and bathymetry used for this model study. Red dots denotes stations to which we will refer later in the text. Bathymetry contour lines have a distance of 50 m. Boundaries of regions are in blue with Bay of Bothnia (BB), Bothnian Sea (BS), Gulf of Finland (GF), Gulf Of Riga (GF), and Baltic Proper (BP). The map was created using the software package GrADS 2.1.1.b0 (http://cola.gmu.edu/grads/, last access: 14 December 2021), using published bathymetry data (Seifert et al., 2008).

2.4 Model setup and simulations

For model testing, we use a coupled system of circulation and biogeochemical model similar to that in Neumann et al. (2021). The circulation model is MOM5.1 (Griffies, 2004) adapted for the Baltic Sea. The horizontal resolution is 3 nautical miles. Vertically, the model is resolved into 152 layers with a layer thickness of 0.5m at the surface and gradually increasing with depth up to 2 m. The circulation model is coupled with a sea ice model Winton (2000) accounting for ice formation and drift. The biogeochemical model ERGOM, described in Sec. 2.1, is coupled with the circulation model via the tracer module which is part of the MOM5.1 code.

The code for the biogeochemical model is generated automatically. Fundamentals are a set of text files describing the biogeochemistry independently of programming language and the host system. Code templates describe physical and numerical aspects and are specific for a certain host, e.g., a circulation model. All the necessary ingredients (the code generation tool, text files, and templates for several systems) can be downloaded from Leibniz Institute for Baltic Sea Research (2015). The same technique is used for example in Neumann et al. (2021).

We run the model for about 70 years (1948–2019) after a spin-up of 50 years. The long simulation time allows us to assess the model performance under different forcing conditions, as for example the eutrophication of the Baltic Sea in the 1970s and the nutrient load reduction beginning in 1990.

Table 2. Average alkalinity concentration and loads in runoff for different Baltic Sea basins and from different authors. BP: Baltic Proper, GR: Gulf of Riga, GF: Gulf of Finland, BS: Bothnian Sea, BB: Bay of Bothnia (6). HS: Hjalmarsson et al. (2008), GS: Gustafsson et al. (2014b), NM: this study.

	Concentration			Load	
Basin	HS	GS	NM	GS	NM
BP	3244	1910	3156	203	340
GR	3117	3140	3638	92	117
GF	835	689	786	73	89
BS	467	271	240	27	17
BB	136	164	174	19	20
total		904	1165	453	606

Alkalinity concentration in $\mu\mathrm{mol\,kg^{-1}}$ and loads in $\mathrm{Gmol\,a^{-1}}$.

2.5 Data

The model has been forced by meteorological data from the coastDat-2 dataset (Geyer and Rockel, 2013). Nutrient loads to the Baltic Sea due to riverine discharge and atmospheric deposition have been compiled based on data from HELCOM assessments (e.g. HELCOM, 2018). Riverine alkalinity follows data provided in Hjalmarsson et al. (2008). In Tab. 2, we compare riverine alkalinity concentration and loads with published data from Hjalmarsson et al. (2008) and Gustafsson et al. (2014b). The data are relatively similar with the exception of the Baltic Proper. Gustafsson et al. (2014b) use considerably lower values, which impacts the total load. Our mean concentrations differ slightly from Hjalmarsson et al. (2008). We used the basin-wide and constant concentration values given in Hjalmarsson et al. (2008) and assigned the data to our model rivers which show inter annual runoff variability. This results in mean concentration deviations. Loads given in Tab. 2 result from runoff and river specific concentrations.

sp$\mathrm{CO_2}$ for model validation have been extracted from the SOCAT (Surface Ocean $\mathrm{CO_2}$ Atlas) data base (https://www.socat.info/). The majority of data are from the voluntary observing ship (VOS) Finnmaid between Lübeck-Travemünde and Helsinki. VOS Finnmaid is a component of the European ICOS (Integrated Carbon Observation System) research infrastructure. Data processing and quality control follow the SOCAT guidelines (Bakker et al., 2016; Pfeil et al., 2013). Additional observation data used for comparison with model results are available from public data bases. Details are given in section *code and data availability*.

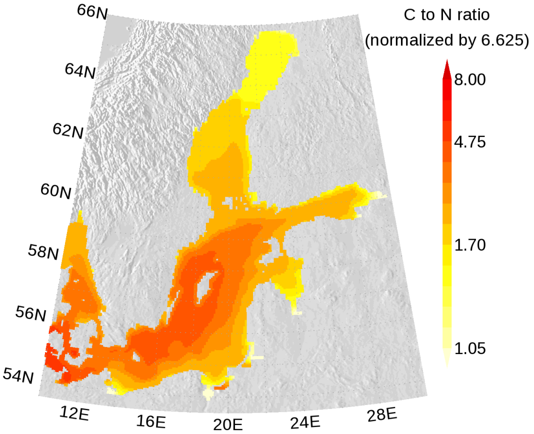

Figure 7. Annual mean elemental carbon to nitrogen ratio in surface organic matter. The ratio is normalized and a ratio of one refers to the classical Redfield ratio. The map was created using the software package GrADS 2.1.1.b0 (http://cola.gmu.edu/grads/, last access: 14 December 2021), using published topography data (Seifert et al., 2008).

3 Results

3.1 How the non-Redfieldian approach works

In this section, we demonstrate how a non-Redfieldian elemental ratio in organic matter (OM) develops due to the above described model extensions. OM involves all forms of model DOM and POM including model phytoplankton, zooplankton, and detritus. We show data averaged over the whole simulation period and seasonal climatologies. The elemental ratios are based on molar concentrations.

In Figs. 7 and 8, the carbon (C) to nitrogen (N) and carbon to phosphorus (P) ratios in organic matter in surface water are shown. In both figures, the elemental ratios are normalized so that a ratio of one is for the classical Redfield ratio. The figures highlight the different nutrient limitation provinces in the Baltic Sea. The C:N ratio is high in the central Baltic Sea where N is a limiting nutrient and consequently the C:P ratio is low. The opposite is in the northern Baltic Sea where P is the limiting nutrient. We have to note that our model approach does not allow for C:N and C:P ratio below Redfield ratios in the DOM and POM fractions. Hence, the elemental ratios in OM are always above one. An exception are river mouths where almost no nutrient limitation keeps the C:N and C:P ratios close to one.

We show the N:P ratio in OM and its seasonality in Fig. 9. Again, the figure shows the separation between the nutrient limitation provinces. N limitation is denoted by a low N:P ratio in the central Baltic Sea and a high N:P ratio shows P limitation in the northern Baltic Sea. During the course of the year, the N:P ratio in the central Baltic Sea increases due to nitrogen fixation by cyanobacteria. The temporal development of the DOM fractions can be

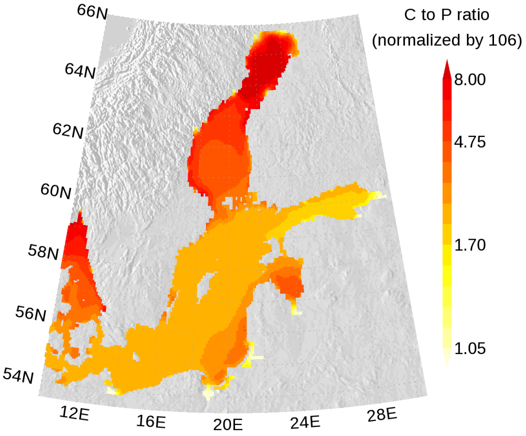

Figure 8. Annual mean elemental carbon to phosphorus ratio in surface organic matter. The ratio is normalized and a ratio of one refers to the classical Redfield ratio. The map was created using the software package GrADS 2.1.1.b0 (http://cola.gmu.edu/grads/, last access: 14 December 2021), using published topography data (Seifert et al., 2008).

seen in Fig. 10. In the N-limited Gotland Sea (Fig. 10a), surplus phosphate is transferred into DOP after depleted N starts limiting phytoplankton growth. With intensified nutrient limitation also DON and DOC will be produced by phytoplankton. In summer, with a higher demand of phosphorus by cyanobacteria, the DOP pool is depleted. In contrast, in the northern part of the Baltic Sea, the Bothnian Bay, surplus nitrogen is transferred into DON (Fig. 10b). Almost no DOP develops. In Fig. 11, we show the surface climatology of simulated $\mathrm{DOC_{obs}}$ (eq. 7) at station BY15 together with observations. Observed DOC concentrations constitute to a large extent of refractory fractions. In contrast, in the model we only consider the labile, autochthonous part of DOC. Therefore, we subtracted 305 µmol $\mathrm{kg^{-1}}$ from the observations which is the mean winter concentration. The annual DOC cycle in the observed data appears less pronounced compared to the modeled $\mathrm{DOC_{obs}}$ cycle.

3.2 Primary production and extracellular production

We consider primary production (PP) as carbon fixation contributing to phytoplankton biomass while extracellular production (EP) is the carbon fixation resulting in DOM (DOC, DON, and DOP state variables). Figure 12 shows the time series and climatology of PP and EP as means of the whole model domain. Carbon fixation is dominated by EP. With increasing nutrient availability beginning in the 1960s, the fraction of PP increases (Fig. 12a). The PP and EP climatology in Fig. 12b shows that PP dominates in spring and fall, and EP dominates in summer. Figure 12c shows PP of the model phytoplankton groups. Most PP occurs in spring mediated by the large cell phytoplankton group LPP. In contrast, most EP is mediated by the small cell phytoplankton group SPP in summer (Fig. 12d).

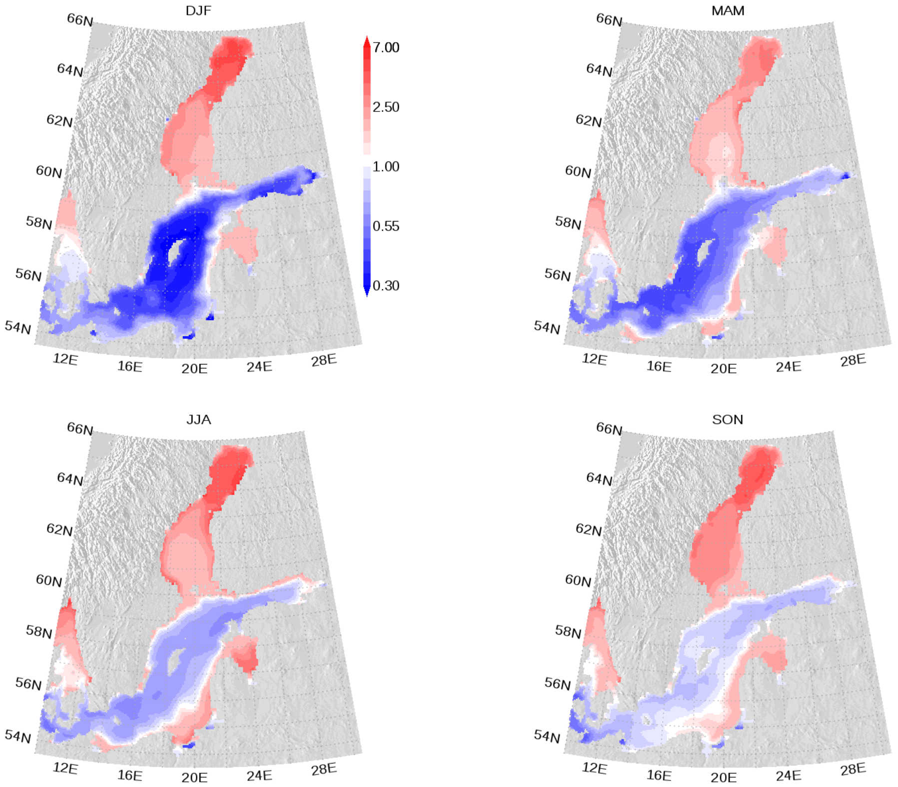

Figure 9. Seasonal mean elemental nitrogen to phosphorus ratio climatology in surface organic matter. The ratio is normalized and a ratio of one refers to the classical Redfield ratio. The map was created using the software package GrADS 2.1.1.b0 (http://cola.gmu.edu/grads/, last access: 14 December 2021), using published topography data (Seifert et al., 2008).

3.3 Assessment of biogeochemical variables

We especially show model data and observations for sea surface carbon dioxide pressure and alkalinity. Other biogeochemical variables are shown in App. A.

3.3.1 Sea surface pressure of carbon dioxide ($spCO_2$)

One motivation to introduce a non-Redfieldian carbon fixation into the ecosystem model ERGOM was the mismatch in observed and simulated $sp\mathrm{CO}_2$ (Kuznetsov et al., 2011, see also Fig. 1). Redfield models are not able to explain the low observed $sp\mathrm{CO}_2$ during summer. Temperature increase and ongoing mineralization in the surface layer increase the $sp\mathrm{CO}_2$ to unrealistic values in the simulations. One conclusion was that still after nutrient limitation, a substantial carbon fixation goes on. Consequently, the carbon fixation is not restricted to the classical Redfield ratio.

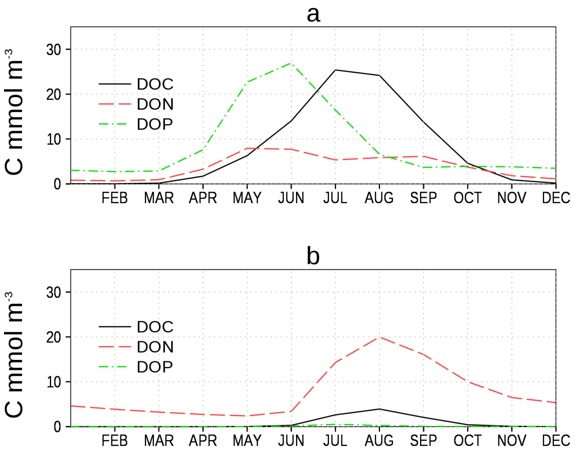

Figure 10. Climatology of surface model DOC, DON, and DOP (in carbon units, Tab. 1 and Eq. 7) at two stations. a) Central station in the Eastern Gotland Sea (BY15), and b) Central Station in the Bothnian Bay (BoB, Fig. 6). Model DON and DOP are converted into carbon units to show all variables on a comparable level.

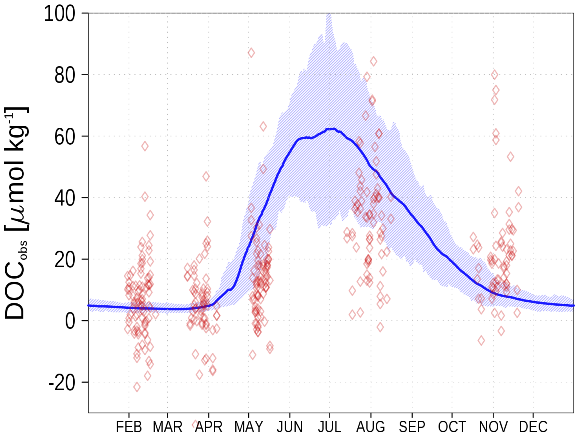

Figure 11. Climatology (1995-2019) of simulated surface DOC$_{\text{obs}}$ (eq. 7) at station BY15 (blue line) and observed DOC (red diamonds). The diamond's opacity reflects the frequency of observations. The shaded area shows the range between the 10th and 90th percentile. From observations, 305 µmol kg^{-1} have been subtracted. Observed DOC data are available from IOW ODIN database (see *code and data availability*).

For the *sp*CO$_2$ benchmark, we use data taken underway from the voluntary observing ship (VOS) Finnmaid regularly traveling between Lübeck-Travemünde and Helsinki. For more details see section 2.5 and Schneider and Müller (2018). The pathway and *sp*CO$_2$ observations taken by VOS Finnmaid and used in this study are shown in

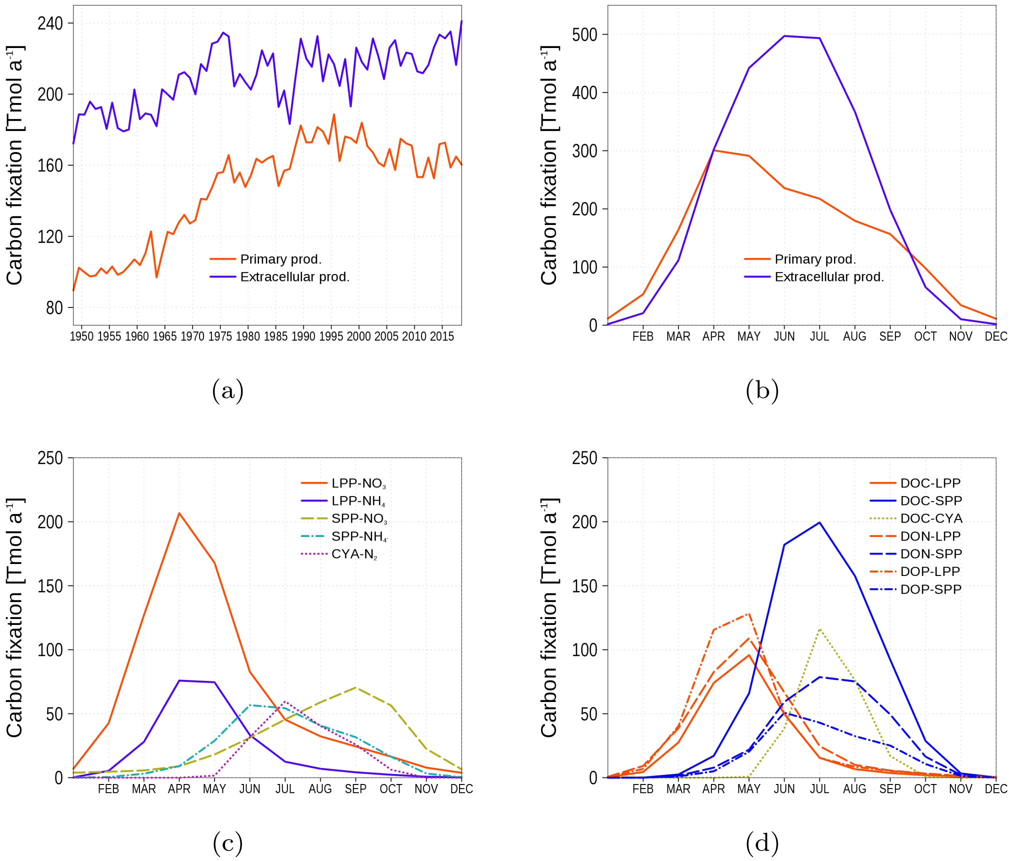

(a) (b)

(c) (d)

Figure 12. Temporal and spatial mean primary and extracelluar carbon fixation by model phytoplankton. a) Time series of annual carbon fixation. b) Climatology of carbon fixation. c) Climatology of primary production related to different uptake processes. LPP-NO3 and LPP-NH4: Carbon fixation by the large cell phytoplankton group related to NO3 and NH4 uptake, respectively. SPP-NO3 and SPP-NH4: The same as for LPP but for the small cell phytoplankton group. CYA-N: Carbon fixation by cyanobacteria related to nitrogen fixation. d) Climatology of extracellular production related to different phytoplankton groups: Red lines are uptake by LPP, blue lines by SPP, and green line by cyanobacteria. Different line styles refer DOC, DON, and DOP. All model variables have been converted into carbon units (Eq. 7).

Fig. 13. From the regions denoted by green rectangles, we have selected data to compare with our model simulation. As can be seen from the pathway's opacity, region f was crossed less frequently than the other regions. The *sp*CO_2 climatology is shown in Fig. 14. The non-Redfieldian carbon fixation keeps the *sp*CO_2 low during summer as seen in the observations. In the northern regions c and e, the spring bloom seems to be delayed in the model. However, the general picture is a strongly improved *sp*CO_2 in the model compared to earlier model versions (e.g. Kuznetsov et al., 2011), as can be seen by comparing to Fig. 1.

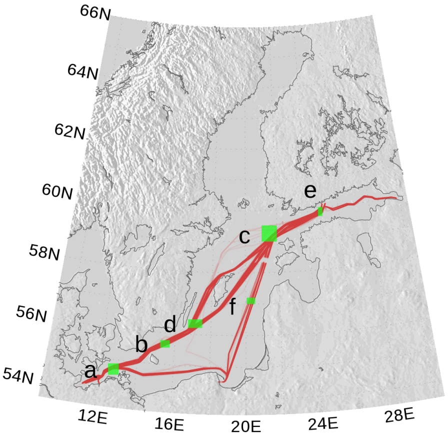

Figure 13. $sp\mathrm{CO}_2$ observations by VOS Finnmaid between 2003 and 2018 used for model analysis (red line). Opacity refers to frequency of observations. a–f denote regions selected (green rectangles) for comparison with model data. The map was created using the software package GrADS 2.1.1.b0 (http://cola.gmu.edu/grads/, last access: 14 December 2021), using published topography data (Seifert et al., 2008).

3.3.2 Alkalinity

Alkalinity in the model is estimated after the equation for `t_alk` in appendix B4. Figure 15 shows the surface alkalinity climatology from observations (red diamonds) and from the model simulation (blue). We show the climatology for six stations from the Kattegat (a) to the Bothnian Bay (f). While in the Kattegat, the simulated alkalinity reflects observations reasonably well, the model's underestimation amounts to roughly 20% in the central Baltic Sea and increases further towards the northern Baltic Sea. This will also have an effect on the total inorganic carbon (DIC) content. However, once in a quasi equilibrium with the atmosphere, the air-sea fluxes will be affected only marginally.

3.3.3 Nutrients

Nutrient surface concentrations are shown in App. A1. We have chosen 6 stations and regions to cover the whole Baltic Sea. Figures A1–A6 show the climatology and time series of simulated nitrate and phosphate together with observations. We find a good model performance for the western Baltic Sea, the central Baltic Sea, and the Gulf of Finland. In the northern Baltic Sea, the Gulf of Bothnia, the model overestimates slightly the nutrient concentrations. Nevertheless, the strong phosphate limitation in this region is well covered.

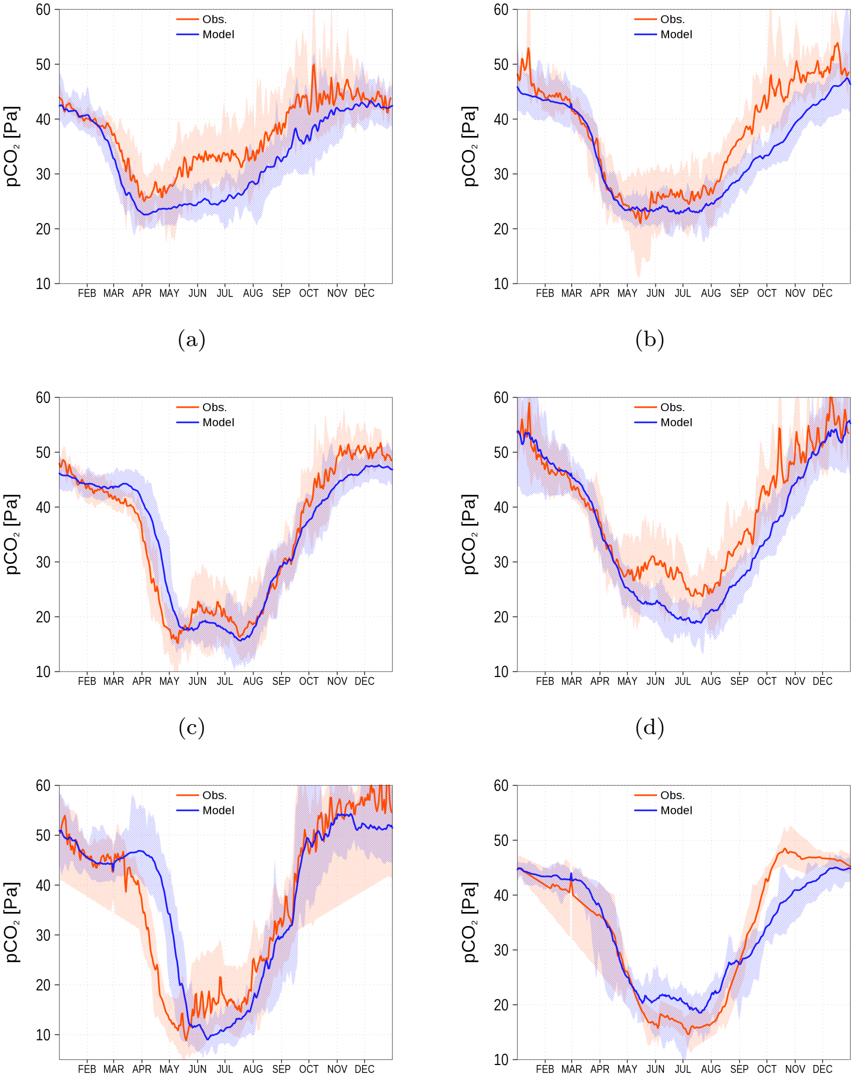

(a) (b) (c) (d) (e) (f)

Figure 14. *sp*CO$_2$ climatology (2003-2018) from observations (red) and from model simulation (blue). Shaded areas show the range between the 10th and 90th percentile. The sub-figures a–f refer to the corresponding regions shown in Fig. 13 by green rectangles a–f. Observations are available from SOCAT (see *code and data availability*).

3.3.4 Oxygen

Oxygen concentrations of the near bottom water are shown in App. A2. Especially in the northern Baltic Sea, simulated concentrations are lower compared to observations.

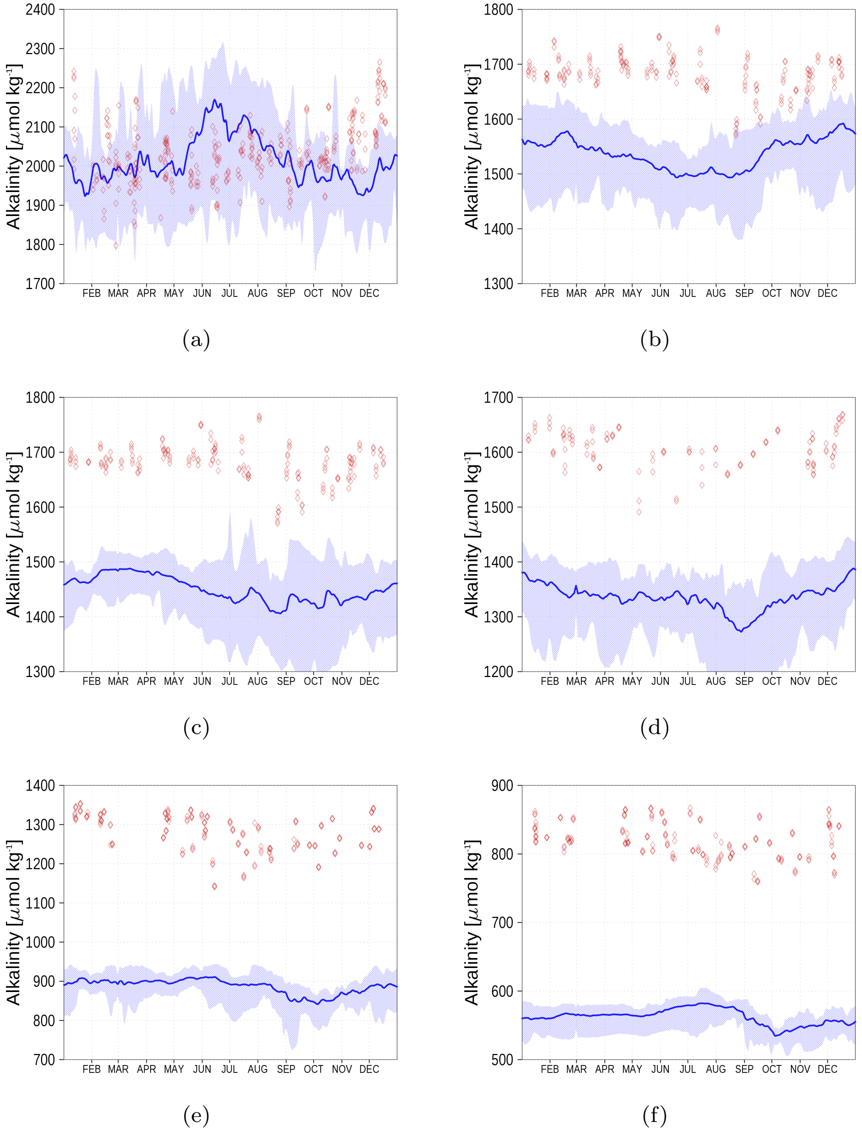

Figure 15. Surface alkalinity climatology (2013-2018) from observations (red) and from model simulatuion (blue). Shaded areas show the range between the 10th and 90th percentile. The subfigures represent stations AH (a), BY1 (b), BY15 (c), BY31 (d), C3 (e), and F9 (f) (Fig. 6). Observed alkalinity data are available from the SHARK database (see *code and data availability*).

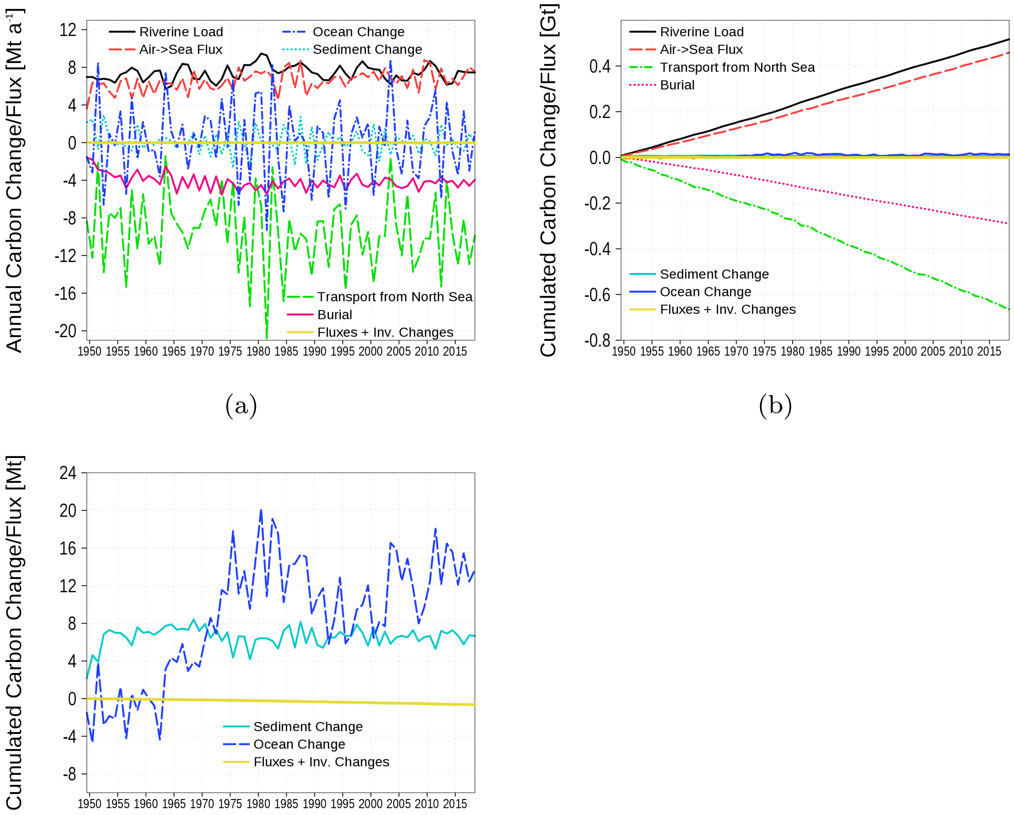

(a)

(b)

(c)

Figure 16. Model-domain integrated carbon budget. Shown are riverine loads, air-sea flux, burial, transport from the North Sea, and changes in the inventory of the ocean (water column) and the sediment. a) Fluxes and inventory change, b) cumulated fluxes, and c) detailed view on the cumulated inventory changes in the ocean and sediment. The yellow line is the sum of all fluxes and inventory changes, and should be zero in a closed budget. Note: We use negative sign for sinks (burial and export towards North Sea).

3.4 Budgets

In this section, we show selected budgets as estimated from the model simulation and demonstrate that the model closes the budget.

3.4.1 Carbon budget

The carbon budget is shown in Fig. 16. The budget considers the inventory change of all carbon containing state variables in the water column and in the sediment. Changes are the result of the boundary fluxes riverine load, air-sea fluxes, transport from and to the North Sea, and burial of carbon in the sediment. The closed budget, which we show with the yellow line, should be zero, a deviation reflects cumulated numerical inaccuracies that are obviously small compared to the simulated signals. In Fig. 16a, annual fluxes and inventory changes are shown. Highest fluxes are the carbon export towards the North Sea and riverine carbon loads followed by air-sea flux and burial. Figures 16b and c show cumulated fluxes and inventory changes. Inventory changes are very small compared to the boundary fluxes. Therefore, we show in Fig. 16c the inventory changes separately. The sediment inventory stays relatively constant. In the water column, carbon inventory increases in response to higher nutrient loads in the 1960s and 70s (loads shown in Figs. 18 and 19).

3.4.2 Alkalinity budget

The alkalinity budget is shown in Fig. 17. The budget considers the inventory change of the alkalinity state variable in the water column. Changes are the result of the boundary fluxes riverine load, and transport from and to the North Sea. In contrast to the carbon budget, the alkalinity budget is not closed (yellow line and Fig. 17c). The increasing sum of boundary fluxes and inventory change, which should cancel out each other in a closed budget, suggests an internal alkalinity source. According to the implemented processes affecting alkalinity (Eq. for `t_alk` in B4), we attribute the alkalinity generation mainly to denitrification. The alkalinity generation is estimated to be roughly 7% of the loads.

3.4.3 Nitrogen budget

The nitrogen budget is shown in Fig. 18 with inventory changes, boundary fluxes, loads, transport from and to the North Sea, burial in the sediment, and the internal sinks (denitrification) and sources (nitrogen fixation by cyanobacteria). The nitrogen load involves riverine, atmospheric, and point source loads. Strongest fluxes are due to loads as nitrogen source and sediment denitrification as sink. A detailed view on cumulated fluxes in Fig. 18c demonstrates that nitrogen fixation is nearly balanced by denitrification in the water column and only a small amount nitrogen is exported towards the North Sea.

3.4.4 Phosphorus budget

The phosphorus budget in Fig. 19 shows inventory changes, boundary fluxes, loads, transport from and to the North Sea, and burial. The phosphorus load involves riverine, atmospheric, and point source loads. In contrast to nitrogen, no internal sinks and sources exist. The most important sink for phosphorus loads is the burial in the sediment. Similar to nitrogen, a small amount of phosphorus is exported towards the North Sea.

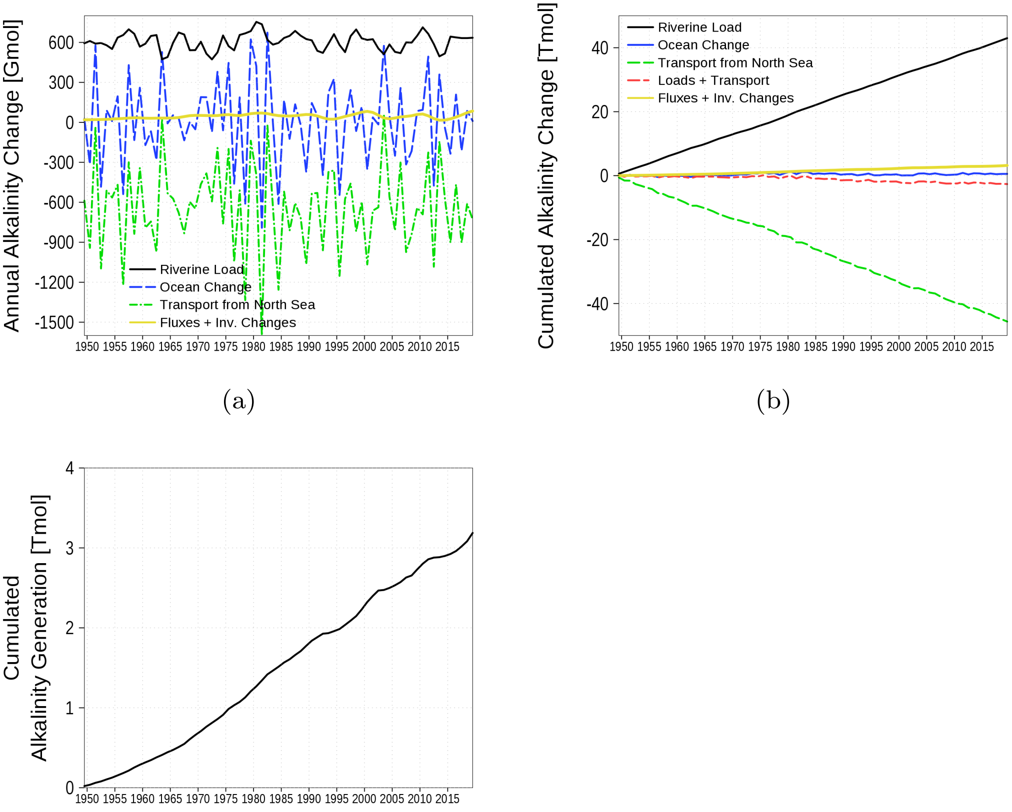

(a) (b)

(c)

Figure 17. Model-domain integrated alkalinity budget. Shown are riverine loads, transport from the North Sea, and changes in the inventory of the ocean. a) Fluxes and inventory change, b) cumulated fluxes and inventory change, and c) residual of the budget which can be attributed to alkalinity generation. The yellow line is the sum of all fluxes and inventory change and should be zero in a closed budget. Note: We use a negative sign for sinks (export towards North Sea).

4 Discussion and conclusion

We present a biogeochemical model for the Baltic Sea which is able to reproduce observed $sp\mathrm{CO}_2$ data. This could be achieved solely by implementing a non-Redfieldian stoichiometry in carbon fixation. We realize this by introducing ER due to primary production. ER results in DOM with a flexible elemental ratio and eventually flocculates into POM which sinks down. This approach reproduces observed $sp\mathrm{CO}_2$, nutrients, and oxygen concentrations reasonably well for the whole Baltic Sea. A different approach is used by Fransner et al. (2018). In their model, in addition to a release of DOC, phytoplankton is formulated as a quota model, that is, within the phytoplankton cells, a certain flexibility of the elemental ratio is allowed. This model is applied for the northern part of the Baltic Sea and

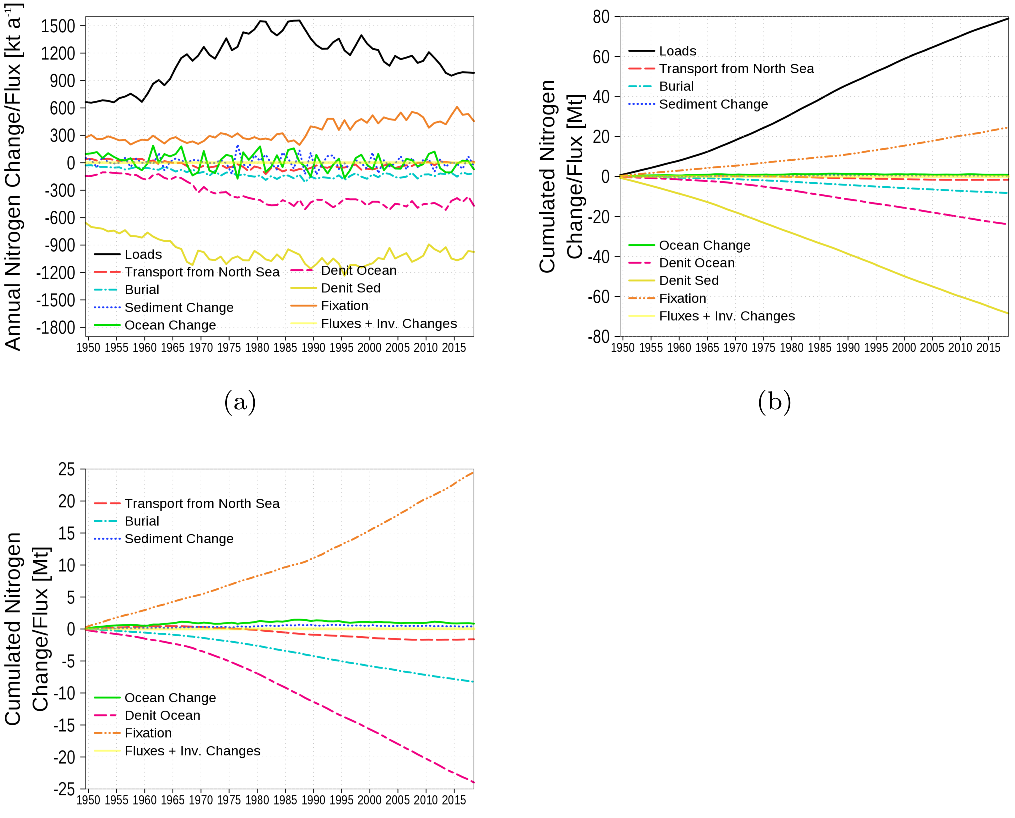

(a)

(b)

(c)

Figure 18. Model-domain integrated nitrogen budget. Shown are loads (riverine, atmospheric, point sources), transport from the North Sea, burial, changes in the inventory of ocean and sediment, denitrification in sediment and ocean, and nitrogen fixation. a) Fluxes and inventory change, b) cumulated fluxes and inventory changes, and c) detailed view without loads and sediment denitrification. The light yellow line is the sum of all fluxes and inventory changes and should be zero in a closed budget. Note: We use negative sign for sinks (burial, denitrification, and export towards North Sea).

reproduces well $sp\text{CO}_2$ and surface nutrient concentrations. The main difference between the models is the quota approach in Fransner et al. (2018) while in our model C/N/P uptake variations are directly transferred into ER. However, we have chosen the fixed ratio (Redfield ratio) in healthy phytoplankton cells because of some evidence from literature (Sec: 1) and less computational effort. We are also convinced that our approach is simpler to handle with respect to higher trophic levels which can rely on a fixed stoichiometry.

A similar model was introduced by Gustafsson et al. (2014a) also using the ER process to increase carbon fixation beyond the Redfield ratio. However, the authors do not show the model's performance with respect to $sp\text{CO}_2$ which might be due to missing or rare observations during this time. Macias et al. (2019) implemented a non-Redfieldian

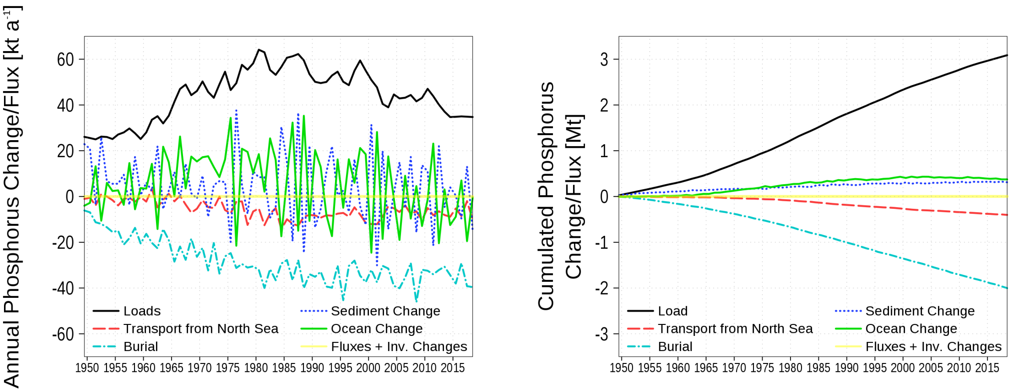

(a) (b)

Figure 19. Model-domain integrated phosphorus budget. Shown are loads (riverine, atmospheric, point sources), transport from the North Sea, burial in the sediment, and changes in the inventory of ocean and sediment. a) Fluxes and inventory change, and b) cumulated fluxes and inventory changes. The light yellow line is the sum of all fluxes and should be zero in a closed budget. Note: We use negative sign for sinks (burial and export towards North Sea).

nutrient uptake in an ecosystem model for the Mediterranean Sea which results in a flexible elemental ratio in phytoplankton. This model gives good results for nutrients N and P but does not consider carbon. A cell quota model for global Earth system models is proposed by Pahlow et al. (2020); Chien et al. (2020). This model also shows an advantage over fixed elemental ratio models with respect to nutrient concentration. However, a proof against variables of the carbon cycle is unfortunately missing.

First evaluations of the simulation show an alkalinity generation of about 50 Gmol a^{-1} (Fig. 17). Gustafsson et al. (2014b, 2019) estimated an alkalinity generation of 84 Gmol a^{-1} and 120 Gmol a^{-1}, respectively. Alkalinity river loads in our model are 600 Gmol a^{-1} and higher compared to loads in Gustafsson et al. (2014b, 2019) (470 Gmol a^{-1}, Tab. 2). Altogether, both models underestimate the alkalinity concentration (Fig. 15) and consequently, sources of alkalinity are missing or underrepresented. Gustafsson et al. (2014b) investigated the contribution of a final pyrite burial in sediments to the missing alkalinity source with an advanced sediment model. However, pyrite burial can explain the missing source only partly. It remains still an open question whether riverine alkalinity loads are underestimated or an unknown source exists, e.g. groundwater discharge.

The Baltic Sea acts as a sink for carbon due to uptake of atmospheric carbon dioxide. The additional carbon is partly buried and the remaining fraction is exported towards the North Sea (Fig. 16). However, the northern Baltic Sea emits carbon dioxide into the atmosphere. Figure 20 shows the horizontal pattern of the mean atmosphere-ocean flux. Sources of carbon dioxide for the atmosphere are the northern Baltic Sea and upwelling regions. The latter are caused by prevailing westerly winds with upwelling near the Swedish coast and in the Gulf of Finland. The upwelled, carbon dioxide rich deep water eventually comes in contact with the atmosphere and equilibriates by outgassing

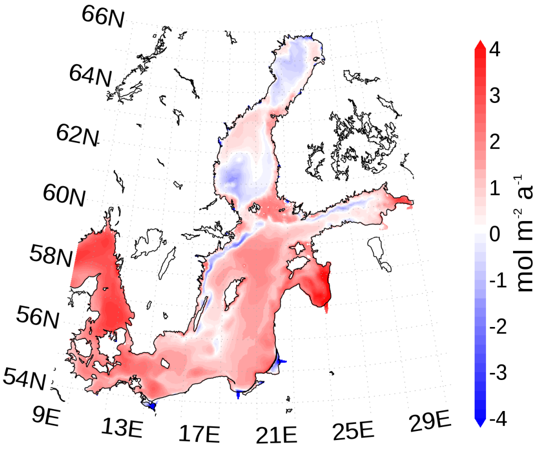

Figure 20. Mean atmosphere-ocean carbon dioxide flux. A positive flux is into the Baltic Sea. The map was created using the software package GrADS 2.1.1.b0 (http://cola.gmu.edu/grads/, last access: 14 December 2021).

Table 3. Total carbon budget for the whole model domain (NM) compared with estimates from Gustafsson et al. (2017, Tab. 6) (GS).

	GS	NM
Riverine loads	10646	7391
Air-sea flux	3878	6525
Export	13416	9614
Burial	909	4077

All carbon fluxes in kt a^{-1} .

of carbon dioxide. For the northern Baltic Sea, we hypothesize that low primary production due to low phosphate concentrations (Fig. A5) favors outgassing of carbon dioxide, which may be imported in subsurface waters from the south.

We compare our carbon budget with estimates from Gustafsson et al. (2017) in Table 3. The most pronounced difference is the 4-fold burial of carbon in our estimates. It corresponds to a rate of 9 $\mathrm{g\,m^{-2}\,a^{-1}}$. Leipe et al. (2010, Fig. 7) estimate an observation based carbon burial rate which is similar to our rate. However, uncertainties in such rates are large, specifically due to a strong spatial heterogeneity of the carbon burial.

Observations of the marine carbon cycle and especially the $sp\mathrm{CO}_2$ provide an additional, independent state variable constraining ecosystem models. Therefore, models able to reproduce the carbon cycle in addition to e.g. nitrogen and phosphorus cycle should be more robust against changes in the forcing conditions (higher predictive capacity). This is especially important if the models will be used for projections or scenario simulations with changing forcing.

As a lot of observational effort in the past focused on N- and P-cycling, proper implementation of the carbon system requires additional observational and experimental data addressing the carbon cycle. For instance, the reason for the mismatch between observational and experimental alkalinity inventories needs to be addressed by re-addressing the alkalinity flux from the riverine input. Clear evidence has been provided for trends of increasing alkalinity in the major basins of the Baltic Sea (Müller et al., 2016) particularly pronounced in the Northern Basins, but a concerted effort to better constrain the alkalinity fluxes from the major riverine sources is currently lacking. Additional contributions from groundwater seepage can contribute to the alkalinity flux from land and have been shown to locally enhance alkalinity, but the importance on a basin-wide scale is unclear (e.g. Szymczycha et al., 2014).

The initial observational finding that carbon loss during the spring bloom continues after nitrogen depletion had originally led to the hypothesis of N-fixation already in late-April (Schneider et al., 2009; Kuznetsov et al., 2011), an interpretation which has been revoked by the authors due to a lack of evidence of any known N-fixing organisms during that time of the year (Schneider and Müller, 2018). However, statistical analysis of observational data clearly revealed an increase in total N in the surface waters of the central Baltic Sea during this period (Eggert and Schneider, 2015), which could not be reproduced by our model. The authors speculated on a potential vertical shuttling of nitrate by the mixotroph mesodynium rubrum, a theory later supported by observations in the Gulf of Finland (Lips and Lips, 2017). Recently, anomalous high carbon fixation in the surface layer under extreme sunny and calm spring conditions in 2018 have been also linked to potential vertical nutrient shuttling (Rehder et al., 2020). However, studies on a process level are needed to explore the mechanism and quantity of a potential nutrient shuttle.

Finally, we present a biogeochemical model for the Baltic Sea reproducing parts of the nutrients and carbon cycle reasonably well. This progress allows now for numerical quantitative studies especially with focus on carbon dynamics in the Baltic Sea under different forcing conditions.

Code and data availability. $sp\mathrm{CO}_2$ data used are available from https://www.socat.info (last access: 14 January 2022). Oceanographic nutrient and oxygen data used for model validation are available from https://www.ices.dk/data/data-portals/Pages/default.aspx (last access: 14 January 2022). DOC data used are available from IOW database ODIN https://odin2.io-warnemuende.de/ (last access:18 February 2022). Alkalinity data used are available from SHARK database https://sharkweb.smhi.se/hamta-data/ (last access: 28 February 2022). The meteorological forcing is archived at https://doi.org/10.1594/WDCC/coastDat-2_COSMO-CLM (last access: 14 January 2022, Geyer and Rockel (2013)).

The code of the biogeochemical model is available at https://ergom.net/ (last access: 14 January 2022). The ocean model "Modular Ocean Model MOM 5-1", used in this study, is available from the developers respository https://github.com/mom-ocean/MOM5 (last access: 14 January 2022).

Model data can be accessed via https://thredds-iow.io-warnemuende.de/thredds/catalogs/projects/integral/catalog__pocNP__V04R25__3nm__agg__time.html (last access: 14 January 2022, Neumann (2021)). All data used in this study for analysis and figures are archived on Zenodo at https://doi.org/10.5281/zenodo.7252134 (last access: 26 October 2022, Neumann (2022)).

The version of the model code used to produce the results in this study is archived on Zenodo at https://doi.org/10.5281/zenodo.7252134 (last access: 26 October 2022, Neumann (2022)). In addition to the source code, the archive includes initial fields and boundary conditions except the meteorological forcing.

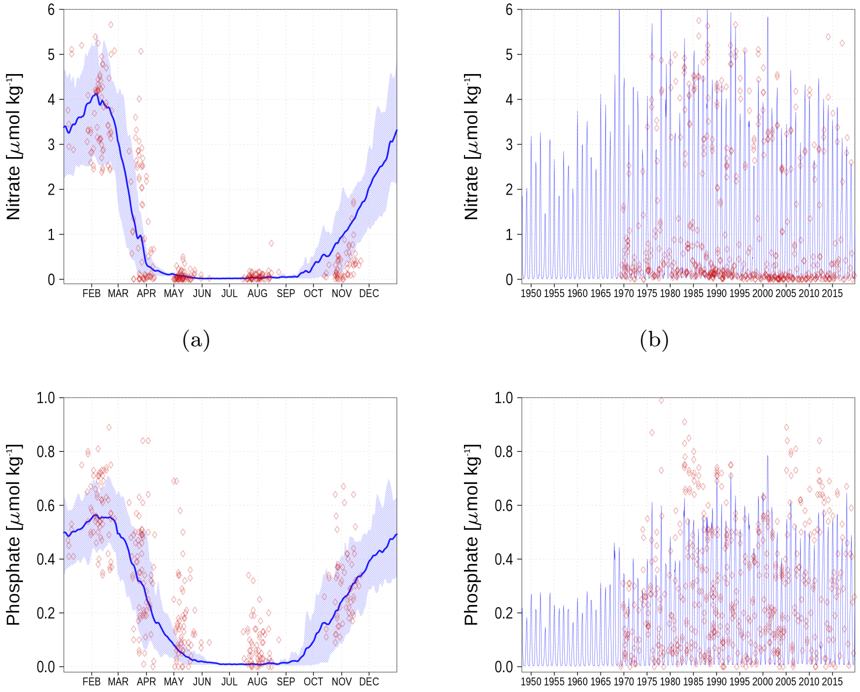

(a) (b)

(c) (d)

Figure A1. Surface nutrients concentrations at station BY1 (Fig. 6). Blue color are model simulations and observations are shown as red diamonds. The blue shaded area is the range between the 10th and 90th percentile. Opacity of the red diamonds reflects the frequency of observations. a: Nitrate climatology, b: Nitrate time series, c: Phosphate climatology, d: Phosphate time series.

Appendix A: Model performance

In this section, we compare model results with observations in order to verify the model performance for biogeochemical variables.

A1 Surface nutrients concentrations

We demonstrate the model performance for surface nutrients at 6 stations and regions, respectively in Figs. A1–A6. For the climatology, we have chosen the time range 1990 until 2018 since observations for some stations are sparse for the period before 1990. Data for nutrients and oxygen have been extracted from the ICES database (see *code and data availability*).

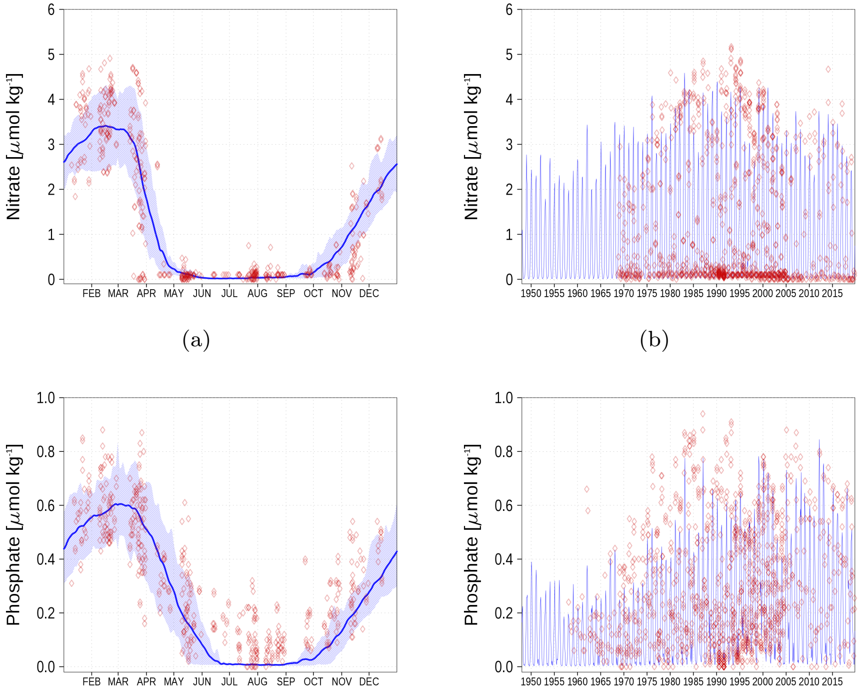

(a) (b)

(c) (d)

Figure A2. Surface nutrients concentrations at station BY5 (Fig. 6). Blue color are model simulations and observations are shown as red diamonds. The blue shaded area is the range between the 10th and 90th percentile. Opacity of the red diamonds reflects the frequency of observations. a: Nitrate climatology, b: Nitrate time series, c: Phosphate climatology, d: Phosphate time series.

A2 Oxygen

In Fig. A7, we show oxygen concentration close to the sea floor at six different stations together with observations. Hydrogen sulfide is represented as negative oxygen equivalents. The simulated oxygen concentration reasonably follows the observations. An exception is the underestimation in the Gulf of Bothnia (Fig. A7d and e). Beginning in 1970, the simulated values start to deviate from the field data.

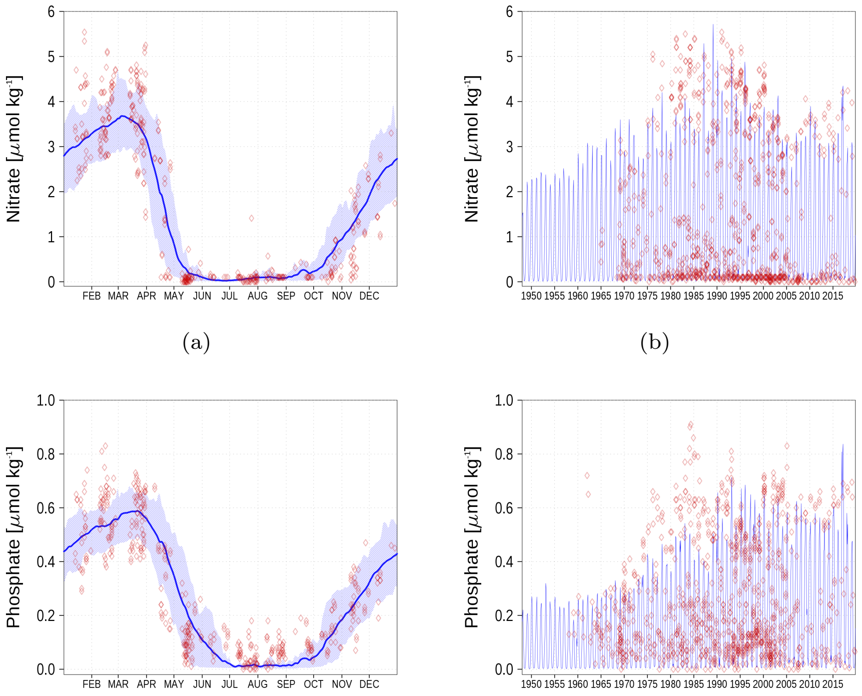

(a) (b)

(c) (d)

Figure A3. Surface nutrients concentrations at station BY15 (Fig. 6). Blue color are model simulations and observations are shown as red diamonds. The blue shaded area is the range between the 10th and 90th percentile. Opacity of the red diamonds reflects the frequency of observations. a: Nitrate climatology, b: Nitrate time series, c: Phosphate climatology, d: Phosphate time series.

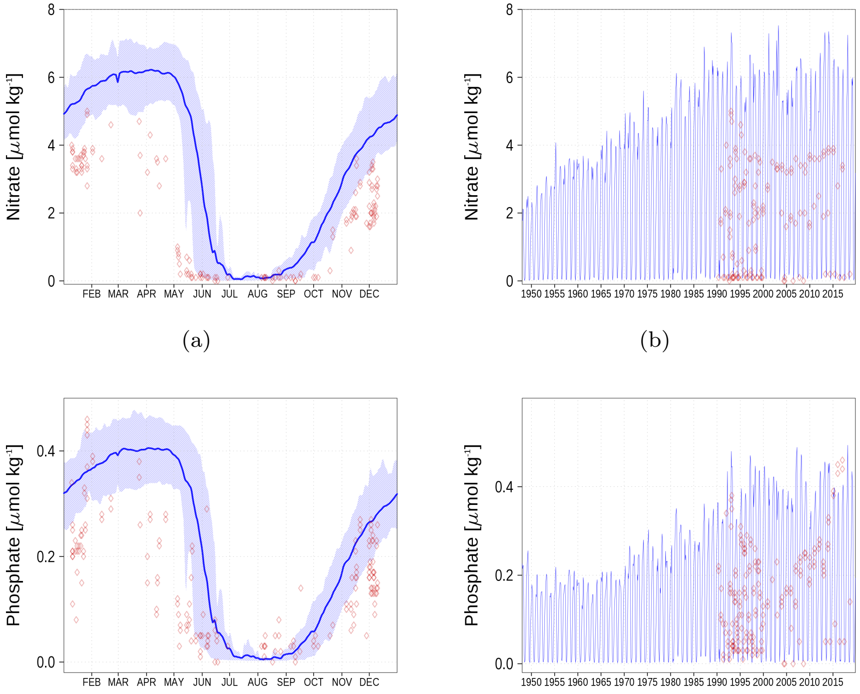

(a) (b)

(c) (d)

Figure A4. Surface nutrients concentrations at station F26 (Fig. 6). Blue color are model simulations and observations are shown as red diamonds. The blue shaded area is the range between the 10th and 90th percentile. Opacity of the red diamonds reflects the frequency of observations. a: Nitrate climatology, b: Nitrate time series, c: Phosphate climatology, d: Phosphate time series.

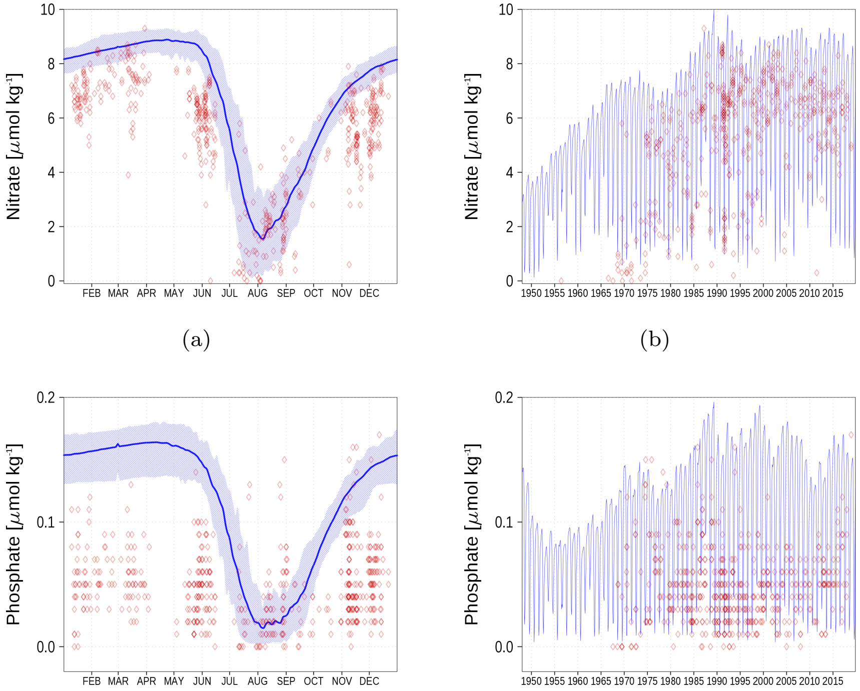

(a) (b)

(c) (d)

Figure A5. Surface nutrients concentrations in the Bothnian Bay (BoB, Fig. 6). Blue color are model simulations and observations are shown as red diamonds. The blue shaded area is the range between the 10th and 90th percentile. Opacity of the red diamonds reflects the frequency of observations. a: Nitrate climatology, b: Nitrate time series, c: Phosphate climatology, d: Phosphate time series.

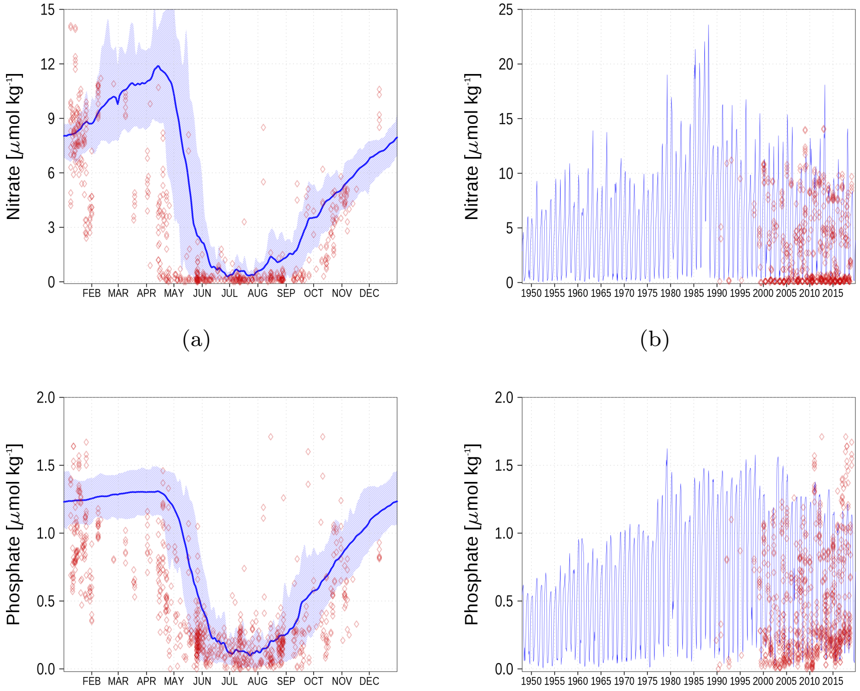

(a) (b)

(c) (d)

Figure A6. Surface nutrients concentrations at station Gulf of Finland (GoF, Fig. 6). Blue color are model simulations and observations are shown as red diamonds. The blue shaded area is the range between the 10th and 90th percentile. Opacity of the red diamonds reflects the frequency of observations. a: Nitrate climatology, b: Nitrate time series, c: Phosphate climatology, d: Phosphate time series.

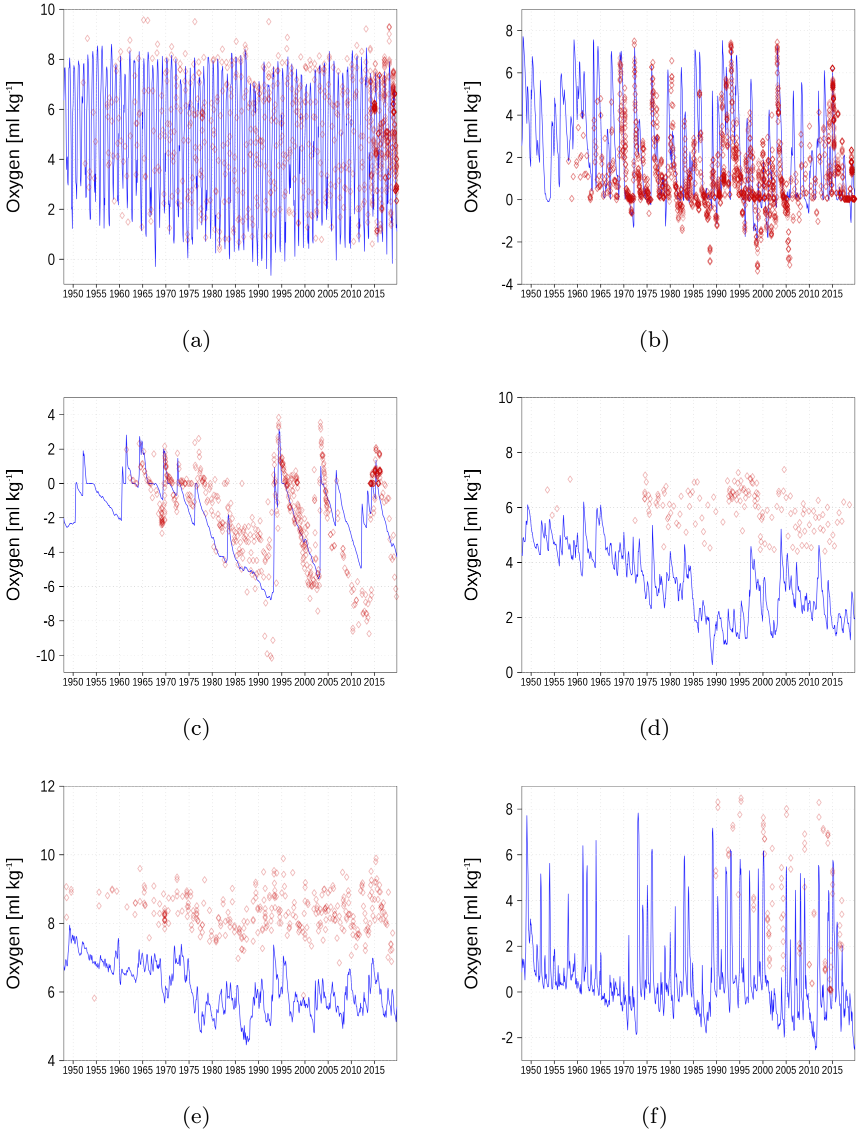

(a) (b)

(c) (d)

(e) (f)

Figure A7. Bottom oxygen concentration at six stations in the Baltic Sea. Negative values denote the presence of hydrogen sulfide. Blue color are model simulations and observations are shown as red diamonds. Opacity of the red diamonds reflects the frequency of observations. a: BY1,b: BY5, c: BY15, d: F26, e: BoB, f: GoF (Fig. 6).

Appendix B: ERGOM Documentation

Contents

B1 Introduction

This is an automatically generated description of the ecosystem model ERGOM version CDOM 1.2 . Model formulation is provided by text files in compliance with the rules of the Code Generation Tool (CGT) by Hagen Radtke (see www.ergom.net).

The ecosystem state variables are concentrations of several substances and are called tracers. In the host ocean model they undergo physical advection, turbulent diffusion or vertical motion as sinking or rising. The ecosystem model component defines their sources or sinks from element turnover through the ecosystem. They are defined and described in Sec. B2.

The following Sec. B3 is the main part of this model description document. It describes the processes changing the tracer concentrations over time. Analogously to chemical processes, two components describe a process:

- A process equation which describes the transformation from precursors (on the left-hand side) to products (on the right-hand side), and
- a turnover rate, describing how fast the process runs.

The time tendency of a tracer can then easily be determined by multiplying the process turnover rate with the stoichiometric ratio in which it consumes or produces the tracer according to the reaction equation.

The document structure reflects the different process types. All processes of one type (e.g. phytoplankton assimilation) are listed together with all their constants and auxiliary variables they depend on. For readability, some constants, such as stoichiometric ratios, will occur repeatedly. We take this compromise for the sake of readability, keeping all information required to understand a specific process in its own section.

For completeness, the tracer equations are given in Sec B4. However, we consider this as a supplementary chapter and suggest to study the model details from Sec. B3 instead.

B2 Description of model state variables (tracers)

Tracers in the water column only	
`t_n2`	**dissolved molecular nitrogen (mol/kg)**
`t_o2`	**dissolved oxygen (mol/kg)**
`t_dic`	**dissolved inorganic carbon, treated as carbon dioxide (mol/kg)**
`t_nh4`	**ammonium (mol/kg)**
`t_no3`	**nitrate (mol/kg)**
`t_po4`	**phosphate (mol/kg)**
`t_spp`	**small-cell phytoplankton (mol/kg)**
opacity =	58.0 m^2/mol
`t_zoo`	**zooplankton (mol/kg)**
`t_h2s`	**hydrogen sulfide (mol/kg)**
`t_sul`	**sulfur (mol/kg)**
`t_alk`	**total alkalinity (mol/kg)**
`t_lip`	**limnic phytoplankton (mol/kg)**
opacity =	58.0 m^2/mol
`t_doc`	**dissolved organic carbon (mol/kg)**
`t_dop`	**phosphorus in dissolved organic carbon in Redfield ratio (mol/kg)**
`t_don`	**nitrogen in dissolved organic carbon in Redfield ratio (mol/kg)**
opacity =	12.6 m^2/mol

continued on next page...

Tracers in the water column only, continued from previous page

`t_cdom`	**colored dissolved organic carbon (mol/kg)**
`t_lpp`	**large-cell phytoplankton (mol/kg)**
vertical speed =	-0.5 m/day
opacity =	58.0 m^2/mol
`t_ipw`	**suspended iron phosphate (mol/kg)**
vertical speed =	-1.0 m/day
`t_cya`	**diazotroph cyanobacteria (mol/kg)**
vertical speed =	1.0 m/day
opacity =	58.0 m^2/mol
`t_det`	**detritus (mol/kg)**
vertical speed =	-4.5 m/day
opacity =	53.2 m^2/mol
`t_poc`	**particulate organic carbon (mol/kg)**
vertical speed =	w_poc_var m/day
`t_pocp`	**phosphorus in particulate organic carbon in Redfield ratio (mol/kg)**
vertical speed =	-0.1 m/day
`t_pocn`	**nitrogen in particulate organic carbon in Redfield ratio (mol/kg)**
vertical speed =	-0.1 m/day

end of table **Tracers in the water column only**

Tracers in water and pore water

end of table **Tracers in water and pore water**

Tracers in fluff and sediment	
`t_sed`	**sediment detritus (mol/m^2)**
`t_ips`	**iron phosphate in sediment (mol/m^2)**
`t_sed_poc`	**sediment particular carbon (mol/m^2)**
`t_sed_pocn`	**sediment particular organic N+C (mol/m^2)**
`t_sed_pocp`	**sediment particular organic P+C (mol/m^2)**

end of table **Tracers in fluff and sediment**

B3 Description of model processes, ordered by process type

5

B3.1 Process type BGC/benthic/bioresuspension

Processes

bio resuspension of sedimentary detritus (sediment only) [mol/m^2/day]

`t_sed -> t_det`

`p_sed_biores_det =` `(r_biores*exp(-0.02*cgt_bottomdepth)*sed_active)*lim_t_o2_6*lim_t_sed_21`

bio resuspension of iron PO4 (sediment only) [mol/m^2/day]

`t_ips -> t_ipw`

`p_ips_biores_ipw =` `(r_biores*exp(-0.02*cgt_bottomdepth)*t_ips)*lim_t_o2_6*lim_t_ips_23`

bio resuspension of sedimentary poc (sediment only) [mol/m^2/day]

`t_sed_poc -> t_poc`

continued on next page...

Processes, continued from previous page

`p_sed_biores_poc =` `(r_biores*exp(-0.02*cgt_bottomdepth)*poc_active)*lim_t_o2_6*lim_t_sed_poc_22`

bio resuspension of sedimentary pocn (sediment only) [mol/m^2/day]

`t_sed_pocn -> t_pocn`

`p_sed_biores_pocn =` `(r_biores*exp(-0.02*cgt_bottomdepth)*pocn_active)*lim_t_o2_6*lim_t_sed_pocn_27`

bio resuspension of sedimentary pocp (sediment only) [mol/m^2/day]

`t_sed_pocp -> t_pocp`

`p_sed_biores_pocp =` `(r_biores*exp(-0.02*cgt_bottomdepth)*pocp_active)*lim_t_o2_6*lim_t_sed_pocp_28`

end of table **Processes**

Auxiliary variables

total carbon in sediment layer [mol/m2]**

`sed_tot =` `t_sed*rfr_c + t_sed_poc + t_sed_pocn*rfr_c + t_sed_pocp*rfr_cp`

total carbon in active sediment layer [mol/m2]**

`sed_tot_active =` `max(0.0,min(sed_tot,sed_max*rfr_c))`

detritus in active sediment layer [mol/m2]**

`sed_active =` `sed_tot_active * t_sed/sed_tot`

poc in active sediment layer [mol/m2]**

`poc_active =` `sed_tot_active * t_sed_poc/sed_tot`

pocn in active sediment layer [mol/m2]**

`pocn_active =` `sed_tot_active * t_sed_pocn/sed_tot`

continued on next page…

Auxiliary variables, continued from previous page

pocp in active sediment layer [mol/m2]**

`pocp_active =          sed_tot_active * t_sed_pocp/sed_tot`

end of table **Auxiliary variables**

Constants

oxygen half-saturation constant for recycling of sediment detritus using oxygen [mol/kg]

`o2_min_sed_resp =      0.000064952`

bio-resuspension rate [1/day]

`r_biores =             0.015`

redfield ratio C/N

`rfr_c =                6.625`

redfield ratio C/P

`rfr_cp =               106.0`

maximum sediment detritus concentration that feels erosion [mol/m2]**

`sed_max =              1.0`

end of table **Constants**

Process limitation factors

`lim_t_o2_6 =           t_o2*t_o2/(t_o2*t_o2+o2_min_sed_resp*o2_min_sed_resp)`

`lim_t_sed_21 =         theta(t_sed-0.0)`

`lim_t_ips_23 =         theta(t_ips-0.0)`

continued on next page. . .

Process limitation factors, continued from previous page

`lim_t_sed_poc_22 =   theta(t_sed_poc-0.0)`

`lim_t_sed_pocn_27 =   theta(t_sed_pocn-0.0)`

`lim_t_sed_pocp_28 =   theta(t_sed_pocp-0.0)`

end of table **Process limitation factors**

B3.2 Process type BGC/benthic/mineralisation

Processes

recycling of sedimentary detritus to ammonium using oxygen (respiration) (sediment only) [mol/m^2/day]

`t_sed + 6.625*t_o2 + 0.8125*h3oplus -> t_nh4 + rfr_p*t_po4 + rfr_c*t_dic + 7.4375*h2o`

`p_sed_resp_nh4 =   (lr_sed_rec*sed_active)*lim_t_sed_21*lim_t_o2_2`

coupled nitrification and denitrification after mineralization of detritus in oxic sediments (sediment only) [mol/m^2/day]

`t_nh4 + 0.75*t_o2 -> 0.5*h2o + h3oplus + 0.5*t_n2`

`p_nh4_nitdenit_n2 =   (frac_denit_sed*(p_sed_resp_nh4+p_sed_pocn_resp)*theta(t_o2-5.0e-6))*lim_t_nh4_11*lim_t_o2_2`

recycling of sedimentary detritus to ammonium using nitrate (denitrification) (sediment only) [mol/m^2/day]

`t_sed + 6.1125*h3oplus + 5.3*t_no3 -> rfr_c*t_dic + rfr_p*t_po4 + t_nh4 + 2.65*t_n2 + 15.3875*h2o`

`p_sed_denit_nh4 =   (lr_sed_rec*sed_active)*(1.0-lim_t_o2_2)*lim_t_no3_3*lim_t_sed_21`

recycling of sedimentary detritus to ammonium using sulfate (sulfate reduction) (sediment only) [mol/m^2/day]

continued on next page. . .

Processes, continued from previous page

```
t_sed + 3.3125*so4 + 7.4375*h3oplus -> t_nh4 + rfr_p*t_po4 + rfr_c*t_dic + 3.3125*
t_h2s + 14.0625*h2o
p_sed_sulf_nh4 =      (lr_sed_rec*sed_active)*(1.0-lim_t_o2_2)*(1.0-lim_t_no3_3)*
                      lim_t_sed_21
```

recycling of sedimentary poc to dic using oxygen (respiration) (sediment only) [mol/m^2/day]

```
t_sed_poc + t_o2 -> t_dic + h2o
p_sed_poc_resp =      (lr_sed_poc_rec*poc_active)*lim_t_sed_poc_22*lim_t_o2_2
```

recycling of sedimentary poc to dic using nitrate (denitrification) (sediment only) [mol/m^2/day]

```
0.8*t_no3 + 0.8*h3oplus + t_sed_poc -> 2.2*h2o + 0.4*t_n2 + t_dic
p_sed_poc_denit =     (lr_sed_poc_rec*poc_active)*(1.0-lim_t_o2_2)*lim_t_no3_3*
                      lim_t_sed_poc_22
```

recycling of sedimentary poc to dic using sulfate (sulfate reduction) (sediment only) [mol/m^2/day]

```
h3oplus + 0.5*so4 + t_sed_poc -> 2.0*h2o + 0.5*t_h2s + t_dic
p_sed_poc_sulf =      (lr_sed_poc_rec*poc_active)*(1.0-lim_t_o2_2)*(1.0-lim_t_no3_3)*
                      lim_t_sed_poc_22
```

recycling of sedimentary pocn to dic and NH4 using oxygen (respiration) (sediment only) [mol/m^2/day]

```
6.625*t_o2 + t_sed_pocn + 0.5*h3oplus -> 6.625*h2o + 6.625*t_dic + t_nh4 + 0.5*ohminus
p_sed_pocn_resp =     (lr_sed_rec*pocn_active)*lim_t_o2_2*lim_t_sed_pocn_27
```

recycling of sedimentary pocp to dic and PO4 using oxygen (respiration) (sediment only) [mol/m^2/day]

```
3*h2o + t_sed_pocp + 106*t_o2 -> 106*h2o + t_po4 + 106*t_dic + 3*h3oplus
p_sed_pocp_resp =     (lr_sed_rec*pocp_active)*lim_t_sed_pocp_28*lim_t_o2_2
```

continued on next page. . .

Processes, continued from previous page

recycling of sedimentary pocn to dic and NH4 using nitrate (denitrification) (sediment only) [mol/m^2/day]

```
t_sed_pocn + 5.3*t_no3 + 5.8*h3oplus -> 6.625*t_dic + t_nh4 + 2.65*t_n2 + 14.575*h2o +
0.5*ohminus
p_sed_pocn_denit =    (lr_sed_rec*pocn_active)*(1.0-lim_t_o2_2)*lim_t_no3_3*
                      lim_t_sed_pocn_27
```

recycling of sedimentary pocp to dic and PO4 using nitrate (denitrification) (sediment only) [mol/m^2/day]

```
t_sed_pocp + 3*ohminus + 84.8*h3oplus + 84.8*t_no3 -> 106*t_dic + t_po4 + 42.4*t_n2 +
236.2*h2o
p_sed_pocp_denit =    (lr_sed_rec*pocp_active)*(1.0-lim_t_o2_2)*lim_t_no3_3*
                      lim_t_sed_pocp_28
```

recycling of sedimentary pocn to dic and NH4 using sulfate (sulfate reduction) (sediment only) [mol/m^2/day]

```
7.125*h3oplus + 3.3125*SO4 + t_pocn -> 0.5*ohminus + 13.25*H2O + 3.3125*t_h2s + t_nh4
+ 6.625*t_dic
p_sed_pocn_sulf =     (lr_sed_rec*pocn_active)*(1.0-lim_t_o2_2)*(1.0-lim_t_no3_3)*
                      lim_t_pocn_14
```

recycling of sedimentary pocp to dic and PO4 using sulfate (sulfate reduction) (sediment only) [mol/m^2/day]

```
t_pocp + 53*so4 + 106*h3oplus + 3*ohminus -> 106*t_dic + 215*h2o + 53*t_h2s + t_po4
p_sed_pocp_sulf =     (lr_sed_rec*pocp_active)*(1.0-lim_t_o2_2)*(1.0-lim_t_no3_3)*
                      lim_t_pocp_13
```

coupled nitrification and denitrification after mineralization of pocn-detritus in oxic sediments (sediment only) [mol/m^2/day]

```
t_nh4 + 0.75*t_o2 -> 0.5*h2o + h3oplus + 0.5*t_n2
```

continued on next page…

Processes, continued from previous page

`(frac_denit_sed*p_sed_pocn_resp*theta(t_o2-5.0e-6))*lim_t_nh4_11*`

`p_nh4_nitdenit_pocn_n2lim_t_o2_2`

`=`

end of table **Processes**

Auxiliary variables

fraction of ammonium that is immediately nitrified and denitrified after remineralization in oxic sediments

`frac_denit_sed =      frac_denit_scal*(0.5+0.5*exp(-0.01*cgt_bottomdepth))`

total carbon in sediment layer [mol/m2]**

`sed_tot =             t_sed*rfr_c + t_sed_poc + t_sed_pocn*rfr_c + t_sed_pocp*rfr_cp`

total carbon in active sediment layer [mol/m2]**

`sed_tot_active =      max(0.0,min(sed_tot,sed_max*rfr_c))`

detritus in active sediment layer [mol/m2]**

`sed_active =          sed_tot_active * t_sed/sed_tot`

recycling rate of sediment detritus, limited by oxygen [1/d]

`lr_sed_rec =          r_sed_rec*exp(q10_sed_rec*cgt_temp)*(1.0-reduced_rec*theta(2*t_h2s-t_o2))`

recycling rate of sediment POC, limited by oxygen [1/d]

`lr_sed_poc_rec =      r_sed_poc_rec*exp(q10_sed_rec*cgt_temp)*(1.0-reduced_rec*theta(2*t_h2s-t_o2))`

poc in active sediment layer [mol/m2]**

`poc_active =          sed_tot_active * t_sed_poc/sed_tot`

continued on next page…

pocn in active sediment layer [mol/m2]**

`pocn_active =         sed_tot_active * t_sed_pocn/sed_tot`

pocp in active sediment layer [mol/m2]**

`pocp_active =         sed_tot_active * t_sed_pocp/sed_tot`

end of table **Auxiliary variables**

Constants

nitrate half-saturation concentration for denitrification in the water column [mol/kg]

`no3_min_sed_denit =   1.423E-7`

q10 rule factor for detritus recycling in the sediment [1/K]

`q10_sed_rec =         0.175`

maximum recycling rate for sedimentary detritus [1/d]

`r_sed_rec =           0.003`

maximum recycling rate for sedimentary POC [1/d]

`r_sed_poc_rec =       0.0005`

redfield ratio C/N

`rfr_c =               6.625`

redfield ratio P/N

`rfr_p =               0.0625`

redfield ratio C/P

`rfr_cp =              106.0`

maximum sediment detritus concentration that feels erosion [mol/m2]**

continued on next page…

Constants, continued from previous page

`sed_max =             1.0`

scaling frac_denit_sed

`frac_denit_scal =     1.0`

decrease recycling in sed under anoxia by reduce_rec

`reduced_rec =         0.8`

end of table **Constants**

Process limitation factors

`lim_t_o2_2 =          theta(t_o2-0.0)`

`lim_t_nh4_11 =        theta(t_nh4-0.0)`

`lim_t_no3_3 =         t_no3*t_no3/(t_no3*t_no3+no3_min_sed_denit*no3_min_sed_denit)`

`lim_t_sed_21 =        theta(t_sed-0.0)`

`lim_t_sed_poc_22 =    theta(t_sed_poc-0.0)`

`lim_t_sed_pocn_27 =   theta(t_sed_pocn-0.0)`

`lim_t_sed_pocp_28 =   theta(t_sed_pocp-0.0)`

`lim_t_pocp_13 =       theta(t_pocp-0.0)`

`lim_t_pocn_14 =       theta(t_pocn-0.0)`

end of table **Process limitation factors**

Processes

retention of phosphate in the sediment under oxic conditions (sediment only) [mol/m^2/day]

`rfr_p*t_po4 + rfr_p*fe3plus -> rfr_p*t_ips`

`p_po4_retent_ips =    (p_sed_resp_nh4*frac_po4retent)*lim_t_o2_4*lim_t_po4_10`

liberation of phosphate from the sediment under anoxic conditions (sediment only) [mol/m^2/day]

`t_ips -> fe3plus + t_po4`

`p_ips_liber_po4 =    (t_ips*r_ips_liber)*lim_t_h2s_5*lim_t_ips_23`

end of table **Processes**

Auxiliary variables

fraction of phosphate which is retained as iron-bound phosphate instead of being released after mineralization in the sediment [1]

`frac_po4retent =    ret_po4_1 + ret_po4_2*theta(cgt_latitude-60.75) + ret_po4_3* theta(cgt_latitude-63.75)`

end of table **Auxiliary variables**

Constants

minimum h2s concentration for liberation of iron phosphate from the sediment [mol/kg]

`h2s_min_po4_liber =   1.0E-6`

oxygen half-saturation concentration for retension of phosphate during sediment denitrification [mol/kg]

`o2_min_po4_retent =   0.0000375`

continued on next page...

Constants, continued from previous page

PO4 liberation rate under anoxic conditions [1/day]

`r_ips_liber =` `0.1`

redfield ratio P/N

`rfr_p =` `0.0625`

PO4 retension in oxic sediments

`ret_po4_1 =` `0.1`

additional PO4 retension in oxic sediments of the Bothnian Sea

`ret_po4_2 =` `0.5`

additional PO4 retension in oxic sediments of the Bothnian Sea

`ret_po4_3 =` `0.13`

end of table **Constants**

Process limitation factors

`lim_t_o2_4 =` `t_o2*t_o2/(t_o2*t_o2+o2_min_po4_retent*o2_min_po4_retent)`

`lim_t_po4_10 =` `theta(t_po4-0.0)`

`lim_t_h2s_5 =` `theta(t_h2s-h2s_min_po4_liber)`

`lim_t_ips_23 =` `theta(t_ips-0.0)`

end of table **Process limitation factors**

5

B3.4 Process type BGC/pelagic/mineralisation

recycling of POC using nitrate (denitrification) [mol/kg/day]

```
t_poc + 0.8*t_no3 + 0.8*h3oplus -> t_dic + 2.2*h2o + 0.4*t_n2
p_poc_denit =         (t_poc*r_poc_rec*exp(q10_det_rec*cgt_temp))*(1.0-lim_t_o2_0)*
                      lim_t_no3_1*lim_t_poc_12
```

Mineralization of POC, e-acceptor sulfate (sulfate reduction) [mol/kg/day]

```
t_poc + 0.5*so4 + h3oplus -> t_dic + 0.5*t_h2s + 2*h2o
p_poc_sulf =          (t_poc*r_poc_rec*exp(q10_det_rec*cgt_temp))*(1.0-lim_t_o2_0)*
                      (1.0-lim_t_no3_1)*lim_t_poc_12
```

respiration of POCP [mol/kg/day]

```
106*t_o2 + t_pocp + 3*H2O -> 106*t_dic + t_po4 + 106*H2O + 3*h3oplus
p_pocp_resp =         (t_pocp * lr_pocp * exp(q10_det_rec * cgt_temp))*lim_t_o2_0*
                      lim_t_pocp_13
```

recycling of POC using nitrate (denitrification) [mol/kg/day]

```
3*ohminus + 84.8*h3oplus + 84.8*t_no3 + t_pocp -> t_po4 + 42.4*t_n2 + 236.2*H2O + 106*
t_dic
p_pocp_denit =        (t_pocp*r_pocp_rec*exp(q10_det_rec*cgt_temp))*(1.0-lim_t_o2_0)*
                      lim_t_no3_1*lim_t_pocp_13
```

Mineralization of POC, e-acceptor sulfate (sulfate reduction) [mol/kg/day]

```
t_pocp + 53*so4 + 106*h3oplus + 3*ohminus -> 106*t_dic + 215*h2o + 53*t_h2s + t_po4
p_pocp_sulf =         (t_pocp*r_pocp_rec*exp(q10_det_rec*cgt_temp))*(1.0-lim_t_o2_0)*
                      (1.0-lim_t_no3_1)*lim_t_pocp_13
```

respiration of POCN [mol/kg/day]

```
0.5*h3oplus + 6.625*t_o2 + t_pocn -> 0.5*ohminus + 6.625*H2O + t_nh4 + 6.625*t_dic
p_pocn_resp =         (t_pocn * lr_pocn * exp(q10_det_rec * cgt_temp))*lim_t_o2_0*
                      lim_t_pocn_14
```

recycling of POCN using nitrate (denitrification) [mol/kg/day]

continued on next page. . .

Processes, continued from previous page

```
5.8*h3oplus + 5.3*t_no3 + t_pocn -> 0.5*ohminus + 14.575*H2O + 2.65*t_n2 + t_nh4 +
6.625*t_dic
p_pocn_denit =       (t_pocn*r_pocn_rec*exp(q10_det_rec*cgt_temp))*(1.0-lim_t_o2_0)*
                     lim_t_no3_1*lim_t_pocn_14
```

Mineralization of POCN, e-acceptor sulfate (sulfate reduction) [mol/kg/day]

```
t_pocn + 3.3125*SO4 + 7.125*h3oplus -> 6.625*t_dic + t_nh4 + 3.3125*t_h2s + 13.25*H2O
+ 0.5*ohminus
p_pocn_sulf =        (t_pocn*r_pocn_rec*exp(q10_det_rec*cgt_temp))*(1.0-lim_t_o2_0)*
                     (1.0-lim_t_no3_1)*lim_t_pocn_14
```

recycling of detritus using oxygen (respiration) [mol/kg/day]

```
t_det + 6.625*t_o2 + 0.8125*h3oplus -> t_nh4 + rfr_p*t_po4 + rfr_c*t_dic + 7.4375*h2o
p_det_resp_nh4 =     (t_det*r_det_rec*exp(q10_det_rec*cgt_temp))*lim_t_o2_0*
                     lim_t_det_20
```

recycling of detritus using nitrate (denitrification) [mol/kg/day]

```
t_det + 5.3*t_no3 + 6.1125*h3oplus -> 2.65*t_n2 + 15.3875*h2o + t_nh4 + rfr_p*t_po4 +
rfr_c*t_dic
p_det_denit_nh4 =    (t_det*r_det_rec*exp(q10_det_rec*cgt_temp))*(1.0-lim_t_o2_0)*
                     lim_t_no3_1*lim_t_det_20
```

recycling of detritus using sulfate (sulfate reduction) [mol/kg/day]

```
7.4375*h3oplus + 3.3125*so4 + t_det -> 14.0625*h2o + 3.3125*t_h2s + rfr_c*t_dic +
rfr_p*t_po4 + t_nh4
p_det_sulf_nh4 =     (t_det*r_det_rec*exp(q10_det_rec*cgt_temp))*(1.0-lim_t_o2_0)*
                     (1.0-lim_t_no3_1)*lim_t_det_20
```

recycling of DOC using nitrate (denitrification) [mol/kg/day]

```
t_doc + 0.8*t_no3 + 0.8*h3oplus -> t_dic + 2.2*h2o + 0.4*t_n2
p_doc_denit =        (t_doc*r_doc_rec*exp(q10_det_rec*cgt_temp))*(1.0-lim_t_o2_0)*
                     lim_t_no3_1*lim_t_doc_29
```

continued on next page…

Mineralization of DOC, e-acceptor sulfate (sulfate reduction) [mol/kg/day]

```
t_doc + 0.5*so4 + h3oplus -> t_dic + 0.5*t_h2s + 2*h2o
p_doc_sulf =          (t_doc*r_doc_rec*exp(q10_det_rec*cgt_temp))*(1.0-lim_t_o2_0)*
                      (1.0-lim_t_no3_1)*lim_t_doc_29
```

respiration of DOP [mol/kg/day]

```
3*H2O + t_dop + 106*t_o2 -> 3*h3oplus + 106*H2O + t_po4 + 106*t_dic
p_dop_resp =          (t_dop * lr_dop * exp(q10_det_rec * cgt_temp))*lim_t_o2_0*
                      lim_t_dop_30
```

recycling of DOP using nitrate (denitrification) [mol/kg/day]

```
t_dop + 84.8*t_no3 + 84.8*h3oplus + 3*ohminus -> 106*t_dic + 236.2*H2O + 42.4*t_n2 +
t_po4
p_dop_denit =         (t_dop*r_dop_rec*exp(q10_det_rec*cgt_temp))*(1.0-lim_t_o2_0)*
                      lim_t_no3_1*lim_t_dop_30
```

Mineralization of DOP, e-acceptor sulfate (sulfate reduction) [mol/kg/day]

```
3*ohminus + 106*h3oplus + 53*so4 + t_dop -> t_po4 + 53*t_h2s + 215*h2o + 106*t_dic
p_dop_sulf =          (t_dop*r_dop_rec*exp(q10_det_rec*cgt_temp))*(1.0-lim_t_o2_0)*
                      (1.0-lim_t_no3_1)*lim_t_dop_30
```

respiration of DON [mol/kg/day]

```
0.5*h3oplus + 6.625*t_o2 + t_don -> 0.5*ohminus + 6.625*H2O + t_nh4 + 6.625*t_dic
p_don_resp =          (t_don * lr_don * exp(q10_det_rec * cgt_temp))*lim_t_o2_0*
                      lim_t_don_31
```

recycling of DON using nitrate (denitrification) [mol/kg/day]

```
5.8*h3oplus + 5.3*t_no3 + t_don -> 0.5*ohminus + 14.575*H2O + 2.65*t_n2 + t_nh4 +
6.625*t_dic
p_don_denit =         (t_don*r_don_rec*exp(q10_det_rec*cgt_temp))*(1.0-lim_t_o2_0)*
                      lim_t_no3_1*lim_t_don_31
```

continued on next page...

Processes, continued from previous page

Mineralization of DON, e-acceptor sulfate (sulfate reduction) [mol/kg/day]

```
7.125*h3oplus + 3.3125*SO4 + t_don -> 0.5*ohminus + 13.25*H2O + 3.3125*t_h2s + t_nh4 +
6.625*t_dic
p_don_sulf =          (t_don*r_don_rec*exp(q10_det_rec*cgt_temp))*(1.0-lim_t_o2_0)*
                      (1.0-lim_t_no3_1)*lim_t_don_31
```

decay of cdom due to light [mol/kg/day]

```
t_cdom ->
p_cdom_decay =        (t_cdom*r_cdom_decay*cgt_light/r_cdom_light)*lim_t_cdom_32
```

end of table **Processes**

Auxiliary variables

dissolved inorganic nitrogen [mol/kg]

```
din =                 t_no3+t_nh4
```

squared DIN [mol2/kg2]

```
din_sq =              din*din
```

squared phosphate [mol2/kg**2]**

```
po4_sq =              t_po4*t_po4
```

modifies pocp recycling towards Redfield ratio if PO4 is depleted

```
ref_p_sw =            (1 - (po4_sq/(rfr_p*din_min_lpp*rfr_p*din_min_lpp+po4_sq)))/(1+
                      exp(6.0*(1-din/(t_po4/rfr_p+epsilon))))
```

modifies pocn recycling towards Redfield ratio if DIN is depleted

```
ref_n_sw =            (1 - (din_sq/(din_min_lpp*din_min_lpp+din_sq)))/(1+exp(6.0*(1-
                      t_po4/rfr_p/(din+epsilon))))
```

continued on next page...

Auxiliary variables, continued from previous page

add an additional POCP recycling if PO4 below Redfield but sufficient DIN

```
lr_pocp =            r_pocp_rec*(1 + fac_enh_rec*ref_p_sw)
```

add an additional DOP recycling if PO4 is below Redfield but sufficient DIN

```
lr_dop =             r_dop_rec*(1 + fac_enh_rec*ref_p_sw)
```

add an additional POCN recycling if DIN below Redfield but sufficient PO4

```
lr_pocn =            r_pocn_rec*(1 + fac_enh_rec*ref_n_sw)
```

add an additional DON recycling if DIN below Redfield but sufficient PO4

```
lr_don =             r_don_rec*(1 + fac_enh_rec*ref_n_sw)
```

end of table **Auxiliary variables**

Constants

DIN half saturation constant for large-cell phytoplankton growth [mol/kg]

```
din_min_lpp =        1.0E-6
```

no division by 0

```
epsilon =            4.5E-17
```

minimum no3 concentration for recycling of detritus using nitrate (denitrification)

```
no3_min_det_denit =  1.0E-9
```

oxygen half-saturation constant for detritus recycling [mol/kg]

```
o2_min_det_resp =    1.0E-6
```

q10 rule factor for recycling [1/K]

```
q10_det_rec =        0.15
```

recycling rate (detritus to ammonium) at 0°C [1/day]

continued on next page…

Constants, continued from previous page

r_det_rec = 0.003

redfield ratio C/N

rfr_c = 6.625

redfield ratio P/N

rfr_p = 0.0625

recycling rate (poc to dic) at 0°C [1/day]

r_poc_rec = 0.003

recycling rate (pocp to dic and po4) at 0°C [1/day]

r_pocp_rec = 0.002

recycling rate (pocn to dic and nh4) at 0°C [1/day]

r_pocn_rec = 0.002

enhance recyclig of DON,POCN/DOP,POCP in case of limiting DIN/DIP

fac_enh_rec = 10.0

recycling rate (doc to dic) at 0°C [1/day]

r_doc_rec = 0.001

recycling rate (don to dic and NH4) at 0°C [1/day]

r_don_rec = 0.001

recycling rate (dop to dic and PO4) at 0°C [1/day]

r_dop_rec = 0.001

decay rate of cdom

r_cdom_decay = 0.0035

continued on next page…

Constants, continued from previous page

PAR intensity controling CDOM decay

`r_cdom_light = 40.0`

end of table **Constants**

Process limitation factors

`lim_t_o2_0 = 1.0-exp(-t_o2/o2_min_det_resp)`

`lim_t_no3_1 = 1.0-exp(-t_no3/no3_min_det_denit)`

`lim_t_doc_29 = theta(t_doc-0.0)`

`lim_t_dop_30 = theta(t_dop-0.0)`

`lim_t_don_31 = theta(t_don-0.0)`

`lim_t_cdom_32 = theta(t_cdom-0.0)`

`lim_t_det_20 = theta(t_det-0.0)`

`lim_t_poc_12 = theta(t_poc-0.0)`

`lim_t_pocp_13 = theta(t_pocp-0.0)`

`lim_t_pocn_14 = theta(t_pocn-0.0)`

end of table **Process limitation factors**

B3.5 Process type BGC/pelagic/phytoplankton

Processes

assimilation of nitrate by large-cell phytoplankton [mol/kg/day]

```
t_no3 + rfr_p*t_po4 + rfr_c*t_dic + 6.4375*h2o + 1.1875*h3oplus -> t_lpp + 8.625*t_o2
p_no3_assim_lpp =     (lpp_plus_lpp0*lr_assim_lpp*t_no3/(din+epsilon))*lim_t_no3_9*
                      lim_t_po4_10*lim_t_dic_8
```

assimilation of ammonium by large-cell phytoplankton [mol/kg/day]

```
7.4375*h2o + rfr_c*t_dic + rfr_p*t_po4 + t_nh4 -> 0.8125*h3oplus + 6.625*t_o2 + t_lpp
p_nh4_assim_lpp =     (lpp_plus_lpp0*lr_assim_lpp*t_nh4/(din+epsilon))*lim_t_dic_8*
                      lim_t_po4_10*lim_t_nh4_11
```

assimilation of nitrate by small-cell phytoplankton [mol/kg/day]

```
t_no3 + rfr_p*t_po4 + rfr_c*t_dic + 6.4375*h2o + 1.1875*h3oplus -> t_spp + 8.625*t_o2
p_no3_assim_spp =     (spp_plus_spp0*lr_assim_spp*t_no3/(din+epsilon))*lim_t_no3_9*
                      lim_t_po4_10*lim_t_dic_8
```

assimilation of ammonium by small-cell phytoplankton [mol/kg/day]

```
7.4375*h2o + rfr_c*t_dic + rfr_p*t_po4 + t_nh4 -> 0.8125*h3oplus + 6.625*t_o2 + t_spp
p_nh4_assim_spp =     (spp_plus_spp0*lr_assim_spp*t_nh4/(din+epsilon))*lim_t_dic_8*
                      lim_t_po4_10*lim_t_nh4_11
```

assimilation of ammonium by limnic phytoplankton [mol/kg/day]

```
t_nh4 + rfr_p*t_po4 + rfr_c*t_dic + 7.4375*h2o -> t_lip + 6.625*t_o2 + 0.8125*h3oplus
p_nh4_assim_lip =     (lip_plus_lip0*lr_assim_lip*t_nh4/(din+epsilon))*lim_t_nh4_11*
                      lim_t_po4_10*lim_t_dic_8
```

assimilation of nitrate by limnic phytoplankton [mol/kg/day]

```
1.1875*h3oplus + 6.4375*h2o + rfr_c*t_dic + rfr_p*t_po4 + t_no3 -> 8.625*t_o2 + t_lip
p_no3_assim_lip =     (lip_plus_lip0*lr_assim_lip*t_no3/(din+epsilon))*lim_t_dic_8*
                      lim_t_po4_10*lim_t_no3_9
```

fixation of dinitrogen by diazotroph cyanobacteria [mol/kg/day]

continued on next page…

```
7.9375*h2o + rfr_c*t_dic + rfr_p*t_po4 + 0.5*t_n2 + 0.1875*h3oplus -> 7.375*t_o2 +
t_cya
p_n2_assim_cya =     (cya_plus_cya0*lr_assim_cya)*lim_t_dic_8*lim_t_po4_10*lim_t_n2_7
```

Production of DOC by LPP [mol/kg/day]

```
h2o + t_dic -> t_o2 + t_doc
p_assim_lpp_doc =    (rfr_c * t_lpp * lr_assim_lpp_doc)*lim_t_dic_8
```

Production of DOC by SPP [mol/kg/day]

```
h2o + t_dic -> t_o2 + t_doc
p_assim_spp_doc =    (rfr_c * t_spp * lr_assim_spp_doc)*lim_t_dic_8
```

Production of DOC by LPP [mol/kg/day]

```
t_dic + h2o -> t_doc + t_o2
p_assim_lip_doc =    (rfr_c * t_lip * lr_assim_lip_doc)*lim_t_dic_8
```

Production of DOC by CYA [mol/kg/day]

```
t_dic + h2o -> t_doc + t_o2
p_assim_cya_doc =    (rfr_c * t_cya * lr_assim_cya_doc)*lim_t_dic_8
```

Production of DOP by LPP [mol/kg/day]

```
3*h3oplus + 106*h2o + t_po4 + 106*t_dic -> 3*h2o + 106*t_o2 + t_dop
p_assim_lpp_dop =    (rfr_p * t_lpp * lr_assim_lpp_dop)*lim_t_po4_10*lim_t_dic_8
```

Production of DOP by SPP [mol/kg/day]

```
106*t_dic + t_po4 + 106*h2o + 3*h3oplus -> t_dop + 106*t_o2 + 3*h2o
p_assim_spp_dop =    (rfr_p * t_spp * lr_assim_spp_dop)*lim_t_dic_8*lim_t_po4_10
```

Production of DOP by LIP [mol/kg/day]

```
3*h3oplus + 106*h2o + t_po4 + 106*t_dic -> 3*h2o + 106*t_o2 + t_dop
p_assim_lip_dop =    (rfr_p * t_lip * lr_assim_lip_dop)*lim_t_po4_10*lim_t_dic_8
```

continued on next page…

Production of DON by LPP [mol/kg/day]

```
rfr_c*t_dic + t_nh4 + 6.625*H2O + ohminus -> t_don + 6.625*t_o2 + H2O
p_nh4_assim_lpp_don = (t_lpp * lr_assim_lpp_don*t_nh4/(din+epsilon))*lim_t_dic_8*
                      lim_t_nh4_11
```

Production of DON by LPP [mol/kg/day]

```
h3oplus + 6.625*H2O + t_no3 + rfr_c*t_dic -> 8.625*t_o2 + t_don
p_no3_assim_lpp_don = (t_lpp * lr_assim_lpp_don*t_no3/(din+epsilon))*lim_t_no3_9*
                      lim_t_dic_8
```

Production of DON by SPP [mol/kg/day]

```
ohminus + 6.625*H2O + t_nh4 + rfr_c*t_dic -> H2O + 6.625*t_o2 + t_don
p_nh4_assim_spp_don = (t_spp * lr_assim_spp_don*t_nh4/(din+epsilon))*lim_t_nh4_11*
                      lim_t_dic_8
```

Production of DON by SPP [mol/kg/day]

```
rfr_c*t_dic + t_no3 + 6.625*H2O + h3oplus -> t_don + 8.625*t_o2
p_no3_assim_spp_don = (t_spp * lr_assim_spp_don*t_no3/(din+epsilon))*lim_t_dic_8*
                      lim_t_no3_9
```

Production of DON by LIP [mol/kg/day]

```
ohminus + 6.625*H2O + t_nh4 + rfr_c*t_dic -> H2O + 6.625*t_o2 + t_don
p_nh4_assim_lip_don = (t_lip * lr_assim_lip_don*t_nh4/(din+epsilon))*lim_t_nh4_11*
                      lim_t_dic_8
```

Production of DON by LIP [mol/kg/day]

```
rfr_c*t_dic + t_no3 + 6.625*H2O + h3oplus -> t_don + 8.625*t_o2
p_no3_assim_lip_don = (t_lip * lr_assim_lip_don*t_no3/(din+epsilon))*lim_t_dic_8*
                      lim_t_no3_9
```

respiration of POC [mol/kg/day]

```
t_poc + t_o2 -> t_dic + h2o
```

continued on next page…

```
p_poc_resp =         (t_poc * r_poc_rec * exp(q10_det_rec * cgt_temp))*lim_t_o2_0*
                     lim_t_poc_12
```

respiration of large-cell phytoplankton [mol/kg/day]

```
t_lpp + 6.625*t_o2 + 0.8125*h3oplus -> don_fraction*t_don + (1-don_fraction)*t_nh4 +
rfr_p*t_po4 + rfr_c*t_dic + 7.4375*h2o
p_lpp_resp_nh4 =     (t_lpp*r_lpp_resp)*lim_t_lpp_15*lim_t_o2_2
```

respiration of small-cell phytoplankton [mol/kg/day]

```
0.8125*h3oplus + 6.625*t_o2 + t_spp -> 7.4375*h2o + rfr_c*t_dic + rfr_p*t_po4 + (1-
don_fraction)*t_nh4 + don_fraction*t_don
p_spp_resp_nh4 =     (t_spp*r_spp_resp)*lim_t_o2_2*lim_t_spp_16
```

respiration of limnic phytoplankton [mol/kg/day]

```
0.8125*h3oplus + 6.625*t_o2 + t_lip -> 7.4375*h2o + rfr_c*t_dic + rfr_p*t_po4 + (1-
don_fraction)*t_nh4 + don_fraction*t_don
p_lip_resp_nh4 =     (t_lip*r_lip_resp)*lim_t_o2_2*lim_t_lip_18
```

respiration of diazotroph cyanobacteria [mol/kg/day]

```
0.8125*h3oplus + 6.625*t_o2 + t_cya -> 7.4375*h2o + rfr_c*t_dic + rfr_p*t_po4 +
don_fraction*t_don + (1-don_fraction)*t_nh4
p_cya_resp_nh4 =     (t_cya*r_cya_resp)*lim_t_o2_2*lim_t_cya_17
```

mortality of large-cell phytoplankton [mol/kg/day]

```
t_lpp -> t_det
p_lpp_mort_det =     (t_lpp*r_pp_mort*(1+9*theta(5.0e-6-t_o2)))*lim_t_lpp_15
```

mortality of small-scale phytoplankton [mol/kg/day]

```
t_spp -> t_det
p_spp_mort_det =     (t_spp*r_pp_mort*(1+9*theta(5.0e-6-t_o2)))*lim_t_spp_16
```

mortality of limnic phytoplankton [mol/kg/day]

continued on next page…

Processes, continued from previous page

```
t_lip -> t_det
p_lip_mort_det =     (t_lip*r_pp_mort*(1+9*theta(5.0e-6-t_o2)))*lim_t_lip_18
```

mortality of diazotroph cyanobacteria [mol/kg/day]

```
t_cya -> t_det
p_cya_mort_det =     (t_cya*r_pp_mort*(1+9*theta(5.0e-6-t_o2)))*lim_t_cya_17
```

mortality of diazotroph cyanobacteria due to strong turbulence [mol/kg/day]

```
t_cya -> t_det
p_cya_mort_det_diff = (t_cya*r_pp_mort*(r_cya_mort_diff*theta(cgt_diffusivity-
                      r_cya_mort_thresh)))*lim_t_cya_17
```

respiration of DOC [mol/kg/day]

```
t_o2 + t_doc -> h2o + t_dic
p_doc_resp =          (t_doc * r_doc_rec * exp(q10_doc_rec * cgt_temp))*lim_t_o2_0*
                      lim_t_doc_29
```

end of table **Processes**

Auxiliary variables

square of positive temperature [°C * °C]

```
temp_sq =             max(0.0,cgt_temp)*max(0.0,cgt_temp)
```

dissolved inorganic nitrogen [mol/kg]

```
din =                 t_no3+t_nh4
```

squared DIN [mol2/kg2]

```
din_sq =              din*din
```

squared phosphate [mol2/kg**2]**

```
po4_sq =              t_po4*t_po4
```

continued on next page…

large-cell phytoplankton plus seed concentration [mol/kg]

```
lpp_plus_lpp0 =       t_lpp+lpp0
```

small-cell phytoplankton plus seed concentration [mol/kg]

```
spp_plus_spp0 =       t_spp+spp0
```

limnic phytoplankton plus seed concentration [mol/kg]

```
lip_plus_lip0 =       t_lip+lip0
```

diazotroph cyanobacteria plus seed concentration [mol/kg]

```
cya_plus_cya0 =       t_cya+cya0
```

light limitation factor for large-cell phytoplankton growth [1]

```
temp1 =               max(cgt_light/2.0,light_opt_lpp)
lim_light_lpp =       cgt_light/temp1*exp(1-cgt_light/temp1)
```

light limitation factor for small-cell phytoplankton growth [1]

```
temp1 =               max(cgt_light/2.0,light_opt_spp)
lim_light_spp =       cgt_light/temp1*exp(1-cgt_light/temp1)
```

light limitation factor for limnic phytoplankton growth [1]

```
temp1 =               max(cgt_light/2.0,light_opt_lip)
lim_light_lip =       cgt_light/temp1*exp(1-cgt_light/temp1)
```

light limitation factor for diazotroph cyanobacteria growth [1]

```
temp1 =               max(cgt_light/2.0,light_opt_cya)
lim_light_cya =       cgt_light/temp1*exp(1-cgt_light/temp1)
```

growth rate of large-cell phytoplankton, limited by DIN, DIP, light and oxygen [1/day]

continued on next page. . .

Auxiliary variables, continued from previous page

`lr_assim_lpp =` `r_lpp_assim*theta(t_o2-2*t_h2s)*min(din_sq/(din_sq+din_min_lpp*din_min_lpp),min(po4_sq/(po4_sq+din_min_lpp*din_min_lpp*rfr_p*rfr_p),lim_light_lpp))`

growth rate of small-cell phytoplankton, limited by DIN, DIP, light, oxygen and temperature [1/day]

`lr_assim_spp =` `r_spp_assim*theta(t_o2-2*t_h2s)*min(din_sq/(din_sq+din_min_spp*din_min_spp),min(po4_sq/(po4_sq+din_min_spp*din_min_spp*rfr_p*rfr_p),lim_light_spp))*(1+temp_sq/(temp_sq+temp_min_spp*temp_min_spp))`

growth rate of limnic phytoplankton, limited by DIN, DIP, light, salt and oxygen [1/day]

`lr_assim_lip =` `r_lip_assim*theta(t_o2-2*t_h2s)*min(din_sq/(din_sq+din_min_lip*din_min_lip),min(po4_sq/(po4_sq+din_min_lip*din_min_lip*rfr_p*rfr_p),lim_light_lip))*(1/(1+exp(cgt_sali*cgt_sali-sali_max_lip*sali_max_lip)))`

growth rate of diazotroph cyanobacteria, limited by DIP, light, oxygen, temperature and salinity [1/day]

`lr_assim_cya =` `r_cya_assim*theta(t_o2-2*t_h2s)*min(po4_sq/(po4_sq+dip_min_cya*dip_min_cya),lim_light_cya)*(1/(1+exp(temp_switch_cya*(temp_min_cya-cgt_temp))))*(1/(1+exp(cgt_sali-sali_max_cya)))*(1/(1+exp(sali_min_cya-cgt_sali)))*(1/(1+exp(nit_switch_cya*(din-nit_max_cya))))`

production rate of DOC by LPP

`lr_assim_lpp_doc =` `fac_doc_assim_lpp * r_lpp_assim * theta(t_o2-2*t_h2s) * min(max(1 - din_sq/(din_sq+din_min_lpp*din_min_lpp),1 - po4_sq/(din_min_lpp*din_min_lpp*rfr_p*rfr_p + po4_sq)), lim_light_lpp)`

production rate of DOC by SPP

continued on next page…

```
lr_assim_spp_doc =    fac_doc_assim_spp * r_spp_assim * theta(t_o2-2*t_h2s) * min(max(1
                      - din_sq/(din_sq+din_min_spp*din_min_spp),1 -
                      po4_sq/(din_min_spp*din_min_spp*rfr_p*rfr_p + po4_sq)),
                      lim_light_spp)*(1+temp_sq/(temp_sq+temp_min_spp*temp_min_spp))
```

production rate of DOC by CYA

```
lr_assim_cya_doc =    fac_doc_assim_cya * r_cya_assim*theta(t_o2-2*t_h2s)*min(1 -
                      po4_sq/(po4_sq+dip_min_cya*dip_min_cya),lim_light_cya)*(1/(1+
                      exp(temp_switch_cya*(temp_min_cya-cgt_temp))))*(1/(1+
                      exp(cgt_sali-sali_max_cya)))*(1/(1+exp(sali_min_cya-cgt_sali)))
```

production rate of DOC by LPP

```
lr_assim_lip_doc =    fac_doc_assim_lip * r_lip_assim * theta(t_o2-2*t_h2s) * min(max(1
                      - din_sq/(din_sq+din_min_lip*din_min_lip),1 -
                      po4_sq/(din_min_lip*din_min_lip*rfr_p*rfr_p + po4_sq)),
                      lim_light_lip)*(1/(1+exp(cgt_sali-sali_max_lip)))
```

production rate of DOP by LPP

```
lr_assim_lpp_dop =    fac_dop_assim * r_lpp_assim * theta(t_o2-2*t_h2s) * min(min(1 -
                      din_sq/(din_sq+din_min_lpp*din_min_lpp),po4_sq/(din_min_lpp*
                      din_min_lpp*rfr_p*rfr_p + po4_sq)), lim_light_lpp)
```

production rate of DOP by SPP

```
lr_assim_spp_dop =    fac_dop_assim * r_spp_assim * theta(t_o2-2*t_h2s) * min(min(1 -
                      din_sq/(din_sq+din_min_spp*din_min_spp),po4_sq/(din_min_spp*
                      din_min_spp*rfr_p*rfr_p + po4_sq)), lim_light_spp)*(1+
                      temp_sq/(temp_sq+temp_min_spp*temp_min_spp))
```

production rate of DOP by LPP

continued on next page...

Auxiliary variables, continued from previous page

```
lr_assim_lip_dop =    fac_dop_assim * r_lip_assim * theta(t_o2-2*t_h2s) * min(min(1 -
                      din_sq/(din_sq+din_min_lip*din_min_lip),po4_sq/(din_min_lip*
                      din_min_lip*rfr_p*rfr_p + po4_sq)), lim_light_lip)*(1/(1+
                      exp(cgt_sali-sali_max_lip)))
```

production rate of DON by LPP

```
lr_assim_lpp_don =    fac_don_assim * r_lpp_assim * theta(t_o2-2*t_h2s) *
                      min(min(din_sq/(din_sq+din_min_lpp*din_min_lpp),1 -
                      po4_sq/(din_min_lpp*din_min_lpp*rfr_p*rfr_p + po4_sq)),
                      lim_light_lpp)
```

production rate of DON by SPP

```
lr_assim_spp_don =    fac_don_assim * r_spp_assim * theta(t_o2-2*t_h2s) *
                      min(min(din_sq/(din_sq+din_min_spp*din_min_spp),1 -
                      po4_sq/(din_min_spp*din_min_spp*rfr_p*rfr_p + po4_sq)),
                      lim_light_spp)*(1+temp_sq/(temp_sq+temp_min_spp*temp_min_spp))
```

production rate of DON by limnic phytoplankton

```
lr_assim_lip_don =    fac_don_assim * r_lip_assim * theta(t_o2-2*t_h2s) *
                      min(min(din_sq/(din_sq+din_min_lip*din_min_lip),1 -
                      po4_sq/(din_min_lip*din_min_lip*rfr_p*rfr_p + po4_sq)),
                      lim_light_lip)*(1/(1+exp(cgt_sali-sali_max_lip)))
```

end of table **Auxiliary variables**

Constants

seed concentration for diazotroph cyanobacteria [mol/kg]

```
cya0 =                9.0E-8
```

DIN half saturation constant for large-cell phytoplankton growth [mol/kg]

```
din_min_lpp =         1.0E-6
```

continued on next page. . .

DIN half saturation constant for small-cell phytoplankton growth [mol/kg]

```
din_min_spp =         1.6E-7
```

DIP half saturation constant for diazotroph cyanobacteria growth [mol/kg]

```
dip_min_cya =         1.0E-8
```

DIN half saturation constant for limnic phytoplankton growth [mol/kg]

```
din_min_lip =         1.0E-6
```

no division by 0

```
epsilon =             4.5E-17
```

optimal light for diazotroph cyanobacteria growth [W/m2]**

```
light_opt_cya =       50.0
```

optimal light for large-cell phytoplankton growth [W/m2]**

```
light_opt_lpp =       35.0
```

optimal light for small-cell phytoplankton growth [W/m2]**

```
light_opt_spp =       50.0
```

optimal light for limnic phytoplankton growth [W/m2]**

```
light_opt_lip =       30.0
```

seed concentration for limnic phytoplankton [mol/kg]

```
lip0 =                4.5E-9
```

seed concentration for large-cell phytoplankton [mol/kg]

```
lpp0 =                4.5E-9
```

oxygen half-saturation constant for detritus recycling [mol/kg]

continued on next page. . .

Constants, continued from previous page

`o2_min_det_resp =     1.0E-6`

q10 rule factor for recycling [1/K]

`q10_det_rec =         0.15`

q10 rule factor for DOC recycling [1/K]

`q10_doc_rec =         0.069`

maximum rate for nutrient uptake of diazotroph cyanobacteria [1/day]

`r_cya_assim =         0.75`

respiration rate of cyanobacteria to ammonium [1/day]

`r_cya_resp =          0.01`

maximum rate for nutrient uptake of large-cell phytoplankton [1/day]

`r_lpp_assim =         1.38`

respiration rate of large phytoplankton to ammonium [1/day]

`r_lpp_resp =          0.075`

maximum rate for nutrient uptake of limnic phytoplankton [1/day]

`r_lip_assim =         1.38`

respiration rate of limnic phytoplankton to ammonium [1/day]

`r_lip_resp =          0.075`

mortality rate of phytoplankton [1/day]

`r_pp_mort =           0.03`

enhanced cya mortality due to strong turbulence

`r_cya_mort_diff =     40.0`

continued on next page…

diffusivity threshold for enhanced cyano mortality

`r_cya_mort_thresh =   0.02`

maximum rate for nutrient uptake of small-cell phytoplankton [1/day]

`r_spp_assim =         0.4`

respiration rate of small phytoplankton to ammonium [1/day]

`r_spp_resp =          0.0175`

redfield ratio C/N

`rfr_c =               6.625`

redfield ratio P/N

`rfr_p =               0.0625`

upper salinity limit - diazotroph cyanobacteria [psu]

`sali_max_cya =        8.0`

lower salinity limit - diazotroph cyanobacteria [psu]

`sali_min_cya =        4.0`

limits cyano growth in DIN reach environment

`nit_max_cya =         5.0E-7`

strengs of DIN control for cyano growth

`nit_switch_cya =      8.0`

lower salinity limit - limnic phytoplankton [psu]

`sali_max_lip =        2.0`

seed concentration for small-cell phytoplankton [mol/kg]

`spp0 =                4.5E-9`

continued on next page. . .

lower temperature limit - diazotroph cyanobacteria [°C]

```
temp_min_cya =       13.5
```

strengs of temperature control for cyano growth

```
temp_switch_cya =    4.0
```

lower temperature limit - small-cell phytoplankton [°C]

```
temp_min_spp =       10.0
```

fraction of DON in respiration products

```
don_fraction =       0.0
```

recycling rate (poc to dic) at 0°C [1/day]

```
r_poc_rec =          0.003
```

factor modifying DOC assimilation rate of large phytoplankton LPP

```
fac_doc_assim_lpp =  1.0
```

factor modifying DOC assimilation rate of cyanobacteria

```
fac_doc_assim_cya =  1.0
```

factor modifying DOC assimilation rate of small phytoplankton SPP

```
fac_doc_assim_spp =  1.0
```

factor modifying DOC assimilation rate of limnic phytoplankton LIP

```
fac_doc_assim_lip =  1.0
```

factor modifying assimilation rate for POCP production

```
fac_dop_assim =      0.5
```

factor modifying assimilation rate for POCN production

continued on next page…

Constants, continued from previous page

`fac_don_assim =       1.0`

recycling rate (doc to dic) at 0°C [1/day]

`r_doc_rec =           0.001`

end of table **Constants**

Process limitation factors

`lim_t_n2_7 =          theta(t_n2-0.0)`

`lim_t_o2_0 =          1.0-exp(-t_o2/o2_min_det_resp)`

`lim_t_o2_2 =          theta(t_o2-0.0)`

`lim_t_dic_8 =         theta(t_dic-0.0)`

`lim_t_nh4_11 =        theta(t_nh4-0.0)`

`lim_t_no3_9 =         theta(t_no3-0.0)`

`lim_t_po4_10 =        theta(t_po4-0.0)`

`lim_t_spp_16 =        theta(t_spp-0.0)`

`lim_t_lip_18 =        theta(t_lip-0.0)`

`lim_t_doc_29 =        theta(t_doc-0.0)`

`lim_t_lpp_15 =        theta(t_lpp-0.0)`

`lim_t_cya_17 =        theta(t_cya-0.0)`

continued on next page…

Process limitation factors, continued from previous page

`lim_t_poc_12 =        theta(t_poc-0.0)`

end of table **Process limitation factors**

5

B3.6 Process type BGC/pelagic/reoxidation

Processes

nitrification [mol/kg/day]

`t_nh4 + 2*t_o2 + h2o -> t_no3 + 2*h3oplus`

`p_nh4_nit_no3 =       (t_nh4*r_nh4_nitrif*exp(q10_nit*cgt_temp))*lim_t_nh4_11* lim_t_o2_2`

oxidation of hydrogen sulfide with oxygen [mol/kg/day]

`0.5*t_o2 + t_h2s -> h2o + t_sul`

`p_h2s_oxo2_sul =      (t_h2s*t_o2*k_h2s_o2*exp(q10_h2s*cgt_temp))*lim_t_o2_2* lim_t_h2s_24`

oxidation of hydrogen sulfide with nitrate [mol/kg/day]

`t_h2s + 0.4*t_no3 + 0.4*h3oplus -> t_sul + 1.6*h2o + 0.2*t_n2`

`p_h2s_oxno3_sul =     (t_h2s*t_no3*k_h2s_no3*exp(q10_h2s*cgt_temp))*lim_t_h2s_24* lim_t_no3_9`

oxidation of elemental sulfur with oxygen [mol/kg/day]

`t_sul + 1.5*t_o2 + 3*h2o -> so4 + 2*h3oplus`

`p_sul_oxo2_so4 =      (t_sul*t_o2*k_sul_o2*exp(q10_h2s*cgt_temp))*lim_t_sul_25* lim_t_o2_2`

oxidation of elemental sulfur with nitrate [mol/kg/day]

`t_sul + 1.2*t_no3 + 1.2*h2o -> so4 + 0.8*h3oplus + 0.6*t_n2`

continued on next page. . .

Processes, continued from previous page

```
p_sul_oxno3_so4 =     (t_sul*t_no3*k_sul_no3*exp(q10_h2s*cgt_temp))*lim_t_sul_25*
                      lim_t_no3_9
```

end of table **Processes**

Auxiliary variables

end of table **Auxiliary variables**

Constants

reaction constant h2s oxidation with no3 [kg/mol/day]

`k_h2s_no3 =            800000.0`

reaction constant h2s oxidation with o2 [kg/mol/day]

`k_h2s_o2 =             800000.0`

reaction constant sul oxidation with no3 [kg/mol/day]

`k_sul_no3 =            20000.0`

reaction constant sul oxidation with o2 [kg/mol/day]

`k_sul_o2 =             20000.0`

q10 rule factor for oxidation of h2s and sul [1/K]

`q10_h2s =              0.0693`

q10 rule factor for nitrification [1/K]

`q10_nit =              0.11`

nitrification rate at 0°C [1/day]

`r_nh4_nitrif =         0.05`

end of table **Constants**

Process limitation factors

```
lim_t_o2_2 =         theta(t_o2-0.0)

lim_t_nh4_11 =       theta(t_nh4-0.0)

lim_t_no3_9 =        theta(t_no3-0.0)

lim_t_h2s_24 =       theta(t_h2s-0.0)

lim_t_sul_25 =       theta(t_sul-0.0)
```

end of table **Process limitation factors**

5

B3.7 Process type BGC/pelagic/zooplankton

Processes

grazing of zooplankton eating large-cell phytoplankton [mol/kg/day]

```
t_lpp -> t_zoo
p_lpp_graz_zoo =     ((t_zoo+zoo0)*lr_graz_zoo*t_lpp/max(food_zoo,epsilon))*
                     lim_t_lpp_15
```

grazing of zooplankton eating small-cell phytoplankton [mol/kg/day]

```
t_spp -> t_zoo
p_spp_graz_zoo =     ((t_zoo+zoo0)*lr_graz_zoo*t_spp/max(food_zoo,epsilon))*
                     lim_t_spp_16
```

grazing of zooplankton eating diazotroph cyanobacteria [mol/kg/day]

```
t_cya -> t_zoo
p_cya_graz_zoo =     ((t_zoo+zoo0)*lr_graz_zoo*(0.5*t_cya)/max(food_zoo,epsilon))*
                     lim_t_cya_17
```

continued on next page...

Processes, continued from previous page

grazing of zooplankton eating limnic phytoplankton [mol/kg/day]

```
t_lip -> t_zoo
p_lip_graz_zoo =      ((t_zoo+zoo0)*lr_graz_zoo*t_lip/max(food_zoo,epsilon))*
                      lim_t_lip_18
```

respiration of zooplankton [mol/kg/day]

```
0.8125*h3oplus + 6.625*t_o2 + t_zoo -> 7.4375*h2o + rfr_c*t_dic + rfr_p*t_po4 + (1-
don_fraction)*t_nh4 + don_fraction*t_don
p_zoo_resp_nh4 =      (zoo_eff*r_zoo_resp)*lim_t_o2_2*lim_t_zoo_19
```

mortality of zooplankton [mol/kg/day]

```
t_zoo -> t_det
p_zoo_mort_det =      (zoo_eff*r_zoo_mort*(1+9*theta(5.0e-6-t_o2)))*lim_t_zoo_19
```

end of table **Processes**

Auxiliary variables

square of positive temperature [°C * °C]

```
temp_sq =             max(0.0,cgt_temp)*max(0.0,cgt_temp)
```

effectice zooplankton concentration assumed for mortality and respiration process [mol/kg]

```
zoo_eff =             t_zoo*t_zoo/zoo_cl
```

suitable food for zooplankton (weighted with food preferences) [mol/kg]

```
food_zoo =            t_lpp+t_spp+t_lip+0.5*t_cya
```

growth rate of zooplankton, limited by food, oxygen and temperature [1/day]

```
lr_graz_zoo =         r_zoo_graz*(1-exp(-food_zoo*food_zoo/(food_min_zoo*food_min_zoo))
                      )*theta(t_o2-2*t_h2s)*(1.0+temp_sq/(temp_opt_zoo*temp_opt_zoo)*
                      exp(2.0-cgt_temp*2.0/temp_opt_zoo))
```

end of table **Auxiliary variables**

Constants

no division by 0

`epsilon =           4.5E-17`

Ivlev phytoplankton concentration for zooplankton grazing [mol/kg]

`food_min_zoo =      4.108E-6`

maximum zooplankton grazing rate [1/day]

`r_zoo_graz =        0.5`

mortality rate of zooplankton [1/day]

`r_zoo_mort =        0.03`

respiration rate of zooplankton [1/day]

`r_zoo_resp =        0.01`

redfield ratio C/N

`rfr_c =             6.625`

redfield ratio P/N

`rfr_p =             0.0625`

optimal temperature for zooplankton grazing [°C]

`temp_opt_zoo =      20.0`

seed concentration for zooplankton [mol/kg]

`zoo0 =              4.5E-9`

zooplankton closure parameter [mol/kg]

`zoo_cl =            9.0E-8`

fraction of DON in respiration products

`don_fraction =      0.0`

continued on next page…

Constants, continued from previous page

end of table **Constants**

Process limitation factors

`lim_t_o2_2 =` `theta(t_o2-0.0)`

`lim_t_spp_16 =` `theta(t_spp-0.0)`

`lim_t_zoo_19 =` `theta(t_zoo-0.0)`

`lim_t_lip_18 =` `theta(t_lip-0.0)`

`lim_t_lpp_15 =` `theta(t_lpp-0.0)`

`lim_t_cya_17 =` `theta(t_cya-0.0)`

end of table **Process limitation factors**

5

B3.8 Process type gas_exchange

Processes

end of table **Processes**

Auxiliary variables

absolute temperature [K]

`temp_k =` `cgt_temp + 273.15`

temporary value assumed for pH [1]

continued on next page...

`ph_temp =` `0.0-log(h3o)/log(10.0)`

calculated iteratively, 10 iterations, initial value = `0.0`

self-ionization constant of Water [mol2/kg2]

`k_water =` `exp( -13847.26 / temp_k + 148.96502 - 23.6521 * log(temp_k) + (118.67/temp_k - 5.977 + 1.0495 * log(temp_k)) * sqrt(cgt_sali) - 0.01615 * cgt_sali)`

Solubility of CO2 [mol/kg/Pa]

`k0_co2 =` `exp(9345.17 / temp_k - 60.2409 + 23.3585 * (log(temp_k) - 4.605170186) + cgt_sali*(0.023517 - 0.00023656 * temp_k + 0.00000047036 *temp_k*temp_k))/101325.0`

Acid dissociation constant CO2 + 2 H2O <-> HCO3- + H3O+ [mol/kg]

`k1_co2 =` `power(10.0,( -3633.86 / temp_k + 61.2172 - 9.6777 * log(temp_k) + 0.011555 * cgt_sali - 0.0001152 * cgt_sali * cgt_sali))`

Acid dissociation constant HCO3- + H2O <-> [CO3 2-] + H3O+ [mol/kg]

`k2_co2 =` `power(10.0,( -471.78 / temp_k - 25.929 + 3.16967 * log(temp_k) + 0.01781 * cgt_sali - 0.0001122 * cgt_sali * cgt_sali))`

Acid dissociation constant of boric acid [mol/kg]

`k_boron =` `exp(( -8966.9 - 2890.53*sqrt(cgt_sali) - 77.942*cgt_sali + 1.728*cgt_sali*sqrt(cgt_sali) - 0.0996*cgt_sali*cgt_sali) / temp_k + 148.0248 + 137.1942*sqrt(cgt_sali) + 1.62142*cgt_sali + (-24.4344 - 25.085*sqrt(cgt_sali) - 0.2474*cgt_sali)*log(temp_k) + 0.053105*sqrt(cgt_sali)*temp_k )`

Acid dissociation constant H3PO4 + H2O <-> [H2PO4 -] + H3O+ [mol/kg]

`k1_po4 =` `exp( -4576.752/temp_k + 115.525 - 18.453*log(temp_k) + (0.69171 - 106.736/temp_k)*sqrt(cgt_sali) - (0.01844 + 0.65643/temp_k)*cgt_sali )`

continued on next page...

Acid dissociation constant [H2PO4 -] + H2O+ <-> [HPO4 2-] + H3O+ [mol/kg]

```
k2_po4 =              exp( -8814.715/temp_k + 172.0883 - 27.927*log(temp_k) + (1.35660
                      - 160.340/temp_k)*sqrt(cgt_sali) - (0.05778 - 0.37335/temp_k)*
                      cgt_sali )
```

Acid dissociation constant [HPO4 2-] + H2O <-> [PO4 3-] + H3O+ [mol/kg]

```
k3_po4 =              exp( -3070.75/temp_k - 18.141 + (2.81197 + 17.27039/temp_k)*
                      sqrt(cgt_sali) - (0.09984 + 44.99486/temp_k)*cgt_sali )
```

Acid dissociation constant H2S + H2O <-> HS- + H3O+ [mol/kg]

```
k1_h2s =              exp( -3131.42/temp_k + 5.818 + 0.368*(power(max(0.0,cgt_sali)
                      ,(1.0/3.0))))
```

total concentration of boron [mol/kg]

```
boron_total =         0.000416 * cgt_sali/35.0
```

boron alkalinity [mol/kg]

```
alk_boron =           boron_total * k_boron / (k_boron + h3o)
```

calculated iteratively, 10 iterations, initial value = `0.0`

hydrogen sulfide alkalinity [mol/kg]

```
alk_h2s =             t_h2s * k1_h2s / (k1_h2s + h3o)
```

calculated iteratively, 10 iterations, initial value = `0.0`

water alkalinity [mol/kg]

```
alk_water =           k_water / h3o - h3o
```

calculated iteratively, 10 iterations, initial value = `0.0`

denominator in phosphate alkalinity formula [mol3/kg3]

```
alk_po4_denominator = (h3o*h3o*h3o + k1_po4*h3o*h3o + k1_po4*k2_po4*h3o + k1_po4*
                      k2_po4*k3_po4)
```

continued on next page...

calculated iteratively, 10 iterations, initial value = `0.0`

phosphate alkalinity [mol/kg]

```
alk_po4 =              t_po4*(k1_po4*k2_po4*h3o + 2.0*k1_po4*k2_po4*k3_po4 - h3o*h3o*
                       h3o) / alk_po4_denominator
```

calculated iteratively, 10 iterations, initial value = `0.0`

denominator in carbonate alkalinity formula [mol2/kg2]

```
alk_co2_denominator = (h3o*h3o + k1_co2*h3o + k1_co2*k2_co2)
```

calculated iteratively, 10 iterations, initial value = `0.0`

carbonate alkalinity [mol/kg]

```
alk_co2 =              t_dic*k1_co2*(h3o+2*k2_co2)/alk_co2_denominator
```

calculated iteratively, 10 iterations, initial value = `0.0`

error in total alkalinity calculation at the assumed pH [mol/kg]

```
alk_residual =         t_alk - alk_co2 - alk_po4 - alk_boron - alk_h2s - alk_water
```

calculated iteratively, 10 iterations, initial value = `0.0`

derivative of phosphate alkalinity with respect to h3o [1]

```
dalkp_dh3o =           t_po4*(0.0-k1_po4*h3o*h3o*h3o*h3o-4*k1_po4*k2_po4*h3o*h3o*h3o-
                       (k1_po4*k1_po4*k2_po4+9*k1_po4*k2_po4*k3_po4)*h3o*h3o-4*k1_po4*
                       k1_po4*k2_po4*k3_po4*h3o-k1_po4*k1_po4*k2_po4*k2_po4*k3_po4)
                       /(alk_po4_denominator*alk_po4_denominator)
```

calculated iteratively, 10 iterations, initial value = `0.0`

derivative of carbonate alkalinity with respect to h3o [1]

```
dalkc_dh3o =           t_dic*(0.0-k1_co2*h3o*h3o-k1_co2*k1_co2*k2_co2-4*k1_co2*k2_co2*
                       h3o)/(alk_co2_denominator*alk_co2_denominator)
```

calculated iteratively, 10 iterations, initial value = `0.0`

derivative of residual_alk with respect to pH [mol/kg]

continued on next page...

`dalkresidual_dpH =` `0.0-log(10.0)*h3o*(alk_boron/(k_boron+h3o)+alk_h2s/(k1_h2s+h3o)+k_water/(h3o*h3o)+1-dalkp_dh3o-dalkc_dh3o)`

calculated iteratively, 10 iterations, initial value = `0.0`

newly determined pH value [1]

`temp1 =` `alk_residual/dalkresidual_dpH`

`ph =` `ph_temp - temp1 + theta(abs(temp1) - 1)*0.5*temp1`

calculated iteratively, 10 iterations, initial value = `0.0`

h3o ion concentration [mol/kg]

`h3o =` `power(10.0,0.0-max(1.0,min(13.0,ph)))`

calculated iteratively, 10 iterations, initial value = `1.0e-8`

co2 partial pressure [Pa]

`pco2 =` `t_dic / k0_co2 / (1 + k1_co2/h3o + k1_co2*k2_co2/h3o/h3o)`

oxygen saturation concentration [mol/kg]

`o2_sat =` `(10.18e0+((5.306e-3-4.8725e-5*cgt_temp)*cgt_temp-0.2785e0)*cgt_temp+cgt_sali*((2.2258e-3+(4.39e-7*cgt_temp-4.645e-5)*cgt_temp)*cgt_temp-6.33e-2))*44.66e0*1e-6`

dissolved molecular nitrogen saturation concentration [mol/kg]

`temp1 =` `log((298.15-cgt_temp)/(273.15+cgt_temp))`

`temp2 =` `temp1*temp1`

`temp3 =` `temp2*temp1`

`n2_sat =` `1e-6*exp(6.42931 + 2.92704*temp1 + 4.32531*temp2 + 4.69149*temp3 + cgt_sali*(0.0 -7.44129e-3 - 8.02566e-3*temp1 - 1.46775e-2*temp2))`

end of table **Auxiliary variables**

Constants

atmospheric partial pressure of CO2 [Pa]

`patm_co2 =           38.0`

piston velocity for co2 surface flux [m/d]

`w_co2_stf =          4.0`

piston velocity for n2 surface flux [m/d]

`w_n2_stf =           5.0`

piston velocity for oxygen surface flux [m/d]

`w_o2_stf =           5.0`

end of table **Constants**

Process limitation factors

`lim_t_n2_7 =         theta(t_n2-0.0)`

`lim_t_o2_2 =         theta(t_o2-0.0)`

`lim_t_dic_8 =        theta(t_dic-0.0)`

end of table **Process limitation factors**

5

B3.9 Process type physics/erosion

Processes

sedimentary detritus erosion (sediment only) [mol/m^2/day]

`t_sed -> t_det`

`p_sed_ero_det =      (erosion_is_active*r_sed_ero*sed_active)*lim_t_sed_21`

continued on next page. . .

erosion of iron PO4 (sediment only) [mol/m^2/day]

`t_ips -> t_ipw`

`p_ips_ero_ipw =      (erosion_is_active*r_ips_ero*t_ips)*lim_t_ips_23`

sedimentary poc erosion (sediment only) [mol/m^2/day]

`t_sed_poc -> t_poc`

`p_sed_ero_poc =      (erosion_is_active*r_sed_ero*poc_active)*lim_t_sed_poc_22`

sedimentary pocn erosion (sediment only) [mol/m^2/day]

`t_sed_pocn -> t_pocn`

`p_sed_ero_pocn =     (erosion_is_active*r_sed_ero*pocn_active)*lim_t_sed_pocn_27`

sedimentary pocp erosion (sediment only) [mol/m^2/day]

`t_sed_pocp -> t_pocp`

`p_sed_ero_pocp =     (erosion_is_active*r_sed_ero*pocp_active)*lim_t_sed_pocp_28`

end of table **Processes**

Auxiliary variables

total carbon in sediment layer [mol/m2]**

`sed_tot =            t_sed*rfr_c + t_sed_poc + t_sed_pocn*rfr_c + t_sed_pocp*rfr_cp`

total carbon in active sediment layer [mol/m2]**

`sed_tot_active =     max(0.0,min(sed_tot,sed_max*rfr_c))`

detritus in active sediment layer [mol/m2]**

`sed_active =         sed_tot_active * t_sed/sed_tot`

switch (1=erosion, 0=no erosion) which depends on the combined bottom stress of currents and waves

continued on next page...

Auxiliary variables, continued from previous page

`erosion_is_active =   theta(cgt_current_wave_stress - critical_stress)`

poc in active sediment layer [mol/m2]**

`poc_active =          sed_tot_active * t_sed_poc/sed_tot`

pocn in active sediment layer [mol/m2]**

`pocn_active =         sed_tot_active * t_sed_pocn/sed_tot`

pocp in active sediment layer [mol/m2]**

`pocp_active =         sed_tot_active * t_sed_pocp/sed_tot`

end of table **Auxiliary variables**

Constants

critical shear stress for sediment erosion [N/m2]

`critical_stress =     0.016`

erosion rate for iron PO4 [1/day]

`r_ips_ero =           6.0`

maximum sediment detritus erosion rate [1/day]

`r_sed_ero =           6.0`

redfield ratio C/N

`rfr_c =               6.625`

redfield ratio C/P

`rfr_cp =              106.0`

maximum sediment detritus concentration that feels erosion [mol/m2]**

`sed_max =             1.0`

continued on next page...

Constants, continued from previous page

end of table **Constants**

Process limitation factors

`lim_t_sed_21 =` `theta(t_sed-0.0)`

`lim_t_ips_23 =` `theta(t_ips-0.0)`

`lim_t_sed_poc_22 =` `theta(t_sed_poc-0.0)`

`lim_t_sed_pocn_27 =` `theta(t_sed_pocn-0.0)`

`lim_t_sed_pocp_28 =` `theta(t_sed_pocp-0.0)`

end of table **Process limitation factors**

5

B3.10 Process type physics/parametrization__deep__burial

Processes

burial of detritus deeper than max__sed (sediment only) [mol/m^2/day]

`t_sed ->`

`p_sed_burial =` `((sed_tot-sed_tot_burial)/cgt_timestep*t_sed/sed_tot)*lim_t_sed_21`

burial of iron PO4 (sediment only) [mol/m^2/day]

`t_ips ->`

`p_ips_burial =` `(fac_ips_burial*(sed_tot-sed_tot_burial)/cgt_timestep*t_ips/sed_tot)*lim_t_ips_23`

continued on next page…

Processes, continued from previous page

burial of poc deeper than max_sed (sediment only) [mol/m^2/day]

```
t_sed_poc ->
p_poc_burial =       ((sed_tot-sed_tot_burial)/cgt_timestep*t_sed_poc/sed_tot)*
                     lim_t_sed_poc_22
```

burial of pocn deeper than max_sed (sediment only) [mol/m^2/day]

```
t_sed_pocn ->
p_pocn_burial =      ((sed_tot-sed_tot_burial)/cgt_timestep*t_sed_pocn/sed_tot)*
                     lim_t_sed_pocn_27
```

burial of pocp deeper than max_sed (sediment only) [mol/m^2/day]

```
t_sed_pocp ->
p_pocp_burial =      ((sed_tot-sed_tot_burial)/cgt_timestep*t_sed_pocp/sed_tot)*
                     lim_t_sed_pocp_28
```

end of table **Processes**

Auxiliary variables

total carbon in sediment layer [mol/m2]**

```
sed_tot =            t_sed*rfr_c + t_sed_poc + t_sed_pocn*rfr_c + t_sed_pocp*rfr_cp
```

total carbon in sediment layer before burial [mol/m2]**

```
sed_tot_burial =     max(0.0,min(sed_tot,sed_burial*rfr_c))
```

end of table **Auxiliary variables**

Constants

redfield ratio C/N

```
rfr_c =              6.625
```

continued on next page...

Constants, continued from previous page

redfield ratio C/P

`rfr_cp =` `106.0`

maximum sediment load before burial

`sed_burial =` `1.0`

reduced burial of t__ips, mimicing resolving iron-P complexes in deeper sediment and subsequent upward PO4 flux

`fac_ips_burial =` `0.5`

end of table **Constants**

Process limitation factors

`lim_t_sed_21 =` `theta(t_sed-0.0)`

`lim_t_ips_23 =` `theta(t_ips-0.0)`

`lim_t_sed_poc_22 =` `theta(t_sed_poc-0.0)`

`lim_t_sed_pocn_27 =` `theta(t_sed_pocn-0.0)`

`lim_t_sed_pocp_28 =` `theta(t_sed_pocp-0.0)`

end of table **Process limitation factors**

5

B3.11 Process type physics/sedimentation

Processes

detritus sedimentation (sediment only) [mol/m^2/day]

continued on next page…

Processes, continued from previous page

```
t_det -> t_sed
p_det_sedi_sed =      ((1.0-erosion_is_active)*(0.0-w_det_sedi)*t_det*cgt_density)*
                      lim_t_det_20
```

sedimentation of iron PO4 (sediment only) [mol/m^2/day]

```
t_ipw -> t_ips
p_ipw_sedi_ips =      ((1.0-erosion_is_active)*(0.0-w_ipw_sedi)*t_ipw*cgt_density)*
                      lim_t_ipw_26
```

poc sedimentation (sediment only) [mol/m^2/day]

```
t_poc -> t_sed_poc
p_poc_sedi_sed =      ((1.0-erosion_is_active)*(0.0-w_poc_var)*t_poc*cgt_density)*
                      lim_t_poc_12
```

pocn sedimentation (sediment only) [mol/m^2/day]

```
t_pocn -> t_sed_pocn
p_pocn_sedi_sed =     ((1.0-erosion_is_active)*(0.0-w_pocn_sedi)*t_pocn*cgt_density)*
                      lim_t_pocn_14
```

pocp sedimentation (sediment only) [mol/m^2/day]

```
t_pocp -> t_sed_pocp
p_pocp_sedi_sed =     ((1.0-erosion_is_active)*(0.0-w_pocp_sedi)*t_pocp*cgt_density)*
                      lim_t_pocp_13
```

end of table **Processes**

Auxiliary variables

switch (1=erosion, 0=no erosion) which depends on the combined bottom stress of currents and waves

```
erosion_is_active =   theta(cgt_current_wave_stress - critical_stress)
```

continued on next page...

Auxiliary variables, continued from previous page

depth dependent POC sinking speed

`w_poc_var =           martin_fac_poc * cgt_bottomdepth * (-1.0)`

end of table **Auxiliary variables**

Constants

critical shear stress for sediment erosion [N/m2]

`critical_stress =     0.016`

sedimentation velocity (negative for downward) [m/day]

`w_det_sedi =          -2.25`

sedimentation velocity for iron PO4 [m/day]

`w_ipw_sedi =          -0.5`

sedimentation velocity (negative for downward) [m/day]

`w_pocp_sedi =         -0.05`

sedimentation velocity (negative for downward) [m/day]

`w_pocn_sedi =         -0.05`

[1/d], depth dependence of POC sinking speed

`martin_fac_poc =      0.01`

end of table **Constants**

Process limitation factors

`lim_t_ipw_26 =        theta(t_ipw-0.0)`

`lim_t_det_20 =        theta(t_det-0.0)`

continued on next page...

Process limitation factors, continued from previous page

`lim_t_poc_12 =` `theta(t_poc-0.0)`

`lim_t_pocp_13 =` `theta(t_pocp-0.0)`

`lim_t_pocn_14 =` `theta(t_pocn-0.0)`

end of table **Process limitation factors**

B3.12 Process type standard

Processes

particle formation from DOC [mol/kg/day]

`t_doc -> t_poc`

`p_doc2pco =` `(t_doc * r_doc2poc)*lim_t_doc_29`

particle formation from DOP [mol/kg/day]

`t_dop -> t_pocp`

`p_dop2pocp =` `(t_dop * r_dop2pocp)*lim_t_dop_30`

particle formation from DON [mol/kg/day]

`t_don -> t_pocn`

`p_don2pocn =` `(t_don * r_don2pocn)*lim_t_don_31`

end of table **Processes**

Auxiliary variables

end of table **Auxiliary variables**

Constants

POC formation rate

`r_doc2poc =` 0.01

POCN formation rate

`r_don2pocn =` 0.01

POCP formation rate

`r_dop2pocp =` 0.01

end of table **Constants**

Process limitation factors

`lim_t_doc_29 =` `theta(t_doc-0.0)`

`lim_t_dop_30 =` `theta(t_dop-0.0)`

`lim_t_don_31 =` `theta(t_don-0.0)`

end of table **Process limitation factors**

B4 Tracer equations

Tracer equations

Change of: dissolved molecular nitrogen

$\frac{d}{dt}$ `t_n2` =

`+ (p_poc_denit)*(0.4)` recycling of POC using nitrate (denitrification)

`+ (p_pocp_denit)*(42.4)` recycling of POC using nitrate (denitrification)

`+ (p_pocn_denit)*(2.65)` recycling of POCN using nitrate (denitrification)

continued on next page…

Tracer equations, continued from previous page

`+ (p_det_denit_nh4)*(2.65)`	recycling of detritus using nitrate (denitrification)
`+ (p_nh4_nitdenit_n2)*(0.5) /(cgt_cellheight*cgt_density)`	coupled nitrification and denitrification after mineralization of detritus in oxic sediments
`+ (p_sed_denit_nh4)*(2.65) /(cgt_cellheight*cgt_density)`	recycling of sedimentary detritus to ammonium using nitrate (denitrification)
`+ (p_sed_poc_denit)*(0.4) /(cgt_cellheight*cgt_density)`	recycling of sedimentary poc to dic using nitrate (denitrification)
`+ (p_h2s_oxno3_sul)*(0.2)`	oxidation of hydrogen sulfide with nitrate
`+ (p_sul_oxno3_so4)*(0.6)`	oxidation of elemental sulfur with nitrate
`+ (p_sed_pocn_denit)*(2.65) /(cgt_cellheight*cgt_density)`	recycling of sedimentary pocn to dic and NH4 using nitrate (denitrification)
`+ (p_sed_pocp_denit)*(42.4) /(cgt_cellheight*cgt_density)`	recycling of sedimentary pocp to dic and PO4 using nitrate (denitrification)
`+ (p_nh4_nitdenit_pocn_n2)*(0.5) /(cgt_cellheight*cgt_density)`	coupled nitrification and denitrification after mineralization of pocn-detritus in oxic sediments
`+ (p_doc_denit)*(0.4)`	recycling of DOC using nitrate (denitrification)
`+ (p_dop_denit)*(42.4)`	recycling of DOP using nitrate (denitrification)
`+ (p_don_denit)*(2.65)`	recycling of DON using nitrate (denitrification)
`- (p_n2_assim_cya)*(0.5)`	fixation of dinitrogen by diazotroph cyanobacteria

continued on next page…

Tracer equations, continued from previous page

Change of: dissolved oxygen

$\frac{d}{dt}$ `t_o2` =

`+ (p_no3_assim_lpp)*(8.625)`	assimilation of nitrate by large-cell phytoplankton
`+ (p_nh4_assim_lpp)*(6.625)`	assimilation of ammonium by large-cell phytoplankton
`+ (p_no3_assim_spp)*(8.625)`	assimilation of nitrate by small-cell phytoplankton
`+ (p_nh4_assim_spp)*(6.625)`	assimilation of ammonium by small-cell phytoplankton
`+ (p_nh4_assim_lip)*(6.625)`	assimilation of ammonium by limnic phytoplankton
`+ (p_no3_assim_lip)*(8.625)`	assimilation of nitrate by limnic phytoplankton
`+ (p_n2_assim_cya)*(7.375)`	fixation of dinitrogen by diazotroph cyanobacteria
`+ p_assim_lpp_doc`	Production of DOC by LPP
`+ p_assim_spp_doc`	Production of DOC by SPP
`+ p_assim_lip_doc`	Production of DOC by LPP
`+ p_assim_cya_doc`	Production of DOC by CYA
`+ (p_assim_lpp_dop)*(106)`	Production of DOP by LPP
`+ (p_assim_spp_dop)*(106)`	Production of DOP by SPP

continued on next page. . .

Tracer equations, continued from previous page

`+ (p_assim_lip_dop)*(106)`	Production of DOP by LIP
`+ (p_nh4_assim_lpp_don)*(6.625)`	Production of DON by LPP
`+ (p_no3_assim_lpp_don)*(8.625)`	Production of DON by LPP
`+ (p_nh4_assim_spp_don)*(6.625)`	Production of DON by SPP
`+ (p_no3_assim_spp_don)*(8.625)`	Production of DON by SPP
`+ (p_nh4_assim_lip_don)*(6.625)`	Production of DON by LIP
`+ (p_no3_assim_lip_don)*(8.625)`	Production of DON by LIP
`- p_poc_resp`	respiration of POC
`- (p_pocp_resp)*(106)`	respiration of POCP
`- (p_pocn_resp)*(6.625)`	respiration of POCN
`- (p_lpp_resp_nh4)*(6.625)`	respiration of large-cell phytoplankton
`- (p_spp_resp_nh4)*(6.625)`	respiration of small-cell phytoplankton
`- (p_lip_resp_nh4)*(6.625)`	respiration of limnic phytoplankton
`- (p_cya_resp_nh4)*(6.625)`	respiration of diazotroph cyanobacteria
`- (p_zoo_resp_nh4)*(6.625)`	respiration of zooplankton
`- (p_nh4_nit_no3)*(2)`	nitrification

continued on next page…

Tracer equations, continued from previous page

`- (p_det_resp_nh4)*(6.625)`	recycling of detritus using oxygen (respiration)
`- (p_sed_resp_nh4)*(6.625) /(cgt_cellheight*cgt_density)`	recycling of sedimentary detritus to ammonium using oxygen (respiration)
`- (p_nh4_nitdenit_n2)*(0.75) /(cgt_cellheight*cgt_density)`	coupled nitrification and denitrification after mineralization of detritus in oxic sediments
`- p_sed_poc_resp/(cgt_cellheight* cgt_density)`	recycling of sedimentary poc to dic using oxygen (respiration)
`- (p_h2s_oxo2_sul)*(0.5)`	oxidation of hydrogen sulfide with oxygen
`- (p_sul_oxo2_so4)*(1.5)`	oxidation of elemental sulfur with oxygen
`- (p_sed_pocn_resp)*(6.625) /(cgt_cellheight*cgt_density)`	recycling of sedimentary pocn to dic and NH4 using oxygen (respiration)
`- (p_sed_pocp_resp)*(106) /(cgt_cellheight*cgt_density)`	recycling of sedimentary pocp to dic and PO4 using oxygen (respiration)
`- (p_nh4_nitdenit_pocn_n2)* (0.75)/(cgt_cellheight* cgt_density)`	coupled nitrification and denitrification after mineralization of pocn-detritus in oxic sediments
`- p_doc_resp`	respiration of DOC
`- (p_dop_resp)*(106)`	respiration of DOP
`- (p_don_resp)*(6.625)`	respiration of DON

continued on next page...

Change of: dissolved inorganic carbon, treated as carbon dioxide

$\frac{d}{dt}$ `t_dic` =

`+ p_poc_resp`	respiration of POC
`+ p_poc_denit`	recycling of POC using nitrate (denitrification)
`+ p_poc_sulf`	Mineralization of POC, e-acceptor sulfate (sulfate reduction)
`+ (p_pocp_resp)*(106)`	respiration of POCP
`+ (p_pocp_denit)*(106)`	recycling of POC using nitrate (denitrification)
`+ (p_pocp_sulf)*(106)`	Mineralization of POC, e-acceptor sulfate (sulfate reduction)
`+ (p_pocn_resp)*(6.625)`	respiration of POCN
`+ (p_pocn_denit)*(6.625)`	recycling of POCN using nitrate (denitrification)
`+ (p_pocn_sulf)*(6.625)`	Mineralization of POCN, e-acceptor sulfate (sulfate reduction)
`+ (p_lpp_resp_nh4)*(rfr_c)`	respiration of large-cell phytoplankton
`+ (p_spp_resp_nh4)*(rfr_c)`	respiration of small-cell phytoplankton
`+ (p_lip_resp_nh4)*(rfr_c)`	respiration of limnic phytoplankton
`+ (p_cya_resp_nh4)*(rfr_c)`	respiration of diazotroph cyanobacteria

continued on next page. . .

Tracer equations, continued from previous page

`+ (p_zoo_resp_nh4)*(rfr_c)`	respiration of zooplankton
`+ (p_det_resp_nh4)*(rfr_c)`	recycling of detritus using oxygen (respiration)
`+ (p_det_denit_nh4)*(rfr_c)`	recycling of detritus using nitrate (denitrification)
`+ (p_det_sulf_nh4)*(rfr_c)`	recycling of detritus using sulfate (sulfate reduction)
`+ (p_sed_resp_nh4)*(rfr_c) /(cgt_cellheight*cgt_density)`	recycling of sedimentary detritus to ammonium using oxygen (respiration)
`+ (p_sed_denit_nh4)*(rfr_c) /(cgt_cellheight*cgt_density)`	recycling of sedimentary detritus to ammonium using nitrate (denitrification)
`+ (p_sed_sulf_nh4)*(rfr_c) /(cgt_cellheight*cgt_density)`	recycling of sedimentary detritus to ammonium using sulfate (sulfate reduction)
`+ p_sed_poc_resp/(cgt_cellheight* cgt_density)`	recycling of sedimentary poc to dic using oxygen (respiration)
`+ p_sed_poc_denit/(cgt_cellheight* cgt_density)`	recycling of sedimentary poc to dic using nitrate (denitrification)
`+ p_sed_poc_sulf/(cgt_cellheight* cgt_density)`	recycling of sedimentary poc to dic using sulfate (sulfate reduction)
`+ (p_sed_pocn_resp)*(6.625) /(cgt_cellheight*cgt_density)`	recycling of sedimentary pocn to dic and NH4 using oxygen (respiration)

continued on next page…

Tracer equations, continued from previous page

+ (p_sed_pocp_resp)*(106) /(cgt_cellheight*cgt_density)	recycling of sedimentary pocp to dic and PO4 using oxygen (respiration)
+ (p_sed_pocn_denit)*(6.625) /(cgt_cellheight*cgt_density)	recycling of sedimentary pocn to dic and NH4 using nitrate (denitrification)
+ (p_sed_pocp_denit)*(106) /(cgt_cellheight*cgt_density)	recycling of sedimentary pocp to dic and PO4 using nitrate (denitrification)
+ (p_sed_pocn_sulf)*(6.625) /(cgt_cellheight*cgt_density)	recycling of sedimentary pocn to dic and NH4 using sulfate (sulfate reduction)
+ (p_sed_pocp_sulf)*(106) /(cgt_cellheight*cgt_density)	recycling of sedimentary pocp to dic and PO4 using sulfate (sulfate reduction)
+ p_doc_resp	respiration of DOC
+ p_doc_denit	recycling of DOC using nitrate (denitrification)
+ p_doc_sulf	Mineralization of DOC, e-acceptor sulfate (sulfate reduction)
+ (p_dop_resp)*(106)	respiration of DOP
+ (p_dop_denit)*(106)	recycling of DOP using nitrate (denitrification)
+ (p_dop_sulf)*(106)	Mineralization of DOP, e-acceptor sulfate (sulfate reduction)
+ (p_don_resp)*(6.625)	respiration of DON
+ (p_don_denit)*(6.625)	recycling of DON using nitrate (denitrification)

continued on next page…

`+ (p_don_sulf)*(6.625)`	Mineralization of DON, e-acceptor sulfate (sulfate reduction)
`- (p_no3_assim_lpp)*(rfr_c)`	assimilation of nitrate by large-cell phytoplankton
`- (p_nh4_assim_lpp)*(rfr_c)`	assimilation of ammonium by large-cell phytoplankton
`- (p_no3_assim_spp)*(rfr_c)`	assimilation of nitrate by small-cell phytoplankton
`- (p_nh4_assim_spp)*(rfr_c)`	assimilation of ammonium by small-cell phytoplankton
`- (p_nh4_assim_lip)*(rfr_c)`	assimilation of ammonium by limnic phytoplankton
`- (p_no3_assim_lip)*(rfr_c)`	assimilation of nitrate by limnic phytoplankton
`- (p_n2_assim_cya)*(rfr_c)`	fixation of dinitrogen by diazotroph cyanobacteria
`- p_assim_lpp_doc`	Production of DOC by LPP
`- p_assim_spp_doc`	Production of DOC by SPP
`- p_assim_lip_doc`	Production of DOC by LPP
`- p_assim_cya_doc`	Production of DOC by CYA
`- (p_assim_lpp_dop)*(106)`	Production of DOP by LPP
`- (p_assim_spp_dop)*(106)`	Production of DOP by SPP

continued on next page…

Tracer equations, continued from previous page

`- (p_assim_lip_dop)*(106)`	Production of DOP by LIP
`- (p_nh4_assim_lpp_don)*(rfr_c)`	Production of DON by LPP
`- (p_no3_assim_lpp_don)*(rfr_c)`	Production of DON by LPP
`- (p_nh4_assim_spp_don)*(rfr_c)`	Production of DON by SPP
`- (p_no3_assim_spp_don)*(rfr_c)`	Production of DON by SPP
`- (p_nh4_assim_lip_don)*(rfr_c)`	Production of DON by LIP
`- (p_no3_assim_lip_don)*(rfr_c)`	Production of DON by LIP

Change of: ammonium

$\frac{d}{dt}$ `t_nh4` =

`+ p_pocn_resp`	respiration of POCN
`+ p_pocn_denit`	recycling of POCN using nitrate (denitrification)
`+ p_pocn_sulf`	Mineralization of POCN, e-acceptor sulfate (sulfate reduction)
`+ (p_lpp_resp_nh4)*((1-don_fraction))`	respiration of large-cell phytoplankton
`+ (p_spp_resp_nh4)*((1-don_fraction))`	respiration of small-cell phytoplankton
`+ (p_lip_resp_nh4)*((1-don_fraction))`	respiration of limnic phytoplankton

continued on next page…

Tracer equations, continued from previous page

`+ (p_cya_resp_nh4)*((1-don_fraction))`	respiration of diazotroph cyanobacteria
`+ (p_zoo_resp_nh4)*((1-don_fraction))`	respiration of zooplankton
`+ p_det_resp_nh4`	recycling of detritus using oxygen (respiration)
`+ p_det_denit_nh4`	recycling of detritus using nitrate (denitrification)
`+ p_det_sulf_nh4`	recycling of detritus using sulfate (sulfate reduction)
`+ p_sed_resp_nh4/(cgt_cellheight*cgt_density)`	recycling of sedimentary detritus to ammonium using oxygen (respiration)
`+ p_sed_denit_nh4/(cgt_cellheight*cgt_density)`	recycling of sedimentary detritus to ammonium using nitrate (denitrification)
`+ p_sed_sulf_nh4/(cgt_cellheight*cgt_density)`	recycling of sedimentary detritus to ammonium using sulfate (sulfate reduction)
`+ p_sed_pocn_resp/(cgt_cellheight*cgt_density)`	recycling of sedimentary pocn to dic and NH4 using oxygen (respiration)
`+ p_sed_pocn_denit/(cgt_cellheight*cgt_density)`	recycling of sedimentary pocn to dic and NH4 using nitrate (denitrification)

continued on next page. . .

`+ p_sed_pocn_sulf/(cgt_cellheight*cgt_density)`	recycling of sedimentary pocn to dic and NH4 using sulfate (sulfate reduction)
`+ p_don_resp`	respiration of DON
`+ p_don_denit`	recycling of DON using nitrate (denitrification)
`+ p_don_sulf`	Mineralization of DON, e-acceptor sulfate (sulfate reduction)
`- p_nh4_assim_lpp`	assimilation of ammonium by large-cell phytoplankton
`- p_nh4_assim_spp`	assimilation of ammonium by small-cell phytoplankton
`- p_nh4_assim_lip`	assimilation of ammonium by limnic phytoplankton
`- p_nh4_assim_lpp_don`	Production of DON by LPP
`- p_nh4_assim_spp_don`	Production of DON by SPP
`- p_nh4_assim_lip_don`	Production of DON by LIP
`- p_nh4_nit_no3`	nitrification
`- p_nh4_nitdenit_n2/(cgt_cellheight cgt_density)`	coupled nitrification and denitrification after mineralization of detritus in oxic sediments

continued on next page…

`- p_nh4_nitdenit_pocn_n2/(cgt_cellh` `cgt_density)`	coupled nitrification and denitrification after mineralization of pocn-detritus in oxic sediments

Change of: nitrate

$\frac{d}{dt}$ `t_no3` =

`+ p_nh4_nit_no3`	nitrification
`- p_no3_assim_lpp`	assimilation of nitrate by large-cell phytoplankton
`- p_no3_assim_spp`	assimilation of nitrate by small-cell phytoplankton
`- p_no3_assim_lip`	assimilation of nitrate by limnic phytoplankton
`- p_no3_assim_lpp_don`	Production of DON by LPP
`- p_no3_assim_spp_don`	Production of DON by SPP
`- p_no3_assim_lip_don`	Production of DON by LIP
`- (p_poc_denit)*(0.8)`	recycling of POC using nitrate (denitrification)
`- (p_pocp_denit)*(84.8)`	recycling of POC using nitrate (denitrification)
`- (p_pocn_denit)*(5.3)`	recycling of POCN using nitrate (denitrification)
`- (p_det_denit_nh4)*(5.3)`	recycling of detritus using nitrate (denitrification)
`- (p_sed_denit_nh4)*(5.3)` `/(cgt_cellheight*cgt_density)`	recycling of sedimentary detritus to ammonium using nitrate (denitrification)

continued on next page…

Tracer equations, continued from previous page

`- (p_sed_poc_denit)*(0.8) /(cgt_cellheight*cgt_density)`	recycling of sedimentary poc to dic using nitrate (denitrification)
`- (p_h2s_oxno3_sul)*(0.4)`	oxidation of hydrogen sulfide with nitrate
`- (p_sul_oxno3_so4)*(1.2)`	oxidation of elemental sulfur with nitrate
`- (p_sed_pocn_denit)*(5.3) /(cgt_cellheight*cgt_density)`	recycling of sedimentary pocn to dic and NH4 using nitrate (denitrification)
`- (p_sed_pocp_denit)*(84.8) /(cgt_cellheight*cgt_density)`	recycling of sedimentary pocp to dic and PO4 using nitrate (denitrification)
`- (p_doc_denit)*(0.8)`	recycling of DOC using nitrate (denitrification)
`- (p_dop_denit)*(84.8)`	recycling of DOP using nitrate (denitrification)
`- (p_don_denit)*(5.3)`	recycling of DON using nitrate (denitrification)

Change of: phosphate

$\frac{d}{dt}$ `t_po4` $=$

`+ p_pocp_resp`	respiration of POCP
`+ p_pocp_denit`	recycling of POC using nitrate (denitrification)
`+ p_pocp_sulf`	Mineralization of POC, e-acceptor sulfate (sulfate reduction)
`+ (p_lpp_resp_nh4)*(rfr_p)`	respiration of large-cell phytoplankton
`+ (p_spp_resp_nh4)*(rfr_p)`	respiration of small-cell phytoplankton

continued on next page…

Tracer equations, continued from previous page

`+ (p_lip_resp_nh4)*(rfr_p)`	respiration of limnic phytoplankton
`+ (p_cya_resp_nh4)*(rfr_p)`	respiration of diazotroph cyanobacteria
`+ (p_zoo_resp_nh4)*(rfr_p)`	respiration of zooplankton
`+ (p_det_resp_nh4)*(rfr_p)`	recycling of detritus using oxygen (respiration)
`+ (p_det_denit_nh4)*(rfr_p)`	recycling of detritus using nitrate (denitrification)
`+ (p_det_sulf_nh4)*(rfr_p)`	recycling of detritus using sulfate (sulfate reduction)
`+ (p_sed_resp_nh4)*(rfr_p)/(cgt_cellheight*cgt_density)`	recycling of sedimentary detritus to ammonium using oxygen (respiration)
`+ (p_sed_denit_nh4)*(rfr_p)/(cgt_cellheight*cgt_density)`	recycling of sedimentary detritus to ammonium using nitrate (denitrification)
`+ (p_sed_sulf_nh4)*(rfr_p)/(cgt_cellheight*cgt_density)`	recycling of sedimentary detritus to ammonium using sulfate (sulfate reduction)
`+ p_ips_liber_po4/(cgt_cellheight*cgt_density)`	liberation of phosphate from the sediment under anoxic conditions
`+ p_sed_pocp_resp/(cgt_cellheight*cgt_density)`	recycling of sedimentary pocp to dic and PO4 using oxygen (respiration)

continued on next page…

`+ p_sed_pocp_denit/(cgt_cellheight* cgt_density)`	recycling of sedimentary pocp to dic and PO4 using nitrate (denitrification)
`+ p_sed_pocp_sulf/(cgt_cellheight* cgt_density)`	recycling of sedimentary pocp to dic and PO4 using sulfate (sulfate reduction)
`+ p_dop_resp`	respiration of DOP
`+ p_dop_denit`	recycling of DOP using nitrate (denitrification)
`+ p_dop_sulf`	Mineralization of DOP, e-acceptor sulfate (sulfate reduction)
`- (p_no3_assim_lpp)*(rfr_p)`	assimilation of nitrate by large-cell phytoplankton
`- (p_nh4_assim_lpp)*(rfr_p)`	assimilation of ammonium by large-cell phytoplankton
`- (p_no3_assim_spp)*(rfr_p)`	assimilation of nitrate by small-cell phytoplankton
`- (p_nh4_assim_spp)*(rfr_p)`	assimilation of ammonium by small-cell phytoplankton
`- (p_nh4_assim_lip)*(rfr_p)`	assimilation of ammonium by limnic phytoplankton
`- (p_no3_assim_lip)*(rfr_p)`	assimilation of nitrate by limnic phytoplankton
`- (p_n2_assim_cya)*(rfr_p)`	fixation of dinitrogen by diazotroph cyanobacteria
`- p_assim_lpp_dop`	Production of DOP by LPP

continued on next page…

`- p_assim_spp_dop`	Production of DOP by SPP
`- p_assim_lip_dop`	Production of DOP by LIP
`- (p_po4_retent_ips)*(rfr_p)` `/(cgt_cellheight*cgt_density)`	retention of phosphate in the sediment under oxic conditions

Change of: small-cell phytoplankton

$\frac{d}{dt}$ `t_spp` $=$

`+ p_no3_assim_spp`	assimilation of nitrate by small-cell phytoplankton
`+ p_nh4_assim_spp`	assimilation of ammonium by small-cell phytoplankton
`- p_spp_graz_zoo`	grazing of zooplankton eating small-cell phytoplankton
`- p_spp_resp_nh4`	respiration of small-cell phytoplankton
`- p_spp_mort_det`	mortality of small-scale phytoplankton

Change of: zooplankton

$\frac{d}{dt}$ `t_zoo` $=$

`+ p_lpp_graz_zoo`	grazing of zooplankton eating large-cell phytoplankton
`+ p_spp_graz_zoo`	grazing of zooplankton eating small-cell phytoplankton

continued on next page...

`+ p_cya_graz_zoo`	grazing of zooplankton eating diazotroph cyanobacteria
`+ p_lip_graz_zoo`	grazing of zooplankton eating limnic phytoplankton
`- p_zoo_resp_nh4`	respiration of zooplankton
`- p_zoo_mort_det`	mortality of zooplankton

Change of: hydrogen sulfide

$\frac{d}{dt}$ `t_h2s` =

`+ (p_poc_sulf)*(0.5)`	Mineralization of POC, e-acceptor sulfate (sulfate reduction)
`+ (p_pocp_sulf)*(53)`	Mineralization of POC, e-acceptor sulfate (sulfate reduction)
`+ (p_pocn_sulf)*(3.3125)`	Mineralization of POCN, e-acceptor sulfate (sulfate reduction)
`+ (p_det_sulf_nh4)*(3.3125)`	recycling of detritus using sulfate (sulfate reduction)
`+ (p_sed_sulf_nh4)*(3.3125) /(cgt_cellheight*cgt_density)`	recycling of sedimentary detritus to ammonium using sulfate (sulfate reduction)
`+ (p_sed_poc_sulf)*(0.5) /(cgt_cellheight*cgt_density)`	recycling of sedimentary poc to dic using sulfate (sulfate reduction)
`+ (p_sed_pocn_sulf)*(3.3125) /(cgt_cellheight*cgt_density)`	recycling of sedimentary pocn to dic and NH4 using sulfate (sulfate reduction)

continued on next page…

Tracer equations, continued from previous page

`+ (p_sed_pocp_sulf)*(53)` `/(cgt_cellheight*cgt_density)`	recycling of sedimentary pocp to dic and PO4 using sulfate (sulfate reduction)
`+ (p_doc_sulf)*(0.5)`	Mineralization of DOC, e-acceptor sulfate (sulfate reduction)
`+ (p_dop_sulf)*(53)`	Mineralization of DOP, e-acceptor sulfate (sulfate reduction)
`+ (p_don_sulf)*(3.3125)`	Mineralization of DON, e-acceptor sulfate (sulfate reduction)
`- p_h2s_oxo2_sul`	oxidation of hydrogen sulfide with oxygen
`- p_h2s_oxno3_sul`	oxidation of hydrogen sulfide with nitrate

Change of: sulfur

$\frac{d}{dt}$ `t_sul` =

`+ p_h2s_oxo2_sul`	oxidation of hydrogen sulfide with oxygen
`+ p_h2s_oxno3_sul`	oxidation of hydrogen sulfide with nitrate
`- p_sul_oxo2_so4`	oxidation of elemental sulfur with oxygen
`- p_sul_oxno3_so4`	oxidation of elemental sulfur with nitrate

Change of: total alkalinity

$\frac{d}{dt}$ `t_alk` =

`+ (1)*(p_pocn_resp)*(0.5)`	respiration of POCN (produces ohminus)

continued on next page…

Tracer equations, continued from previous page

`+ (1)*(p_pocn_denit)*(0.5)`	recycling of POCN using nitrate (denitrification) (produces ohminus)
`+ (1)*(p_pocn_sulf)*(0.5)`	Mineralization of POCN, e-acceptor sulfate (sulfate reduction) (produces ohminus)
`+ (1)*(p_sed_pocn_resp)*(0.5)` `/(cgt_cellheight*cgt_density)`	recycling of sedimentary pocn to dic and NH4 using oxygen (respiration) (produces ohminus)
`+ (1)*(p_sed_pocn_denit)*(0.5)` `/(cgt_cellheight*cgt_density)`	recycling of sedimentary pocn to dic and NH4 using nitrate (denitrification) (produces ohminus)
`+ (1)*(p_sed_pocn_sulf)*(0.5)` `/(cgt_cellheight*cgt_density)`	recycling of sedimentary pocn to dic and NH4 using sulfate (sulfate reduction) (produces ohminus)
`+ (1)*(p_don_resp)*(0.5)`	respiration of DON (produces ohminus)
`+ (1)*(p_don_denit)*(0.5)`	recycling of DON using nitrate (denitrification) (produces ohminus)
`+ (1)*(p_don_sulf)*(0.5)`	Mineralization of DON, e-acceptor sulfate (sulfate reduction) (produces ohminus)
`- (1)*(p_nh4_assim_lpp_don)`	Production of DON by LPP (consumes ohminus)
`- (1)*(p_nh4_assim_spp_don)`	Production of DON by SPP (consumes ohminus)
`- (1)*(p_nh4_assim_lip_don)`	Production of DON by LIP (consumes ohminus)
`- (1)*(p_pocp_denit)*(3)`	recycling of POC using nitrate (denitrification) (consumes ohminus)

continued on next page…

Tracer equations, continued from previous page

`- (1)*(p_pocp_sulf)*(3)`	Mineralization of POC, e-acceptor sulfate (sulfate reduction) (consumes ohminus)
`- (1)*(p_sed_pocp_denit)*(3) /(cgt_cellheight*cgt_density)`	recycling of sedimentary pocp to dic and PO4 using nitrate (denitrification) (consumes ohminus)
`- (1)*(p_sed_pocp_sulf)*(3) /(cgt_cellheight*cgt_density)`	recycling of sedimentary pocp to dic and PO4 using sulfate (sulfate reduction) (consumes ohminus)
`- (1)*(p_dop_denit)*(3)`	recycling of DOP using nitrate (denitrification) (consumes ohminus)
`- (1)*(p_dop_sulf)*(3)`	Mineralization of DOP, e-acceptor sulfate (sulfate reduction) (consumes ohminus)
`+ (-1)*(p_nh4_assim_lpp)* (0.8125)`	assimilation of ammonium by large-cell phytoplankton (produces h3oplus)
`+ (-1)*(p_nh4_assim_spp)* (0.8125)`	assimilation of ammonium by small-cell phytoplankton (produces h3oplus)
`+ (-1)*(p_nh4_assim_lip)* (0.8125)`	assimilation of ammonium by limnic phytoplankton (produces h3oplus)
`+ (-1)*(p_pocp_resp)*(3)`	respiration of POCP (produces h3oplus)
`+ (-1)*(p_nh4_nit_no3)*(2)`	nitrification (produces h3oplus)
`+ (-1)*(p_nh4_nitdenit_n2) /(cgt_cellheight*cgt_density)`	coupled nitrification and denitrification after mineralization of detritus in oxic sediments (produces h3oplus)

continued on next page…

Tracer equations, continued from previous page

`+ (-1)*(p_sul_oxo2_so4)*(2)`	oxidation of elemental sulfur with oxygen (produces h3oplus)
`+ (-1)*(p_sul_oxno3_so4)*(0.8)`	oxidation of elemental sulfur with nitrate (produces h3oplus)
`+ (-1)*(p_sed_pocp_resp)*(3) /(cgt_cellheight*cgt_density)`	recycling of sedimentary pocp to dic and PO4 using oxygen (respiration) (produces h3oplus)
`+ (-1)*(p_nh4_nitdenit_pocn_n2) /(cgt_cellheight*cgt_density)`	coupled nitrification and denitrification after mineralization of pocn-detritus in oxic sediments (produces h3oplus)
`+ (-1)*(p_dop_resp)*(3)`	respiration of DOP (produces h3oplus)
`- (-1)*(p_no3_assim_lpp)* (1.1875)`	assimilation of nitrate by large-cell phytoplankton (consumes h3oplus)
`- (-1)*(p_no3_assim_spp)* (1.1875)`	assimilation of nitrate by small-cell phytoplankton (consumes h3oplus)
`- (-1)*(p_no3_assim_lip)* (1.1875)`	assimilation of nitrate by limnic phytoplankton (consumes h3oplus)
`- (-1)*(p_n2_assim_cya)*(0.1875)`	fixation of dinitrogen by diazotroph cyanobacteria (consumes h3oplus)
`- (-1)*(p_assim_lpp_dop)*(3)`	Production of DOP by LPP (consumes h3oplus)
`- (-1)*(p_assim_spp_dop)*(3)`	Production of DOP by SPP (consumes h3oplus)
`- (-1)*(p_assim_lip_dop)*(3)`	Production of DOP by LIP (consumes h3oplus)

continued on next page. . .

`- (-1)*(p_no3_assim_lpp_don)`	Production of DON by LPP (consumes h3oplus)
`- (-1)*(p_no3_assim_spp_don)`	Production of DON by SPP (consumes h3oplus)
`- (-1)*(p_no3_assim_lip_don)`	Production of DON by LIP (consumes h3oplus)
`- (-1)*(p_poc_denit)*(0.8)`	recycling of POC using nitrate (denitrification) (consumes h3oplus)
`- (-1)*(p_poc_sulf)`	Mineralization of POC, e-acceptor sulfate (sulfate reduction) (consumes h3oplus)
`- (-1)*(p_pocp_denit)*(84.8)`	recycling of POC using nitrate (denitrification) (consumes h3oplus)
`- (-1)*(p_pocp_sulf)*(106)`	Mineralization of POC, e-acceptor sulfate (sulfate reduction) (consumes h3oplus)
`- (-1)*(p_pocn_resp)*(0.5)`	respiration of POCN (consumes h3oplus)
`- (-1)*(p_pocn_denit)*(5.8)`	recycling of POCN using nitrate (denitrification) (consumes h3oplus)
`- (-1)*(p_pocn_sulf)*(7.125)`	Mineralization of POCN, e-acceptor sulfate (sulfate reduction) (consumes h3oplus)
`- (-1)*(p_lpp_resp_nh4)*(0.8125)`	respiration of large-cell phytoplankton (consumes h3oplus)
`- (-1)*(p_spp_resp_nh4)*(0.8125)`	respiration of small-cell phytoplankton (consumes h3oplus)

continued on next page…

`- (-1)*(p_lip_resp_nh4)*(0.8125)`	respiration of limnic phytoplankton (consumes h3oplus)
`- (-1)*(p_cya_resp_nh4)*(0.8125)`	respiration of diazotroph cyanobacteria (consumes h3oplus)
`- (-1)*(p_zoo_resp_nh4)*(0.8125)`	respiration of zooplankton (consumes h3oplus)
`- (-1)*(p_det_resp_nh4)*(0.8125)`	recycling of detritus using oxygen (respiration) (consumes h3oplus)
`- (-1)*(p_det_denit_nh4)*(6.1125)`	recycling of detritus using nitrate (denitrification) (consumes h3oplus)
`- (-1)*(p_det_sulf_nh4)*(7.4375)`	recycling of detritus using sulfate (sulfate reduction) (consumes h3oplus)
`- (-1)*(p_sed_resp_nh4)*(0.8125)/(cgt_cellheight*cgt_density)`	recycling of sedimentary detritus to ammonium using oxygen (respiration) (consumes h3oplus)
`- (-1)*(p_sed_denit_nh4)*(6.1125)/(cgt_cellheight*cgt_density)`	recycling of sedimentary detritus to ammonium using nitrate (denitrification) (consumes h3oplus)
`- (-1)*(p_sed_sulf_nh4)*(7.4375)/(cgt_cellheight*cgt_density)`	recycling of sedimentary detritus to ammonium using sulfate (sulfate reduction) (consumes h3oplus)
`- (-1)*(p_sed_poc_denit)*(0.8)/(cgt_cellheight*cgt_density)`	recycling of sedimentary poc to dic using nitrate (denitrification) (consumes h3oplus)

continued on next page…

Tracer equations, continued from previous page

`- (-1)*(p_sed_poc_sulf) /(cgt_cellheight*cgt_density)`	recycling of sedimentary poc to dic using sulfate (sulfate reduction) (consumes h3oplus)
`- (-1)*(p_h2s_oxno3_sul)*(0.4)`	oxidation of hydrogen sulfide with nitrate (consumes h3oplus)
`- (-1)*(p_sed_pocn_resp)*(0.5) /(cgt_cellheight*cgt_density)`	recycling of sedimentary pocn to dic and NH4 using oxygen (respiration) (consumes h3oplus)
`- (-1)*(p_sed_pocn_denit)*(5.8) /(cgt_cellheight*cgt_density)`	recycling of sedimentary pocn to dic and NH4 using nitrate (denitrification) (consumes h3oplus)
`- (-1)*(p_sed_pocp_denit)*(84.8) /(cgt_cellheight*cgt_density)`	recycling of sedimentary pocp to dic and PO4 using nitrate (denitrification) (consumes h3oplus)
`- (-1)*(p_sed_pocn_sulf)*(7.125) /(cgt_cellheight*cgt_density)`	recycling of sedimentary pocn to dic and NH4 using sulfate (sulfate reduction) (consumes h3oplus)
`- (-1)*(p_sed_pocp_sulf)*(106) /(cgt_cellheight*cgt_density)`	recycling of sedimentary pocp to dic and PO4 using sulfate (sulfate reduction) (consumes h3oplus)
`- (-1)*(p_doc_denit)*(0.8)`	recycling of DOC using nitrate (denitrification) (consumes h3oplus)
`- (-1)*(p_doc_sulf)`	Mineralization of DOC, e-acceptor sulfate (sulfate reduction) (consumes h3oplus)
`- (-1)*(p_dop_denit)*(84.8)`	recycling of DOP using nitrate (denitrification) (consumes h3oplus)
`- (-1)*(p_dop_sulf)*(106)`	Mineralization of DOP, e-acceptor sulfate (sulfate reduction) (consumes h3oplus)

continued on next page…

Tracer equations, continued from previous page

`- (-1)*(p_don_resp)*(0.5)`	respiration of DON (consumes h3oplus)
`- (-1)*(p_don_denit)*(5.8)`	recycling of DON using nitrate (denitrification) (consumes h3oplus)
`- (-1)*(p_don_sulf)*(7.125)`	Mineralization of DON, e-acceptor sulfate (sulfate reduction) (consumes h3oplus)
`+ (2)*(p_pocp_resp)`	respiration of POCP (produces t_po4)
`+ (2)*(p_pocp_denit)`	recycling of POC using nitrate (denitrification) (produces t_po4)
`+ (2)*(p_pocp_sulf)`	Mineralization of POC, e-acceptor sulfate (sulfate reduction) (produces t_po4)
`+ (2)*(p_lpp_resp_nh4)*(rfr_p)`	respiration of large-cell phytoplankton (produces t_po4)
`+ (2)*(p_spp_resp_nh4)*(rfr_p)`	respiration of small-cell phytoplankton (produces t_po4)
`+ (2)*(p_lip_resp_nh4)*(rfr_p)`	respiration of limnic phytoplankton (produces t_po4)
`+ (2)*(p_cya_resp_nh4)*(rfr_p)`	respiration of diazotroph cyanobacteria (produces t_po4)
`+ (2)*(p_zoo_resp_nh4)*(rfr_p)`	respiration of zooplankton (produces t_po4)

continued on next page…

Tracer equations, continued from previous page

`+ (2)*(p_det_resp_nh4)*(rfr_p)`	recycling of detritus using oxygen (respiration) (produces t_po4)
`+ (2)*(p_det_denit_nh4)*(rfr_p)`	recycling of detritus using nitrate (denitrification) (produces t_po4)
`+ (2)*(p_det_sulf_nh4)*(rfr_p)`	recycling of detritus using sulfate (sulfate reduction) (produces t_po4)
`+ (2)*(p_sed_resp_nh4)*(rfr_p) /(cgt_cellheight*cgt_density)`	recycling of sedimentary detritus to ammonium using oxygen (respiration) (produces t_po4)
`+ (2)*(p_sed_denit_nh4)*(rfr_p) /(cgt_cellheight*cgt_density)`	recycling of sedimentary detritus to ammonium using nitrate (denitrification) (produces t_po4)
`+ (2)*(p_sed_sulf_nh4)*(rfr_p) /(cgt_cellheight*cgt_density)`	recycling of sedimentary detritus to ammonium using sulfate (sulfate reduction) (produces t_po4)
`+ (2)*(p_ips_liber_po4) /(cgt_cellheight*cgt_density)`	liberation of phosphate from the sediment under anoxic conditions (produces t_po4)
`+ (2)*(p_sed_pocp_resp) /(cgt_cellheight*cgt_density)`	recycling of sedimentary pocp to dic and PO4 using oxygen (respiration) (produces t_po4)
`+ (2)*(p_sed_pocp_denit) /(cgt_cellheight*cgt_density)`	recycling of sedimentary pocp to dic and PO4 using nitrate (denitrification) (produces t_po4)
`+ (2)*(p_sed_pocp_sulf) /(cgt_cellheight*cgt_density)`	recycling of sedimentary pocp to dic and PO4 using sulfate (sulfate reduction) (produces t_po4)
`+ (2)*(p_dop_resp)`	respiration of DOP (produces t_po4)

continued on next page…

Tracer equations, continued from previous page

`+ (2)*(p_dop_denit)`	recycling of DOP using nitrate (denitrification) (produces t_po4)
`+ (2)*(p_dop_sulf)`	Mineralization of DOP, e-acceptor sulfate (sulfate reduction) (produces t_po4)
`- (2)*(p_no3_assim_lpp)*(rfr_p)`	assimilation of nitrate by large-cell phytoplankton (consumes t_po4)
`- (2)*(p_nh4_assim_lpp)*(rfr_p)`	assimilation of ammonium by large-cell phytoplankton (consumes t_po4)
`- (2)*(p_no3_assim_spp)*(rfr_p)`	assimilation of nitrate by small-cell phytoplankton (consumes t_po4)
`- (2)*(p_nh4_assim_spp)*(rfr_p)`	assimilation of ammonium by small-cell phytoplankton (consumes t_po4)
`- (2)*(p_nh4_assim_lip)*(rfr_p)`	assimilation of ammonium by limnic phytoplankton (consumes t_po4)
`- (2)*(p_no3_assim_lip)*(rfr_p)`	assimilation of nitrate by limnic phytoplankton (consumes t_po4)
`- (2)*(p_n2_assim_cya)*(rfr_p)`	fixation of dinitrogen by diazotroph cyanobacteria (consumes t_po4)
`- (2)*(p_assim_lpp_dop)`	Production of DOP by LPP (consumes t_po4)
`- (2)*(p_assim_spp_dop)`	Production of DOP by SPP (consumes t_po4)
`- (2)*(p_assim_lip_dop)`	Production of DOP by LIP (consumes t_po4)

continued on next page...

Tracer equations, continued from previous page

`- (2)*(p_po4_retent_ips)*(rfr_p) /(cgt_cellheight*cgt_density)`	retention of phosphate in the sediment under oxic conditions (consumes t_po4)

Change of: sediment detritus

$\frac{d}{dt}\,\texttt{t\_sed} =$

`+ p_det_sedi_sed`	detritus sedimentation
`- p_sed_resp_nh4`	recycling of sedimentary detritus to ammonium using oxygen (respiration)
`- p_sed_denit_nh4`	recycling of sedimentary detritus to ammonium using nitrate (denitrification)
`- p_sed_sulf_nh4`	recycling of sedimentary detritus to ammonium using sulfate (sulfate reduction)
`- p_sed_ero_det`	sedimentary detritus erosion
`- p_sed_biores_det`	bio resuspension of sedimentary detritus
`- p_sed_burial`	burial of detritus deeper than max_sed

Change of: iron phosphate in sediment

$\frac{d}{dt}\,\texttt{t\_ips} =$

`+ (p_po4_retent_ips)*(rfr_p)`	retention of phosphate in the sediment under oxic conditions
`+ p_ipw_sedi_ips`	sedimentation of iron PO4

continued on next page…

Tracer equations, continued from previous page

`- p_ips_liber_po4`	liberation of phosphate from the sediment under anoxic conditions
`- p_ips_ero_ipw`	erosion of iron PO4
`- p_ips_biores_ipw`	bio resuspension of iron PO4
`- p_ips_burial`	burial of iron PO4

Change of: limnic phytoplankton

$\frac{d}{dt}$ `t_lip` $=$

`+ p_nh4_assim_lip`	assimilation of ammonium by limnic phytoplankton
`+ p_no3_assim_lip`	assimilation of nitrate by limnic phytoplankton
`- p_lip_graz_zoo`	grazing of zooplankton eating limnic phytoplankton
`- p_lip_resp_nh4`	respiration of limnic phytoplankton
`- p_lip_mort_det`	mortality of limnic phytoplankton

Change of: dissolved organic carbon

$\frac{d}{dt}$ `t_doc` $=$

`+ p_assim_lpp_doc`	Production of DOC by LPP
`+ p_assim_spp_doc`	Production of DOC by SPP
`+ p_assim_lip_doc`	Production of DOC by LPP
`+ p_assim_cya_doc`	Production of DOC by CYA

continued on next page…

Tracer equations, continued from previous page

`- p_doc2pco`	particle formation from DOC
`- p_doc_resp`	respiration of DOC
`- p_doc_denit`	recycling of DOC using nitrate (denitrification)
`- p_doc_sulf`	Mineralization of DOC, e-acceptor sulfate (sulfate reduction)

Change of: phosphorus in dissolved organic carbon in Redfield ratio

$\frac{d}{dt}$ `t_dop` $=$

`+ p_assim_lpp_dop`	Production of DOP by LPP
`+ p_assim_spp_dop`	Production of DOP by SPP
`+ p_assim_lip_dop`	Production of DOP by LIP
`- p_dop2pocp`	particle formation from DOP
`- p_dop_resp`	respiration of DOP
`- p_dop_denit`	recycling of DOP using nitrate (denitrification)
`- p_dop_sulf`	Mineralization of DOP, e-acceptor sulfate (sulfate reduction)

Change of: nitrogen in dissolved organic carbon in Redfield ratio

$\frac{d}{dt}$ `t_don` $=$

`+ p_nh4_assim_lpp_don`	Production of DON by LPP

continued on next page. . .

Tracer equations, continued from previous page

`+ p_no3_assim_lpp_don`	Production of DON by LPP
`+ p_nh4_assim_spp_don`	Production of DON by SPP
`+ p_no3_assim_spp_don`	Production of DON by SPP
`+ p_nh4_assim_lip_don`	Production of DON by LIP
`+ p_no3_assim_lip_don`	Production of DON by LIP
`+ (p_lpp_resp_nh4)* (don_fraction)`	respiration of large-cell phytoplankton
`+ (p_spp_resp_nh4)* (don_fraction)`	respiration of small-cell phytoplankton
`+ (p_lip_resp_nh4)* (don_fraction)`	respiration of limnic phytoplankton
`+ (p_cya_resp_nh4)* (don_fraction)`	respiration of diazotroph cyanobacteria
`+ (p_zoo_resp_nh4)* (don_fraction)`	respiration of zooplankton
`- p_don2pocn`	particle formation from DON
`- p_don_resp`	respiration of DON
`- p_don_denit`	recycling of DON using nitrate (denitrification)

continued on next page…

Tracer equations, continued from previous page

`- p_don_sulf`	Mineralization of DON, e-acceptor sulfate (sulfate reduction)

Change of: sediment particular carbon

$\frac{d}{dt}\,\texttt{t\_sed\_poc} =$

`+ p_poc_sedi_sed`	poc sedimentation
`- p_sed_poc_resp`	recycling of sedimentary poc to dic using oxygen (respiration)
`- p_sed_poc_denit`	recycling of sedimentary poc to dic using nitrate (denitrification)
`- p_sed_poc_sulf`	recycling of sedimentary poc to dic using sulfate (sulfate reduction)
`- p_sed_ero_poc`	sedimentary poc erosion
`- p_sed_biores_poc`	bio resuspension of sedimentary poc
`- p_poc_burial`	burial of poc deeper than max_sed

Change of: sediment particular organic N+C

$\frac{d}{dt}\,\texttt{t\_sed\_pocn} =$

`+ p_pocn_sedi_sed`	pocn sedimentation
`- p_sed_ero_pocn`	sedimentary pocn erosion
`- p_sed_biores_pocn`	bio resuspension of sedimentary pocn

continued on next page…

Tracer equations, continued from previous page

`- p_pocn_burial`	burial of pocn deeper than max_sed
`- p_sed_pocn_resp`	recycling of sedimentary pocn to dic and NH4 using oxygen (respiration)
`- p_sed_pocn_denit`	recycling of sedimentary pocn to dic and NH4 using nitrate (denitrification)

Change of: sediment particular organic P+C

$\frac{d}{dt}$ `t_sed_pocp` =

`+ p_pocp_sedi_sed`	pocp sedimentation
`- p_sed_ero_pocp`	sedimentary pocp erosion
`- p_sed_biores_pocp`	bio resuspension of sedimentary pocp
`- p_pocp_burial`	burial of pocp deeper than max_sed
`- p_sed_pocp_resp`	recycling of sedimentary pocp to dic and PO4 using oxygen (respiration)
`- p_sed_pocp_denit`	recycling of sedimentary pocp to dic and PO4 using nitrate (denitrification)

Change of: colored dissolved organic carbon

$\frac{d}{dt}$ `t_cdom` =

`- p_cdom_decay`	decay of cdom due to light

Change of: large-cell phytoplankton

continued on next page…

Tracer equations, continued from previous page

$\frac{d}{dt}$ `t_lpp` =

`+ p_no3_assim_lpp`	assimilation of nitrate by large-cell phytoplankton
`+ p_nh4_assim_lpp`	assimilation of ammonium by large-cell phytoplankton
`- p_lpp_graz_zoo`	grazing of zooplankton eating large-cell phytoplankton
`- p_lpp_resp_nh4`	respiration of large-cell phytoplankton
`- p_lpp_mort_det`	mortality of large-cell phytoplankton

Change of: suspended iron phosphate

$\frac{d}{dt}$ `t_ipw` =

`+ p_ips_ero_ipw/(cgt_cellheight* cgt_density)`	erosion of iron PO4
`+ p_ips_biores_ipw/(cgt_cellheight* cgt_density)`	bio resuspension of iron PO4
`- p_ipw_sedi_ips/(cgt_cellheight* cgt_density)`	sedimentation of iron PO4

Change of: diazotroph cyanobacteria

$\frac{d}{dt}$ `t_cya` =

`+ p_n2_assim_cya`	fixation of dinitrogen by diazotroph cyanobacteria

continued on next page...

Tracer equations, continued from previous page

`- p_cya_graz_zoo`	grazing of zooplankton eating diazotroph cyanobacteria
`- p_cya_resp_nh4`	respiration of diazotroph cyanobacteria
`- p_cya_mort_det`	mortality of diazotroph cyanobacteria
`- p_cya_mort_det_diff`	mortality of diazotroph cyanobacteria due to strong turbulence

Change of: detritus

$\frac{d}{dt}$ `t_det` =

`+ p_lpp_mort_det`	mortality of large-cell phytoplankton
`+ p_spp_mort_det`	mortality of small-scale phytoplankton
`+ p_lip_mort_det`	mortality of limnic phytoplankton
`+ p_cya_mort_det`	mortality of diazotroph cyanobacteria
`+ p_cya_mort_det_diff`	mortality of diazotroph cyanobacteria due to strong turbulence
`+ p_zoo_mort_det`	mortality of zooplankton
`+ p_sed_ero_det/(cgt_cellheight* cgt_density)`	sedimentary detritus erosion
`+ p_sed_biores_det/(cgt_cellheight* cgt_density)`	bio resuspension of sedimentary detritus

continued on next page. . .

`- p_det_resp_nh4`	recycling of detritus using oxygen (respiration)
`- p_det_denit_nh4`	recycling of detritus using nitrate (denitrification)
`- p_det_sulf_nh4`	recycling of detritus using sulfate (sulfate reduction)
`- p_det_sedi_sed/(cgt_cellheight* cgt_density)`	detritus sedimentation

Change of: particulate organic carbon

$\frac{d}{dt}$ `t_poc` =

`+ p_sed_ero_poc/(cgt_cellheight* cgt_density)`	sedimentary poc erosion
`+ p_sed_biores_poc/(cgt_cellheight* cgt_density)`	bio resuspension of sedimentary poc
`+ p_doc2pco`	particle formation from DOC
`- p_poc_resp`	respiration of POC
`- p_poc_denit`	recycling of POC using nitrate (denitrification)
`- p_poc_sulf`	Mineralization of POC, e-acceptor sulfate (sulfate reduction)

continued on next page…

`- p_poc_sedi_sed/(cgt_cellheight* cgt_density)`	poc sedimentation

Change of: phosphorus in particulate organic carbon in Redfield ratio

$\frac{d}{dt}$ `t_pocp` =

`+ p_sed_ero_pocp/(cgt_cellheight* cgt_density)`	sedimentary pocp erosion
`+ p_sed_biores_pocp/(cgt_cellheight cgt_density)`	bio resuspension of sedimentary pocp
`+ p_dop2pocp`	particle formation from DOP
`- p_pocp_resp`	respiration of POCP
`- p_pocp_denit`	recycling of POC using nitrate (denitrification)
`- p_pocp_sulf`	Mineralization of POC, e-acceptor sulfate (sulfate reduction)
`- p_pocp_sedi_sed/(cgt_cellheight* cgt_density)`	pocp sedimentation
`- p_sed_pocp_sulf/(cgt_cellheight* cgt_density)`	recycling of sedimentary pocp to dic and PO4 using sulfate (sulfate reduction)

continued on next page…

Tracer equations, continued from previous page

Change of: nitrogen in particulate organic carbon in Redfield ratio

$\frac{d}{dt}$ `t_pocn` =

`+ p_sed_ero_pocn/(cgt_cellheight* cgt_density)`	sedimentary pocn erosion
`+ p_sed_biores_pocn/(cgt_cellheigh cgt_density)`	bio resuspension of sedimentary pocn
`+ p_don2pocn`	particle formation from DON
`- p_pocn_resp`	respiration of POCN
`- p_pocn_denit`	recycling of POCN using nitrate (denitrification)
`- p_pocn_sulf`	Mineralization of POCN, e-acceptor sulfate (sulfate reduction)
`- p_pocn_sedi_sed/(cgt_cellheight* cgt_density)`	pocn sedimentation
`- p_sed_pocn_sulf/(cgt_cellheight* cgt_density)`	recycling of sedimentary pocn to dic and NH4 using sulfate (sulfate reduction)

end of table **Tracer equations**

Author contributions. TN, HR, BC, and MS developed and implemented the model. TN performed the model simulations. All authors contributed to writing the manuscript.

Competing interests. The authors declare that they have no conflict of interest.

Acknowledgements. Computational power was provided by the North-German Supercomputing Alliance (HLRN). Financial support by the BONUS INTEGRAL 363 project (Grant No. 03F0773A) is gratefully acknowledged. We wish to thank Bernd Schneider, and Henry Bitting for many pieces of advise and discussion.

References

Bakker, D. C. E., Pfeil, B., Landa, C. S., Metzl, N., O'Brien, K. M., Olsen, A., Smith, K., Cosca, C., Harasawa, S., Jones, S. D., Nakaoka, S., Nojiri, Y., Schuster, U., Steinhoff, T., Sweeney, C., Takahashi, T., Tilbrook, B., Wada, C., Wanninkhof, R., Alin, S. R., Balestrini, C. F., Barbero, L., Bates, N. R., Bianchi, A. A., Bonou, F., Boutin, J., Bozec, Y., Burger, E. F., Cai, W.-J., Castle, R. D., Chen, L., Chierici, M., Currie, K., Evans, W., Featherstone, C., Feely, R. A., Fransson, A., Goyet, C., Greenwood, N., Gregor, L., Hankin, S., Hardman-Mountford, N. J., Harlay, J., Hauck, J., Hoppema, M., Humphreys, M. P., Hunt, C. W., Huss, B., Ibánhez, J. S. P., Johannessen, T., Keeling, R., Kitidis, V., Körtzinger, A., Kozyr, A., Krasakopoulou, E., Kuwata, A., Landschützer, P., Lauvset, S. K., Lefèvre, N., Lo Monaco, C., Manke, A., Mathis, J. T., Merlivat, L., Millero, F. J., Monteiro, P. M. S., Munro, D. R., Murata, A., Newberger, T., Omar, A. M., Ono, T., Paterson, K., Pearce, D., Pierrot, D., Robbins, L. L., Saito, S., Salisbury, J., Schlitzer, R., Schneider, B., Schweitzer, R., Sieger, R., Skjelvan, I., Sullivan, K. F., Sutherland, S. C., Sutton, A. J., Tadokoro, K., Telszewski, M., Tuma, M., van Heuven, S. M. A. C., Vandemark, D., Ward, B., Watson, A. J., and Xu, S.: A multi-decade record of high-quality $f\mathrm{CO_2}$ data in version 3 of the Surface Ocean $\mathrm{CO_2}$ Atlas (SOCAT), Earth System Science Data, 8, 383–413, https://doi.org/10.5194/essd-8-383-2016, 2016.

Carlson, C. A. and Hansell, D. A.: Chapter 3 - DOM Sources, Sinks, Reactivity, and Budgets, in: Biogeochemistry of Marine Dissolved Organic Matter, edited by Carlson, D. A. and Hansell, C. A., pp. 65 – 126, Academic Press, Boston, Second edn., https://doi.org/10.1016/B978-0-12-405940-5.00003-0, 2015.

Carlson, C. A., Ducklow, H. W., Hansell, D. A., and Smith Jr., W. O.: Organic carbon partitioning during spring phytoplankton blooms in the Ross Sea polynya and the Sargasso Sea, Limnology and Oceanography, 43, 375–386, https://doi.org/10.4319/lo.1998.43.3.0375, 1998.

Chien, C.-T., Pahlow, M., Schartau, M., and Oschlies, A.: Optimality-based non-Redfield plankton–ecosystem model (OPEM v1.1) in UVic-ESCM 2.9 – Part 2: Sensitivity analysis and model calibration, Geoscientific Model Development, 13, 4691–4712, https://doi.org/10.5194/gmd-13-4691-2020, 2020.

Droop, M. R.: SOME THOUGHTS ON NUTRIENT LIMITATION IN ALGAE1, Journal of Phycology, 9, 264–272, https://doi.org/https://doi.org/10.1111/j.1529-8817.1973.tb04092.x, 1973.

Eggert, A. and Schneider, B.: A nitrogen source in spring in the surface mixed-layer of the Baltic Sea: Evidence from total nitrogen and total phosphorus data, Journal of Marine Systems, 148, 39–47, https://doi.org/doi.org/10.1016/j.jmarsys.2015.01.005, 2015.

Engel, A.: Direct relationship between CO2 uptake and transparent exopolymer particles production in natural phytoplankton, Journal of Plankton Research, 24, 49–53, https://doi.org/10.1093/plankt/24.1.49, 2002.

Engel, A., Thoms, S., Riebesell, U., Rochelle-Newall, E., and Zondervan, I.: Polysaccharide aggregation as a potential sink of marine dissolved organic carbon, Nature, 428, 929–932, https://doi.org/10.1038/nature02453, 2004.

Eppley, R. W.: Temperature and phytoplankton growth, Fish. Bull., 70, 1063–1085, 1972.

Fransner, F., Gustafsson, E., Tedesco, L., Vichi, M., Hordoir, R., Roquet, F., Spilling, K., Kuznetsov, I., Eilola, K., Mörth, C.-M., Humborg, C., and Nycander, J.: Non-Redfieldian Dynamics Explain Seasonal pCO2 Drawdown in the Gulf of Bothnia, Journal of Geophysical Research: Oceans, 123, 166–188, https://doi.org/10.1002/2017JC013019, 2018.

Geyer, B. and Rockel, B.: coastDat-2 COSMO-CLM Atmospheric Reconstruction [data set], https://doi.org/10.1594/WDCC/coastDat-2_COSMO-CLM, 2013.

Griffies, S. M.: Fundamentals of Ocean Climate Models, Princeton University Press, Princeton, NJ, 2004.

Gustafsson, E., Deutsch, B., Gustafsson, B., Humborg, C., and Mörth, C.-M.: Carbon cycling in the Baltic Sea ? The fate of allochthonous organic carbon and its impact on air-sea CO2 exchange, Journal of Marine Systems, 129, 289–302, https://doi.org/10.1016/j.jmarsys.2013.07.005, 2014a.

Gustafsson, E., Wällstedt, T., Humborg, C., Mörth, C.-M., and Gustafsson, B. G.: External total alkalinity loads versus internal generation: The influence of nonriverine alkalinity sources in the Baltic Sea, Global Biogeochemical Cycles, 28, 1358–1370, https://doi.org/10.1002/2014GB004888, 2014b.

Gustafsson, E., Savchuk, O. P., Gustafsson, B. G., and Müller-Karulis, B.: Key processes in the coupled carbon, nitrogen, and phosphorus cycling of the Baltic Sea, Biogeochemistry, 134, 301–317, https://doi.org/10.1007/s10533-017-0361-6, 2017.

Gustafsson, E., Hagens, M., Sun, X., Reed, D. C., Humborg, C., Slomp, C. P., and Gustafsson, B. G.: Sedimentary alkalinity generation and long-term alkalinity development in the Baltic Sea, Biogeosciences, 16, 437–456, https://doi.org/10.5194/bg-16-437-2019, 2019.

Hansell, D. A., Carlson, C. A., Repeta, D. J., and Schlitzer, R.: Dissolved Organic Matter in the Ocean: A Controversy Stimulates New Insights, Oceanography, 22, 202–211, https://doi.org/10.5670/oceanog.2009.109, 2009.

HELCOM: Sources and pathways of nutrients to the Baltic Sea., Balt. Sea Environ. Proc. No. 153, 2018.

Hjalmarsson, S., Wesslander, K., Anderson, L. G., Omstedt, A., Perttilä, M., and Mintrop, L.: Distribution, long-term development and mass balance calculation of total alkalinity in the Baltic Sea, Continental Shelf Research, 28, 593–601, https://doi.org/10.1016/j.csr.2007.11.010, 2008.

Ho, T.-Y., Quigg, A., Finkel, Z. V., Milligan, A. J., Wyman, K., Falkowski, P. G., and Morel, F. M. M.: The Elemental Composition of Some Marine Phytoplankton, Journal of Phycology, 39, 1145–1159, https://doi.org/10.1111/j.0022-3646.2003.03-090.x, 2003.

Hoikkala, L., Kortelainen, P., Soinne, H., and Kuosa, H.: Dissolved organic matter in the Baltic Sea, Journal of Marine Systems, 142, 47–61, https://doi.org/10.1016/j.jmarsys.2014.10.005, 2015.

Kreus, M., Schartau, M., Engel, A., Nausch, M., and Voss, M.: Variations in the elemental ratio of organic matter in the central Baltic Sea: Part I?Linking primary production to remineralization, Continental Shelf Research, 100, 25–45, https://doi.org/10.1016/j.csr.2014.06.015, 2015.

Kriest, I., Oschlies, A., and Khatiwala, S.: Sensitivity analysis of simple global marine biogeochemical models, Global Biogeochemical Cycles, 26, https://doi.org/10.1029/2011GB004072, 2012.

Kuznetsov, I., Neumann, T., and Burchard, H.: Model study on the ecosystem impact of a variable C:N:P ratio for cyanobacteria in the Baltic Proper, Ecological Modelling, 219, 107–114, https://doi.org/10.1016/j.ecolmodel.2008.08.002, 2008.

Kuznetsov, I., Neumann, T., Schneider, B., and Yakushev, E.: Processes regulating pCO(2) in the surface waters of the central eastern Gotland Sea: a model study, OCEANOLOGIA, 53, 745–770, https://doi.org/10.5697/oc.53-3.745, 2011.

Larsson, U., Hajdu, S., Walve, J., and Elmgren, R.: Baltic Sea nitrogen fixation estimated from the summer increase in upper mixed layer total nitrogen, Limnology and Oceanography, 46, 811–820, https://doi.org/10.4319/lo.2001.46.4.0811, 2001.

Leibniz Institute for Baltic Sea Research: ERGOM: Ecological ReGional Ocean Model, https://ergom.net/, last access: 10 March 2022, 2015.

Leipe, T., Tauber, F., Vallius, H., Virtasalo, J., Uścinowicz, S., Kowalski, N., Hille, S., Lindgren, S., and Myllyvirta, T.: Particulate organic carbon (POC) in surface sediments of the Baltic Sea, Geo-Marine Letters, 31, 175–188, https://doi.org/10.1007/s00367-010-0223-x, 2010.

Lips, I. and Lips, U.: The Importance of Mesodinium rubrum at Post-Spring Bloom Nutrient and Phytoplankton Dynamics in the Vertically Stratified Baltic Sea, Frontiers in Marine Science, 4, https://doi.org/10.3389/fmars.2017.00407, 2017.

Macias, D., Huertas, I. E., Garcia-Gorriz, E., and Stips, A.: Non-Redfieldian dynamics driven by phytoplankton phosphate frugality explain nutrient and chlorophyll patterns in model simulations for the Mediterranean Sea, Progress in Oceanography, 173, 37–50, https://doi.org/10.1016/j.pocean.2019.02.005, 2019.

Martin, J. H., Knauer, G. A., Karl, D. M., and Broenkow, W. W.: VERTEX: carbon cycling in the northeast Pacific, Deep Sea Research Part A. Oceanographic Research Papers, 34, 267–285, https://doi.org/10.1016/0198-0149(87)90086-0, 1987.

Martiny, A. C., Talarmin, A., Mouginot, C., Lee, J. A., Huang, J. S., Gellene, A. G., and Caron, D. A.: Biogeochemical interactions control a temporal succession in the elemental composition of marine communities, Limnology and Oceanography, 61, 531–542, https://doi.org/10.1002/lno.10233, 2016.

Monod, J.: The growth of bacterial cultures, Ann. Rev. Microbiol., 3, 371–394, 1949.

Müller, J. D., Schneider, B., and Rehder, G.: Long-term alkalinity trends in the Baltic Sea and their implications for CO2-induced acidification, Limnology and Oceanography, 61, 1984–2002, https://doi.org/doi.org/10.1002/lno.10349, 2016.

Nausch, M., Nausch, G., Lass, H. U., Mohrholz, V., Nagel, K., Siegel, H., and Wasmund, N.: Phosphorus input by upwelling in the eastern Gotland Basin (Baltic Sea) in summer and its effects on filamentous cyanobacteria, Estuarine, Coastal and Shelf Science, 83, 434–442, https://doi.org/https://doi.org/10.1016/j.ecss.2009.04.031, 2009.

Neumann, T.: ERGOM 1.2 model hindcast 1948-2019 [data set], https://thredds-iow.io-warnemuende.de/thredds/catalogs/projects/integral/catalog_pocNP_V04R25_3nm_agg_time.html, last access: 10 March 2022, 2021.

Neumann, T.: Model code and boundary data for "Non-Redfield carbon model for the Baltic Sea (ERGOM version 1.2) – Implementation and Budget estimates" paper [code], https://doi.org/10.5281/zenodo.7252134, last access: 26 October 2022, 2022.

Neumann, T., Fennel, W., and Kremp, C.: Experimental simulations with an ecosystem model of the Baltic Sea: A nutrient load reduction experiment, Global Biogeochemical Cycles, 16, 7–1–7–19, https://doi.org/10.1029/2001GB001450, 2002.

Neumann, T., Koponen, S., Attila, J., Brockmann, C., Kallio, K., Kervinen, M., Mazeran, C., Müller, D., Philipson, P., Thulin, S., Väkevä, S., and Ylöstalo, P.: Optical model for the Baltic Sea with an explicit CDOM state variable: a case study with Model ERGOM (version 1.2), Geoscientific Model Development, 14, 5049–5062, https://doi.org/10.5194/gmd-14-5049-2021, 2021.

Omstedt, A., Gustafsson, E., and Wesslander, K.: Modelling the uptake and release of carbon dioxide in the Baltic Sea surface water, Continental Shelf Research, 29, 870–885, https://doi.org/10.1016/j.csr.2009.01.006, 2009.

Omstedt, A., Humborg, C., Pempkowiak, J., Perttilä, M., Rutgersson, A., Schneider, B., and Smith, B.: Biogeochemical Control of the Coupled CO2-O2 System of the Baltic Sea: A Review of the Results of Baltic-C, Ambio, 43, 49–59, https://doi.org/10.1007/s13280-013-0485-4, 2014.

Pahlow, M., Chien, C.-T., Arteaga, L. A., and Oschlies, A.: Optimality-based non-Redfield plankton–ecosystem model (OPEM v1.1) in UVic-ESCM 2.9 – Part 1: Implementation and model behaviour, Geoscientific Model Development, 13, 4663–4690, https://doi.org/10.5194/gmd-13-4663-2020, 2020.

Pfeil, B., Olsen, A., Bakker, D. C. E., Hankin, S., Koyuk, H., Kozyr, A., Malczyk, J., Manke, A., Metzl, N., Sabine, C. L., Akl, J., Alin, S. R., Bates, N., Bellerby, R. G. J., Borges, A., Boutin, J., Brown, P. J., Cai, W.-J., Chavez, F. P., Chen, A., Cosca, C., Fassbender, A. J., Feely, R. A., González-Dávila, M., Goyet, C., Hales, B., Hardman-Mountford, N., Heinze, C., Hood, M., Hoppema, M., Hunt, C. W., Hydes, D., Ishii, M., Johannessen, T., Jones, S. D., Key, R. M., Körtzinger, A., Landschützer, P., Lauvset, S. K., Lefèvre, N., Lenton, A., Lourantou, A., Merlivat, L., Midorikawa, T., Mintrop, L., Miyazaki, C., Murata, A., Nakadate, A., Nakano, Y., Nakaoka, S., Nojiri, Y., Omar, A. M., Padin, X. A., Park, G.-H., Paterson, K., Perez, F. F., Pierrot, D., Poisson, A., Ríos, A. F., Santana-Casiano, J. M., Salisbury, J., Sarma, V. V. S. S., Schlitzer, R., Schneider, B., Schuster, U., Sieger, R., Skjelvan, I., Steinhoff, T., Suzuki, T., Takahashi, T., Tedesco, K., Telszewski, M., Thomas, H., Tilbrook, B., Tjiputra, J., Vandemark, D., Veness, T., Wanninkhof, R., Watson, A. J., Weiss, R., Wong, C. S., and Yoshikawa-Inoue, H.: A uniform, quality controlled Surface Ocean CO_2 Atlas (SOCAT), Earth System Science Data, 5, 125–143, https://doi.org/10.5194/essd-5-125-2013, 2013.

Redfield, A. C., Ketchum, B. H., and Richards, B. H.: The influence of organisms on the composotion of sea water, in: The Sea, edited by Hill, L., vol. 2, pp. 26 – 77, Interscience, New York, 1963.

Rehder, G., Müller, J., Bittig, H., Kahru, M., Kaitala, S., Schneider, B., Siiriä, S.-M., Tuomi, L., and Wasmund, N.: Extreme productivity patterns during the spring bloom 2018 in the central Baltic Sea suggest vertical nutrient shuttling: Unforeseen surprises for the fight against eutrophication in a warming world?, in: All abstracts for the ICOS Science Conference 2020, ICOS Integrated Carbon Observation System, https://www.icos-cp.eu/sc2020/abstracts#143, 2020.

Schneider, B. and Müller, J. D.: Surface Water Biogeochemistry as Derived from pCO2 Observations, pp. 49–92, Springer International Publishing, Cham, https://doi.org/10.1007/978-3-319-61699-5_5, 2018.

Schneider, B., Kaitala, S., Raateoja, M., and Sadkowiak, B.: A nitrogen fixation estimate for the Baltic Sea based on continuous pCO2 measurements on a cargo ship and total nitrogen data, Continental Shelf Research, 29, 1535–1540, https://doi.org/10.1016/j.csr.2009.04.001, 2009.

Seifert, T., Tauber, F., and Kayser, B.: Digital topography of the Baltic Sea [data set], https://www.io-warnemuende.de/topography-of-the-baltic-sea.html, last access: 27 July 2020, 2008.

Sharoni, S. and Halevy, I.: Nutrient ratios in marine particulate organic matter are predicted by the population structure of well-adapted phytoplankton, Science Advances, 6, eaaw9371, https://doi.org/10.1126/sciadv.aaw9371, 2020.

Steele, J. H.: The structure of marine ecosystems, Cambridge Havard University Press, 1974.

Szymczycha, B., Maciejewska, A., Winogradow, A., and Pempkowiak, J.: Could submarine groundwater discharge be a significant carbon source to the southern Baltic Sea?, Oceanologia, 56, 327–347, https://doi.org/10.5697/oc.56-2.327, 2014.

Wan, Z., Jonasson, L., and Bi, H.: N/P ratio of nutrient uptake in the Baltic Sea, Ocean Science, 7, 693–704, https://doi.org/10.5194/os-7-693-2011, 2011.

Wetz, M. S. and Wheeler, P. A.: Release of dissolved organic matter by coastal diatoms, Limnology and Oceanography, 52, 798–807, https://doi.org/10.4319/lo.2007.52.2.0798, 2007.

Winton, M.: A Reformulated Three-Layer Sea Ice Model, Journal of Atmospheric and Oceanic Technology, 17, 525–531, https://doi.org/10.1175/1520-0426(2000)017<0525:ARTLSI>2.0.CO;2, 2000.